

*2/11/74*

NASA CONTRACTOR  
REPORT

*CR 134324*

IMPLEMENTATION AND EXTENSION OF THE  
IMPULSE TRANSFER FUNCTION METHOD FOR FUTURE  
APPLICATION TO THE SPACE SHUTTLE PROJECT

Volume I - Analysis and Correlation Studies

By

M. Mantus and H. Pardo

Grumman Aerospace Corporation  
Bethpage, New York 11714

April 1973

*NAS 9 - 12333*

Prepared for

NASA-MANNED SPACECRAFT CENTER  
Houston, Texas 77058

Reproduced by  
NATIONAL TECHNICAL  
INFORMATION SERVICE  
US Department of Commerce  
Springfield, VA. 22151

E74-28334  
Unclas  
42571  
G3/31  
CSCCL 22B  
(NASA-CR-134324) IMPLEMENTATION AND  
EXTENSION OF THE IMPULSE TRANSFER  
FUNCTION METHOD FOR FUTURE APPLICATION TO  
THE SPACE SHUTTLE (Grumman Aerospace  
Corp.)

PRICES SUBJECT TO CHANGE

*1182*

NASA CONTRACTOR  
REPORT

IMPLEMENTATION AND EXTENSION OF THE  
IMPULSE TRANSFER FUNCTION METHOD FOR FUTURE  
APPLICATION TO THE SPACE SHUTTLE PROJECT

Volume I - Analysis and Correlation Studies

By

M. Mantus and H. Pardo

Grumman Aerospace Corporation  
Bethpage, New York 11714

April 1973

Prepared for

NASA-MANNED SPACECRAFT CENTER  
Houston, Texas 77058

FOREWORD

The work reported herein was performed by the Grumman Aerospace Corporation for the NASA-Manned Spacecraft Center under Contract No. NAS 9-12333. The period of performance was from February 1972 through March 1973.

Mr. M. Mantus of the Grumman Aerospace Corporation was the Project Manager for the contract; G. Patterson was in charge of computer program development for Grumman Data Systems. The authors wish to extend thanks to many Grumman personnel who contributed to the successful completion of the work. Outstanding were D. Ives and E. Lerner for assistance on filtering methods, L. Mitchell for help with the modal analysis, M. Bernstein for assistance with Shuttle considerations, F. Bunce, R. Hilderman, W. Lansing, A. Alberi, and E. Kelly for reviewing the results, and J. Smedfjeld for guidance during the latter stages of the work. Thanks are also extended to R. Rosello, H. Coddling, P. Kraft, P. Mulvehill, and R. Quinn, Grumman Data Systems personnel, who were major contributors to the successful data processing effort.

Mr. T. Modlin was the MSC Technical Monitor. His assistance in all phases of the program is gratefully acknowledged.

## TABLE OF CONTENTS

Section	Page
1. Introduction and Summary.....	1
2. Background on ITF Development .....	5
3. Data Acquisition and Processing.....	15
4. Results .....	20
a. Comparison of Drop Test Results with Predictions Using ITF Data.....	25
b. Comparison of Drop Test Results, Predictions Using ITF's and Predictions from Modal Analysis.....	47
c. LM Modal Characteristics from ITF Data.....	61
5. Considerations for ITF Testing the Shuttle.....	63
6. Conclusions and Recommendations.....	75
7. References.....	79
Appendices	
A. Suspension System Considerations.....	81
B. Instrumentation List.....	86
C. Summary of LTA-11 Impulse Testing.....	90
D. Sample Impulse and Response Time Histories.....	92
E. LTA-11 Finite Element Idealization.....	95
F. LTA-11 Mode Survey Results.....	101

## 1-INTRODUCTION AND SUMMARY

The work performed under this contract was the second step in a two phase program to develop and implement the test/analysis technique known as the "Impulse Transfer Function" (ITF) method for possible application to the Space Shuttle project. The first phase of the program, funded by the Langley Research Center under Contract No. NAS 1-10635-2, was concerned with testing a realistic spacecraft structure and a partial verification of the accuracy of the ITF approach. Results of this effort are reported in Reference 1.

The second phase effort has been primarily devoted to computer programming, data processing, and a correlation study that employed data collected in the first phase test.

The primary objective of the Langley contract was to demonstrate that standard test procedures and equipment could be used to collect a significant number of transfer functions from tests of the Lunar Module test article LTA-11. The testing consisted of suspending the vehicle from the apex fittings of the outrigger trusses through a set of air springs to simulate the "free-free" state. Impulsive loadings were delivered, one at a time, at each of the landing gear's attachment points, in three mutually perpendicular directions; thus a total of 36 impulses were applied to the vehicle. Time histories of each pulse were recorded on magnetic tape along with 40 channels of strain gage response and 28 channels of accelerometer response. Since an automated data processing system was not available, oscillograph playbacks were made of all 2400 time histories as a check on the validity of the data taken. In addition, one channel of instrumentation was processed to determine its response to a set of forcing functions from a prior LTA-11 drop test. This prediction was compared with drop test results as a first measure of accuracy.

Based on our work for Langley it was concluded that an ITF test of a realistic structure could be conducted expeditiously; the one-channel correlation study indicated that the ITF approach was promising with regard to accuracy.

Under the present contract, computer programming and data processing of the test data taken for Langley was completed. This consisted of first converting to digital form all the data originally collected on analog tapes, and then storing the data in a disk pack on the IBM 370 computer. Programming of the Duhamel integral that is used to predict time history response from ITF data when a set of forcing functions is specified was also completed. As summarized in Volume II of this report, the data processing system is now available at NASA/MSC on the Univac 1108, where tape is used for permanent storage, and at Grumman on the IBM 370 computer, where a random access, easily expandable, disk pack is the permanent storage device. A subroutine is available that allows convenient transfer of data from the Grumman disk pack to the MSC tape storage system.

Using the computer system at Grumman, an extensive correlation study has been conducted to compare internal response as predicted by the ITF technique with results of the LTA-11 drop test program. Section 4a of this report details this work; filtering methods employed to remove spurious effects caused by the suspension system used to support the vehicle for ITF testing are also discussed. The time history comparison that is presented covers every channel that was common to both the drop test and ITF test programs -- a total of 40 channels.

Many channels of the correlation results of Section 4a show excellent agreement in both high frequency content and peak amplitude, even when such difficult-to-measure quantities as shear strain are involved. Other channels indicate that peak amplitude can often be predicted in cases where wave-form correlation leaves something to be desired. In channels where correlation is poor, known or suspected reasons for the discrepancy annotate the time history.

Section 4b shows a comparison of drop test results, ITF predictions, and conventional modal analysis predictions. Modal analysis was based on a LM finite element math model identified as "Big Spring IV." Since the modes predicted using this model were not exceptionally accurate when compared to ground vibration survey results, the relatively good correlation indicated in the response time histories of Section 4b was a welcome surprise. However, it can be readily seen that ITF results are most frequently the more accurate. Again, where discrepancies exist, and reasons are known or suspected, they are amended to the plots. As in the case for the first correlation study, all channels that are common to the drop test, the ITF program, and the modal analysis have been compared.

Two additional areas were covered in the present contract. The first was concerned with determining the feasibility of using the LTA-11 ITF data to compute modal information for the LM. This task was undertaken by the TRW Systems Group under subcontract to Grumman; their work is summarized in References 2 and 3. TRW demonstrated that the frequencies of the lowest modes could be accurately computed from ITF data. Mode shape data, on the other hand, did not compare well with ground vibration results. It is probable that the test problem used in this work (the LM vehicle) was too complex for accurate mode shape prediction without further development work. As explained in Section 4c, it is our opinion that a possibility for determining modal data from ITF's presently exists for applications on simpler airplane-type structures.

The last area of study involved a preliminary investigation of how ITF testing could be applied to the Shuttle. Such items as loading and vehicle support conditions, impulse magnitude, and instrumentation requirements were considered. This work is reported in Section 5.

- - - - -

Section 2, which follows, gives a brief description of the ITF method, its mathematical foundation, and a summary of the assumptions upon which the method is based. Section 3 is concerned with data acquisition and processing. While much of the material contained in Sections 2 and 3 can be found in other reports prepared by Grumman, e.g., Reference 1, it is repeated here so that this report will be reasonably self-contained. As mentioned previously, Section 4 deals with correlation results, while Section 5 outlines considerations for ITF testing on the Shuttle. Section 6 summarizes our conclusions and recommendations on the use of the ITF technique. Miscellaneous material is included in the appendices.

## 2-BACKGROUND ON ITF DEVELOPMENT

The Impulse Transfer Function (ITF) technique is a combined test and analysis method that can be useful for determining internal structural response due to transient forcing functions. As an example of the way the ITF approach can be used, consider the problem of computing the response of an aircraft or the LM to landing forces. The required test program for using the ITF method would consist of supporting the vehicle to simulate a "free-free" state, applying impulses at all the gear attachment points, and measuring the time history responses, e.g., strain, load, acceleration, that are induced by the impulses. Once the collected data is processed and available on a digital computer, the response to long duration applied gear forces could be computed using Duhamel's integral.

The technique is based on the fact that, for a linear structure, the dynamic response to any applied loading can be represented by the superposition of the responses to an equivalent series of impulsive loadings. Figure 2-1 provides a graphical illustration of the technique. A given time history of applied load,  $F_j(t)$ , is approximated by a series of pulses which are sufficiently short to be considered impulses. Since the response to an impulse is proportional to its magnitude (area), the time-history of response to each of the pulses is computed by multiplying the response to a unit impulse,  $h_{ij}(t)$ , (known as an ITF) by the area under the pulse. The responses are then superimposed, with the proper time shifts, to produce the response,  $R_{ij}(t)$ , to the applied loading. A series approximation of Duhamel's integral is used to perform the necessary calculations, as shown in Figure 2-1.

The transfer functions employed in this analytical procedure are obtained experimentally by applying short-duration pulses which approximate impulses,

one at a time, to each point in the structure where load is to be applied. Time histories of these pulses, as well as the responses (strains, accelerations, etc.) at selected locations throughout the structure are recorded. Dividing the response time-history at  $i$  (called a response point) due to the pulse applied at  $j$  (called a loading point) by the area under the pulse yields the Impulse Transfer Function,  $h_{ij}(t)$ . The process is illustrated in Figure 2-2.

Total response at  $i$ , in a structure loaded at several points, is obtained by summing the individual response to each applied load. This procedure is shown in Figure 2-3.

When the ITF technique was first considered, a number of valid questions concerning the difficulty of experimentally determining ITF's were raised. These had significant bearing on the feasibility of the technique. Among them were: Could a pulse be applied with sufficiently short duration to provide a good approximation to an impulse and of sufficiently high amplitude to excite measureable response in a large, complex structure? Could the applied pulse and response be measured accurately?

The only way to answer these questions was to actually try the technique, and so a modest test-analysis program was initiated at Grumman. The test article used was a solid, uniform circular beam suspended to simulate a free-free condition and instrumented to measure strain response. Using a pendulum device, a short-duration loading was applied and recorded along with the strain responses. Impulse transfer functions were then computed from the test results. Subsequently, long-duration pulses were applied, and the attendant measured responses were compared with those calculated by using the ITF data. Except for a scale factor on amplitude, due to inaccurate measurement of the impulse magnitude, good agreement was indicated. This effort, which is reported in Reference 4, demonstrated that a sufficiently short duration pulse could indeed be applied and the response to it could be accurately measured. Poor accuracy in the applied pulse measurement was attributed to the crude instrumentation used in the program. The question of delivering a high pulse amplitude for a large structure was not answered since the test article was not representative in this respect.

Based on the promise shown in the initial study, a more ambitious program was undertaken using the LTA-3 Lunar Module test article. The structure was suspended in a free-free configuration and instrumented to measure strain and acceleration response at a number of locations. An electrodynamic shaker, programmed with an exact-wave-form synthesizer to produce a single pulse, replaced the pendulum. The shaker was selected because it could apply high amplitude pulses and could readily be used to load various points in the structure in any desired direction. A more suitable force transducer eliminated the previous difficulties encountered in pulse measurement, but the 5,000 force-pound shaker initially employed provided too small a pulse to excite measurable response at points remote from the point of load application. A 15,000 force-pound shaker was then substituted and proved more than adequate in exciting measurable response at the most remote of the instrumented points. These were as far as 15 feet away, on the vehicle's aft equipment bay. Figure 2-4 shows a typical impulse and several ITF's obtained for various amplitude short-duration pulses. Excellent repeatability of experimentally determined ITF's is illustrated.

In addition to the impulse loadings, relatively long duration pulses were applied to the test article and the responses measured. The ITF method was then used to predict response. A comparison of the measured and predicted response at a single point is shown in Figure 2-5, along with the time history of the long duration pulse. Reference 5 contains an extensive sample of LTA-3 results. Of the 40 comparisons, half showed predicted peak amplitude agreement within 10% and within 5 milliseconds in time of occurrence. Some had peak amplitude predictions within 5% agreement. In general, all records showed good waveform agreement.

The reason that Grumman has diligently pursued the development of the ITF method is that it can be a valuable supplement to current analytical and experimental techniques and offers certain advantages over both.

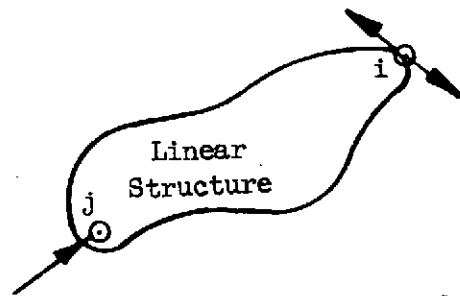
Compared with a purely analytical approach to transient response calculations the ITF's provide a more realistic representation of the

structure than that afforded by usual modal analysis methods. The system's mass, damping and stiffness properties are not needed, since these properties are implicitly reflected in the ITF's, and thus the approximations usually involved in their determination are eliminated. The method is particularly advantageous when dealing with large complex structural systems, such as the Space Shuttle, which do not yield readily to analysis. This is not intended to imply that modal and transient response analysis will be replaced. Since the ITF approach requires hardware to be available before it can be employed, conventional analysis procedures will still be needed in the design stages.

Conventional aerospace practice makes extensive use of testing, including mode surveys and dynamic simulation, such as drop testing. Modal information obtained from tests is still difficult to use to predict internal load distributions, stress levels, and component accelerations. Dynamic simulations verify the integrity of the structure, but do not yield basic information which can be applied to conditions that were not tested or which arise after testing is completed. Measured ITF's, on the other hand, would be available for calculation of responses to any loading condition. A considerable reduction in cost can be effected by using the ITF technique to reduce the number of loading conditions to be simulated, as well as to study loading conditions which are difficult to simulate in a test. It should be noted that the instrumentation required for impulse testing is normally found on simulation test articles; thus, no additional cost would be incurred in this area. One further advantage of the ITF technique lies in the fact that testing may be accomplished at low load levels, minimizing the inherent risk of premature failure and resulting structural damage which exists in simulation. The above discussion is particularly applicable to the Shuttle, due to its size and complexity, and the variety of transient loading conditions to which it will be subjected.

The ITF technique can be profitably applied to the Shuttle program through the use of "replica" models to provide design information, or through the use of full scale impulse testing which can be employed in checking

conventional modal transient response analysis. Shuttle transient loading conditions which can be handled by the method include: lift-off (engine start-up and vehicle release), end of boost, separation, docking and landing. Further discussion of the applicability of the ITF technique to the Space Shuttle may be found in Section 5 of this report and in Reference 6.



$F_j(t)$  = Any force applied at j

$R_{ij}(t)$  = Response at i due to  $F_j(t)$

$$R_{ij}(t) = \Delta t [F_j(t_0)h_{ij}(t) + F_j(t_1)h_{ij}(t-\Delta t) + F_j(t_2)h_{ij}(t-2\Delta t)]$$

$$= \Delta t \sum_{k=0}^{t/\Delta t} F_j(t_k)h_{ij}(t-k\Delta t)$$

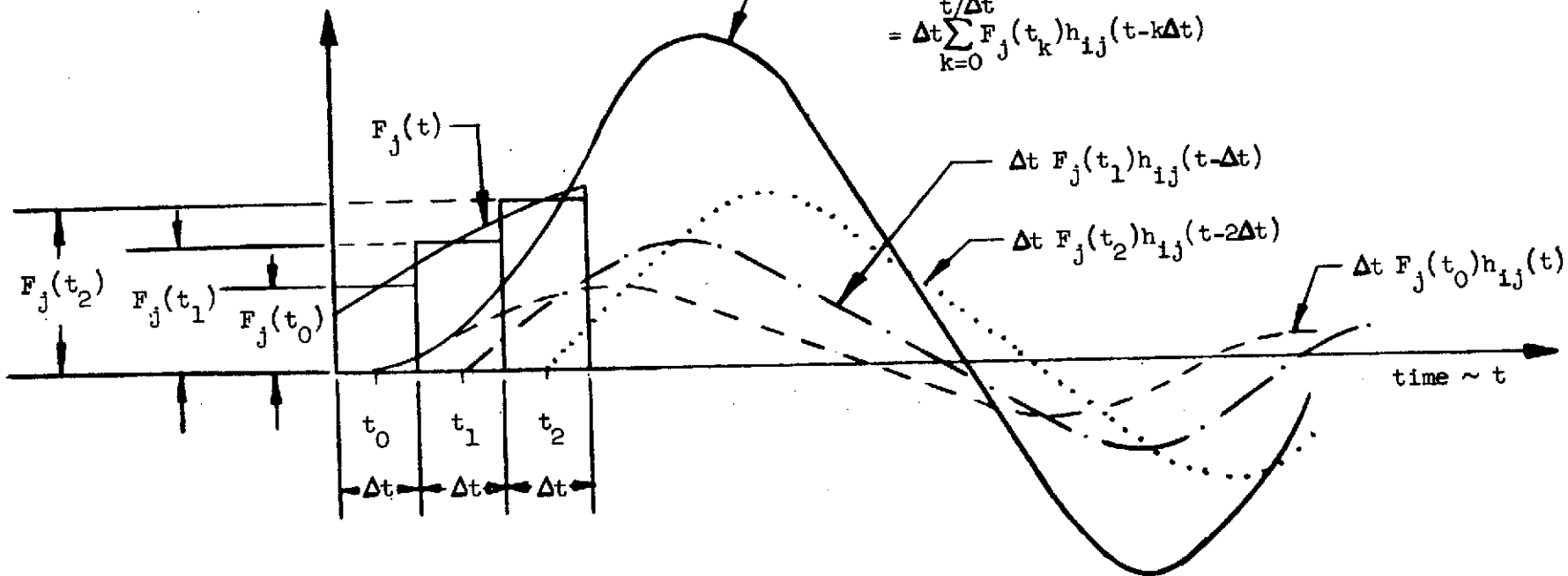
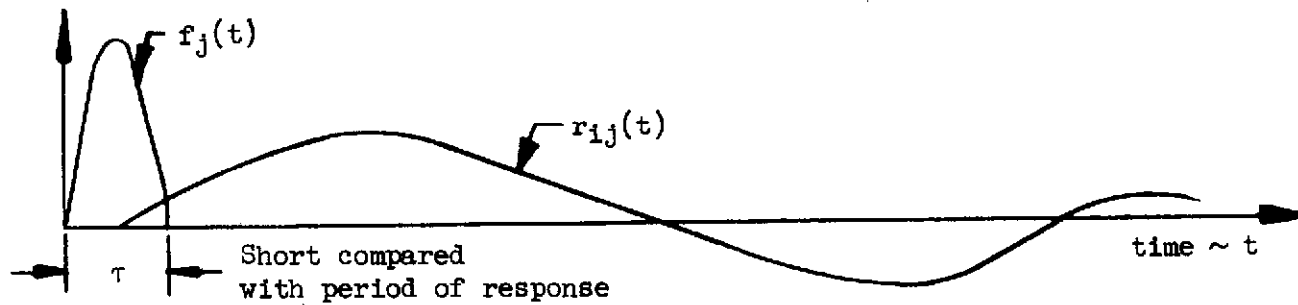
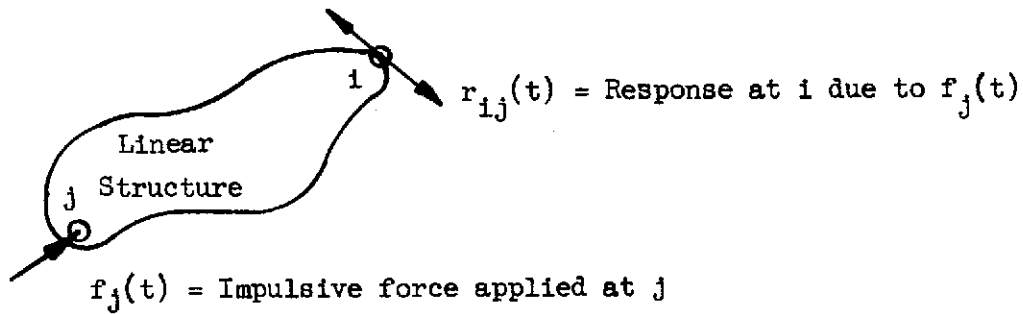


Figure 2-1 - Computing Response Using Impulse Transfer Functions

Apply  $f_j(t)$  and measure  $r_{ij}(t)$  &  $f_j(t)$  :



$$I_j = \text{Impulse magnitude} = \int_0^{\tau} f_j(t) dt$$

$$h_{ij}(t) = \text{Impulse transfer function between i \& j}$$

$$= r_{ij}(t) / I_j$$

Figure 2-2 - Measuring Impulse Transfer Function

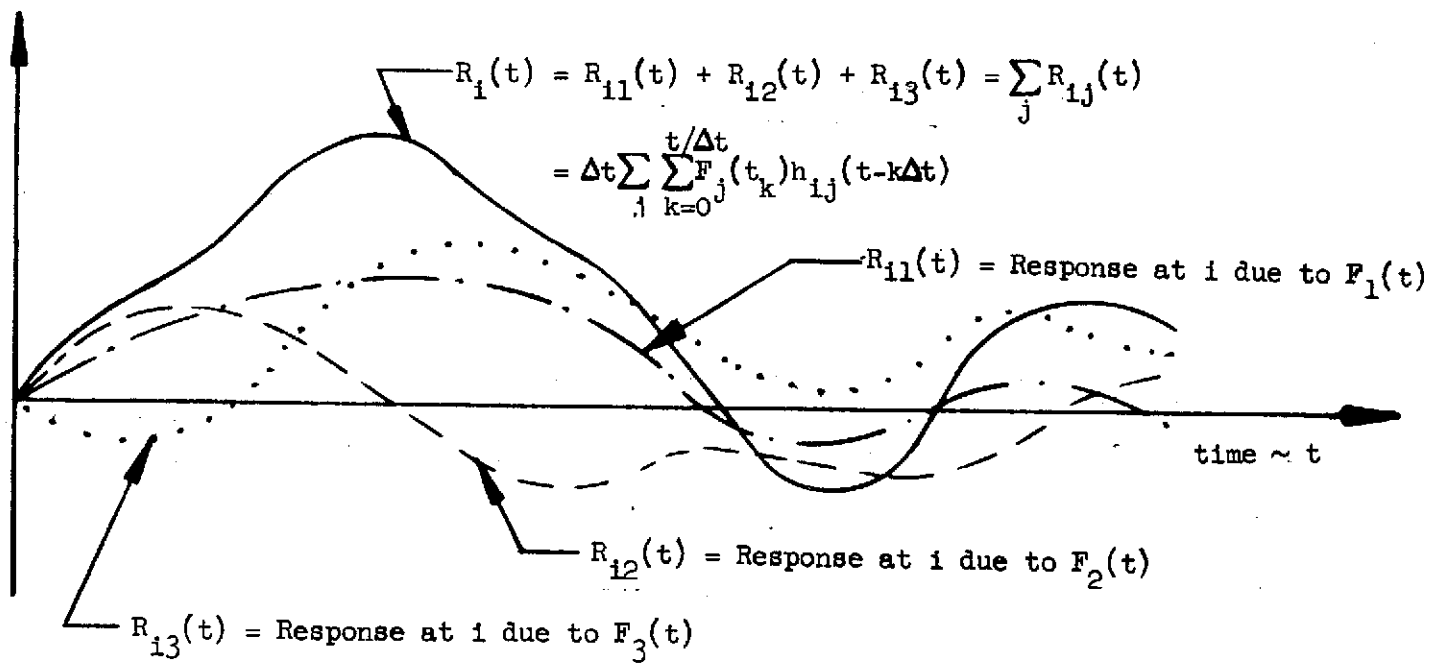
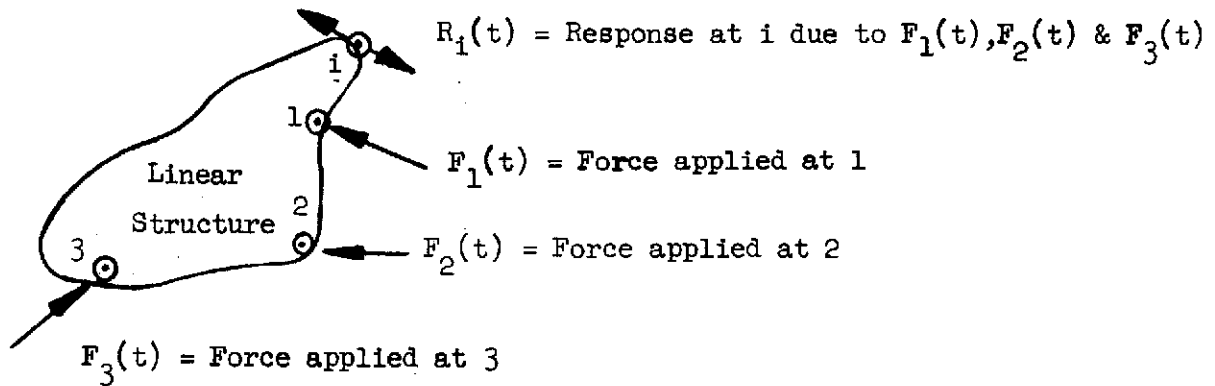


Figure 2-3 - Computing Response to a Number of Applied Forces

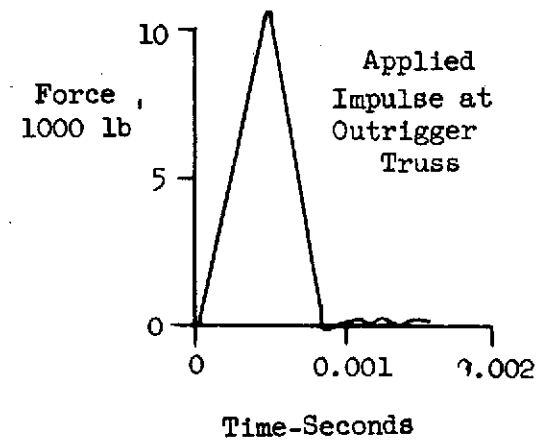
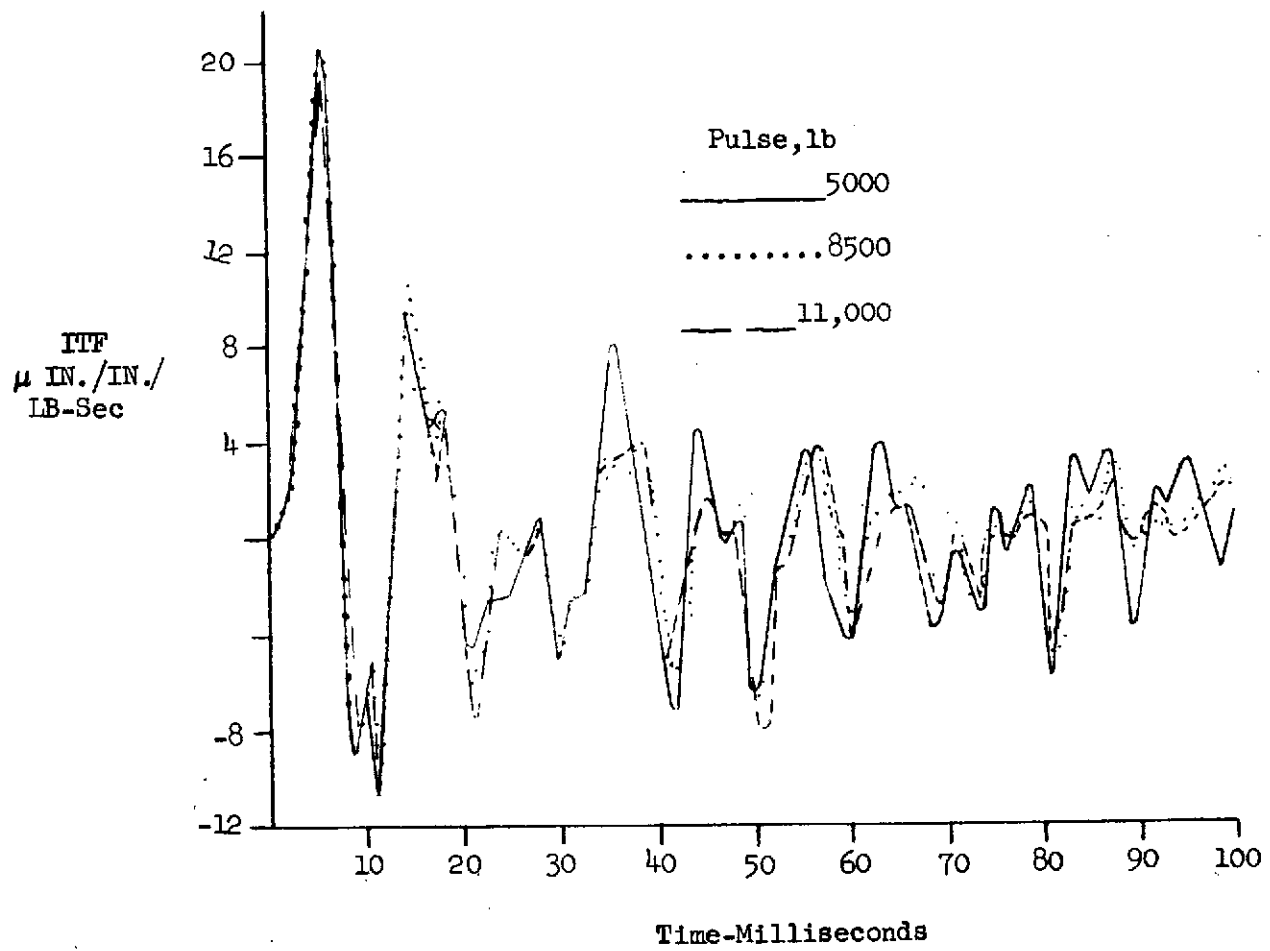


Figure 2-4 - Left-Hand Forward Interstage Fitting Impulse Transfer Function

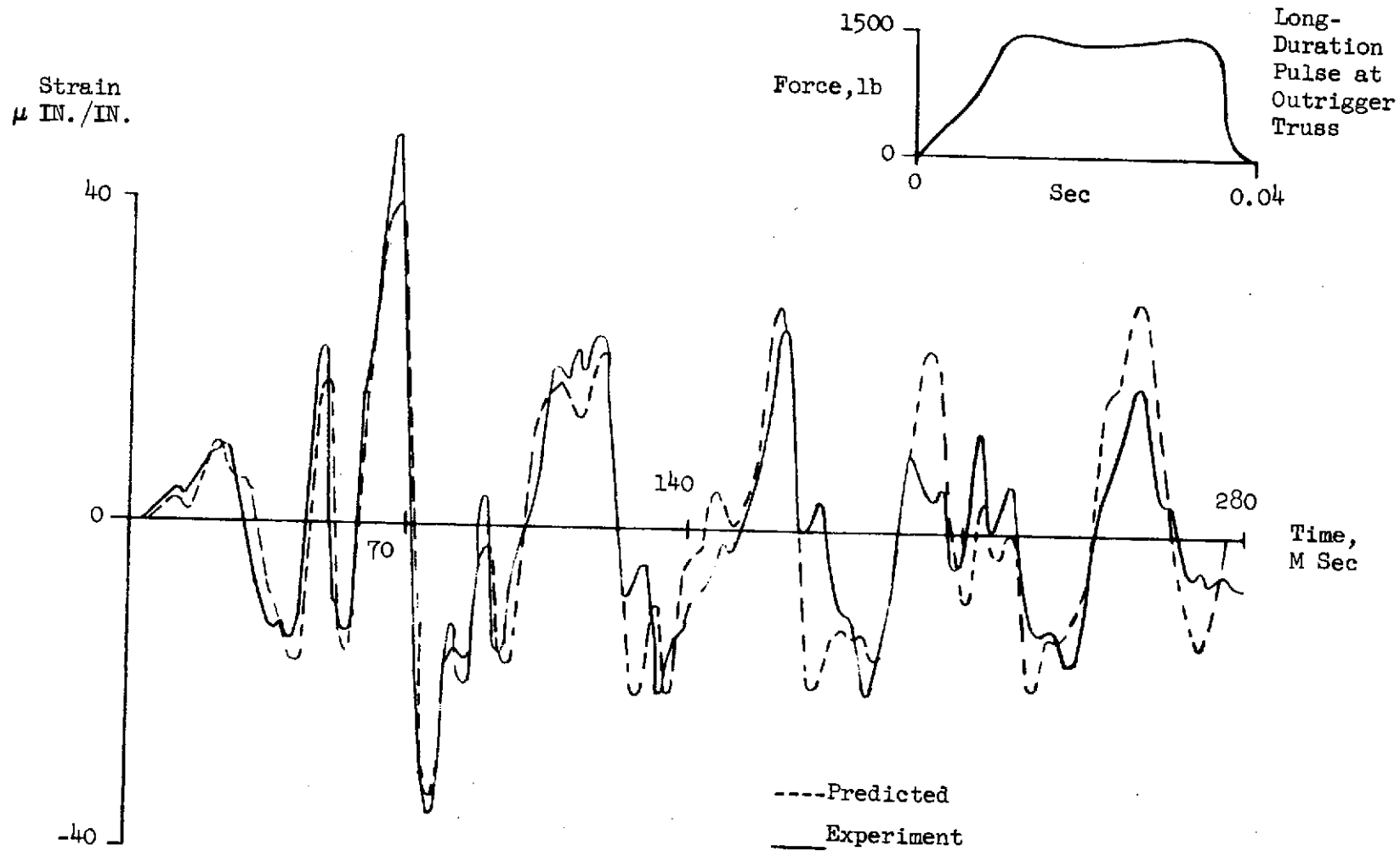


Figure 2-5 - Right-Hand Aft Equipment Bay Lower Outboard Strut Response

### 3-DATA ACQUISITION AND PROCESSING

As mentioned previously, the data used in this effort was collected during testing conducted for Langley, Reference 1. The test article was a structurally complete LM vehicle, designated as the LTA-11. It consisted of the LTA-3 ascent stage mated to the LTA-11 descent stage. In addition to it being structurally complete, most major mass items and systems were either mass-represented or inert production units. This vehicle had been used in several LM structural test programs, including the May 1970 series of drop tests.

The test article was installed in a structural steel frame that provided the hoist and support points required to position the vehicle, as well as the points necessary to install the suspension system. The vehicle was supported at each outrigger apex fitting by a hydraulic actuator and an air spring arranged in tandem. The actuators were used to provide for vertical positioning while the air springs simulated the "free-free" state.

The impulses were generated using an electrodynamic shaker (Ling Model 335), programmed through an Exact Waveform Synthesizer, to drive an impact head into a striker plate mounted at the impact point on the vehicle. Both the impact head and the striker plate were fabricated from a cemented tungsten carbide alloy; this high modulus of elasticity material had been used with success in previous testing. A Kistler 905A force transducer, mounted in the impact head, was used to measure the applied pulse.

Schematic representations of the test set-up and impulse generating and monitoring systems are shown in Figures 3-1 and 3-2.

Impulses were applied to the freely suspended vehicle at each of the apex fittings and at the points where gear components are attached to the deployment trusses. At each point, 3 mutually perpendicular pulses were applied. Thus,

the vehicle was excited by 36, individually applied impulsive loads. Sample time histories of these impulses along with sample responses are shown in Appendix D.

Vehicle responses, both strain and acceleration, were measured close to and remote from the points of load application. Forty strain gage measurements were selected from those used in the LM qualification drop test program based on their response to the various drop test conditions. Twenty-eight accelerometers were selected from those used in the LTA-11 mode survey for their usefulness in identifying the 5 lowest modes of vibration of the LM in the landing configuration.

A detailed list of this instrumentation is presented in Appendix B.

Response of all the instrumentation to an applied pulse was recorded on magnetic tape and played back immediately on an oscillograph. These oscillograph records were inspected to insure that all channels were operational and that response did not exceed the range assigned to it. In addition to the responses, the time history of the applied pulse was also recorded on analog magnetic tape. Permanent oscillograph playbacks were made at a later time to further insure the validity of the data taken. The original tapes collected during the test program, provided the basic data for the effort of the present contract.

Volume II of this report discusses data processing in some detail, so discussion here will be brief. The original test tapes store the recorded responses to an impulse, the impulse time history, as well as some calibration information, all in analog form. The first step in data processing is to convert the analog information to a digital form. This analog-to-digital conversion was accomplished by the Grumman LM Data Reduction Station using a standard package. The tapes that result have been called Phase 1 digital tapes.

The next step in the processing involves mainly storing of the ITF data; the computer code that performs the operation is identified as Program I-ITF Program. It stores the ITF time histories, at a prescribed time interval, in

a disk pack on the IBM 370 and in a tape storage data bank on the Univac 1108. In addition to basic time history data, calibration information and applied impulse magnitudes are stored. Output options include listing and automatic plotting.

Response prediction using the stored ITF data is performed in the second program, Program II-Response Program. This code takes scale factor and time history data from the data bank and forcing function time histories as input data, and performs the Duhamel integration and the superposition discussed in the previous section of this report. Output is in both printed and plotted form.

Filtering of the ITF data to remove undesirable suspension system effects is performed in the Response Program. During the course of this contract several methods of performing digital filtering were explored. These included least-square curve fitting, steady state methods that are frequently employed for aircraft flight testing, and a Fourier Transform approach. The latter method appeared to perform the filtering most accurately and was therefore programmed. The approach consists of the following steps. First, each ITF is transformed from the time domain to the frequency domain using a Grumman developed Fast-Fourier Transform computer subroutine; both real and imaginary components are computed. Low frequencies are eliminated by setting terms that define the real and imaginary components at the low frequencies to zero. The truncated frequency domain transfer functions are transformed back into the time domain using the same computer subroutine. The revised time history responses are considered ITF's and are used as such in the Response Program. (It should be noted that for computation efficiency, the method programmed is somewhat different from that described above. However, the overall result is identical.) The effect of filtering is demonstrated in the section which follows along with the complete results of the correlation efforts.

It is interesting to note that for the data processing of this contract, a total of 4 hours of computer time was required by the ITF Program to store the 2400 ITF's, on the IBM disk pack. The predictions that were made using the Response Program required 5 minutes of computer time, for all 40 channels, including the filtering computations.

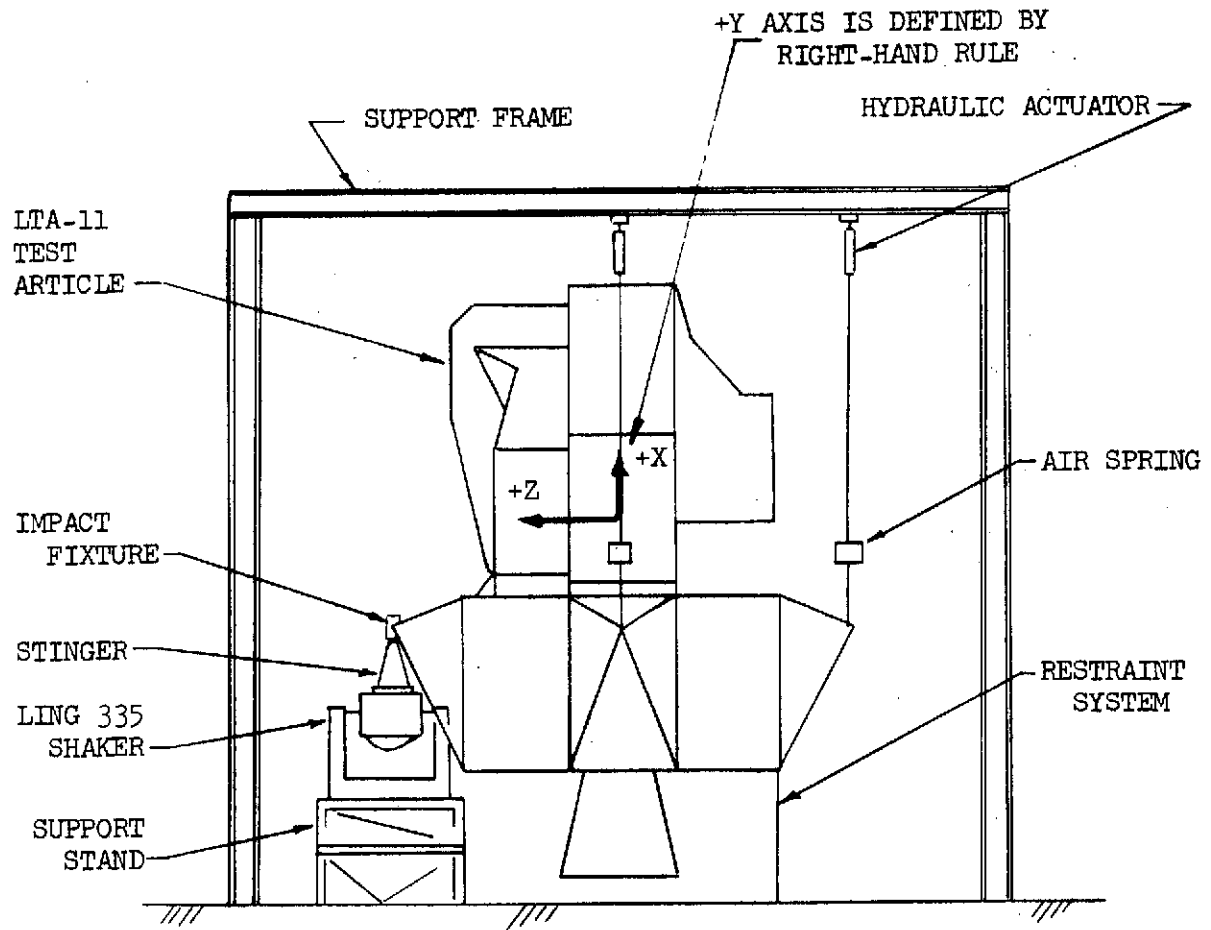


Figure 3-1 - Schematic Representation of the Impulse Test Set-Up

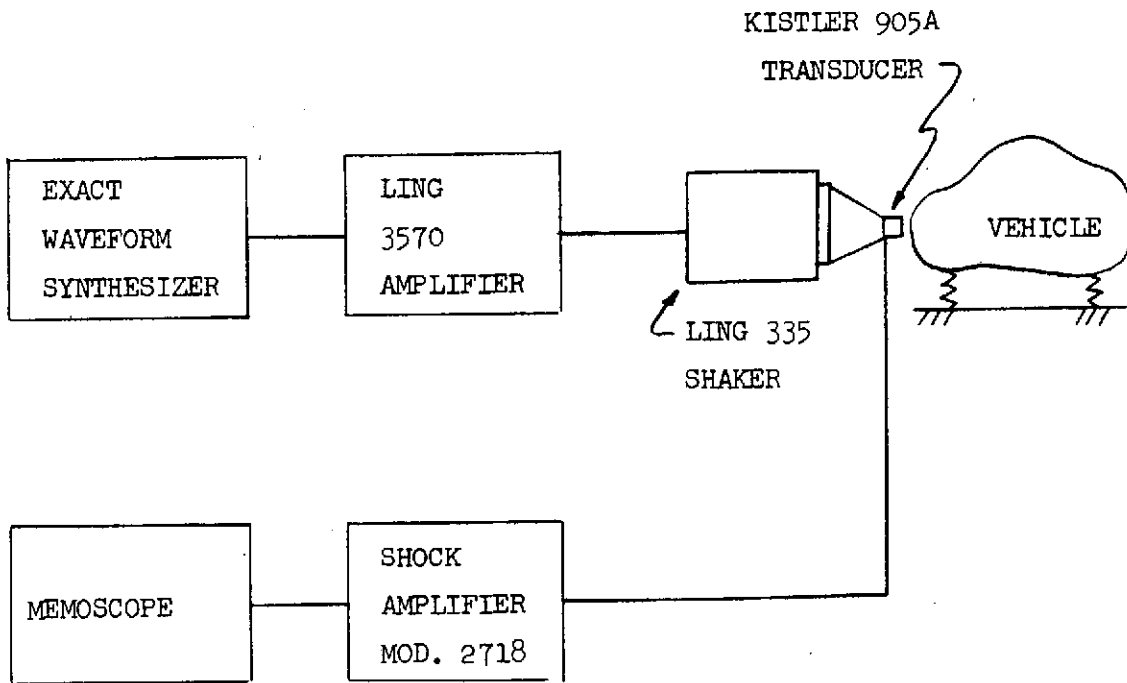


Figure 3-2 - Equipment for Generating and Monitoring Impulses

#### 4-RESULTS

The correlation effort of this contract consisted of two parts. The first, and most important, was a study into the accuracy of predicting transient response using the IITF method. The second involved a study into the feasibility of using IITF data to predict modal information. Data for the LTA-11 was used in these studies.

For the transient response study, results predicted from IITF's are compared with those obtained from drop testing (Section 4a) and those computed using traditional modal analysis methods, (Section 4b). Modal data derived from the IITF's are discussed in Reference 2 and 3 and in Section 4c.

The drop test selected for study was a level landing where all four footpads impact horizontal platforms designed to restrain the pads against in-plane motion. In this landing the primary rigid body acceleration of the vehicle is in the vertical direction. Translational acceleration in other directions, and rotational accelerations of the vehicle are small and only arise because of slight differences in the load-stroke characteristics of the landing gear energy absorbing devices, and asymmetries in the vehicle's mass distribution.

Figure 4-1 illustrates the forcing functions applied to the vehicle in the drop test. These forces were computed from measurements recorded during drop testing in the following manner. For the drop tests, each member of the outrigger trusses and each member of the deployment trusses was instrumented to record axial force. After the test, the member forces were resolved and summed into X, Y, and Z components at each of the points where a landing gear member attaches to the basic structure. These processed time histories are illustrated in Figure 4-1. Note, that of the 36 possible applied forces only 24 are shown; the remainder are very close to zero due to the nature of the landing condition. For example, since the landing induces only vertical

rigid body acceleration and each gear is loading the structure in an identical manner, there are only two non-zero forces at each apex fitting. These are a vertical component of load and a horizontal component directed toward the center of the vehicle. At the deployment truss connection points, only horizontal forces exist since in this drop test the secondary struts were almost parallel to the horizontal plane. Thus a total of 12 loads (4 from the apex fittings and 8 from the deployment trusses) are taken as zero.

Before proceeding to a complete discussion of the correlation study, some results that illustrate the effect Fourier Transform filtering are in order. Figure 4-2 shows a sample of these results for two channels of data. Drop test time history responses are shown dashed while unfiltered predictions using ITF data are shown as dashed-dot curves. Predictions, where the ITF's were filtered to remove components below 1.6, 3.2 and 5.2 Hz using the Fourier method, are also shown. From this sample and from results on additional channels, it became evident that removing frequency content below 3.2 or 5.2 Hz yielded results that correlated reasonably well with the drop test. Since no firm data existed on the frequencies that were actually introduced by the suspension and since 5.2 Hz was below the lowest LM elastic frequency, this value was used in the filtering that was employed in all the correlation work described subsequently.

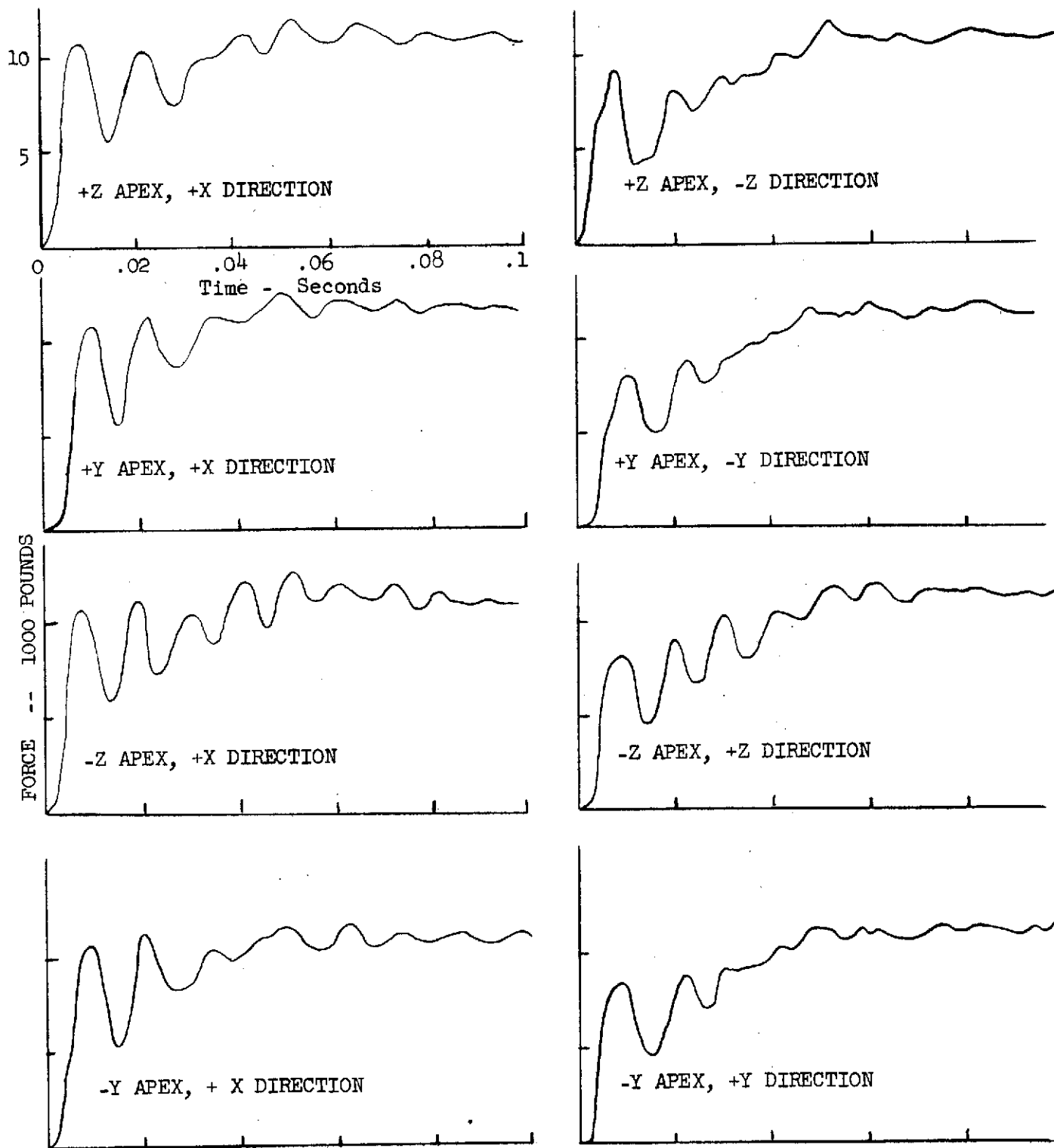


Figure 4-1a - Forces Applied to Outrigger Truss Apex Fittings From Drop Test  
Used in Correlation Study

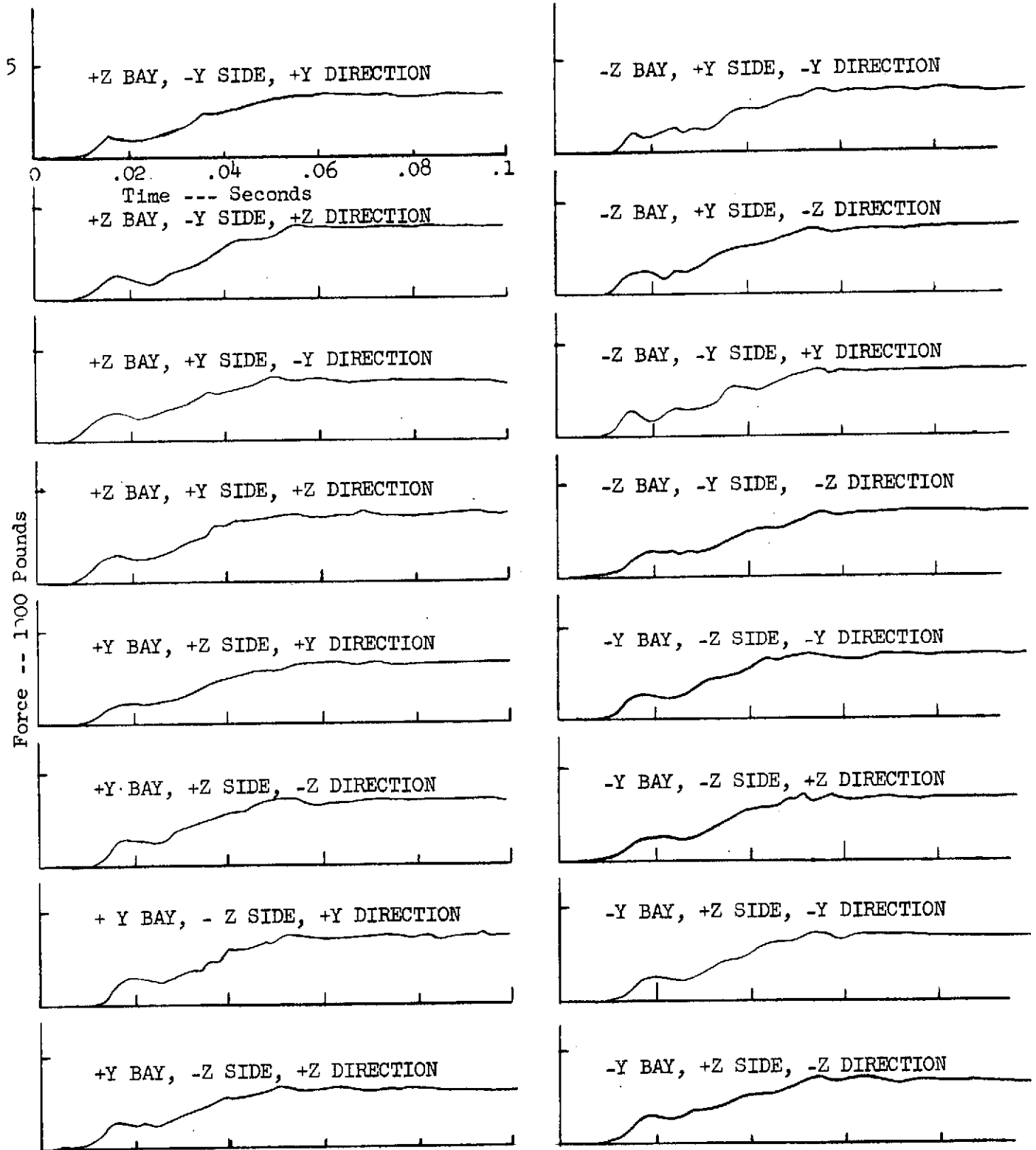


Figure 4-1b - Forces Applied to Deployment Trusses From Drop Test Used in the Correlation Study

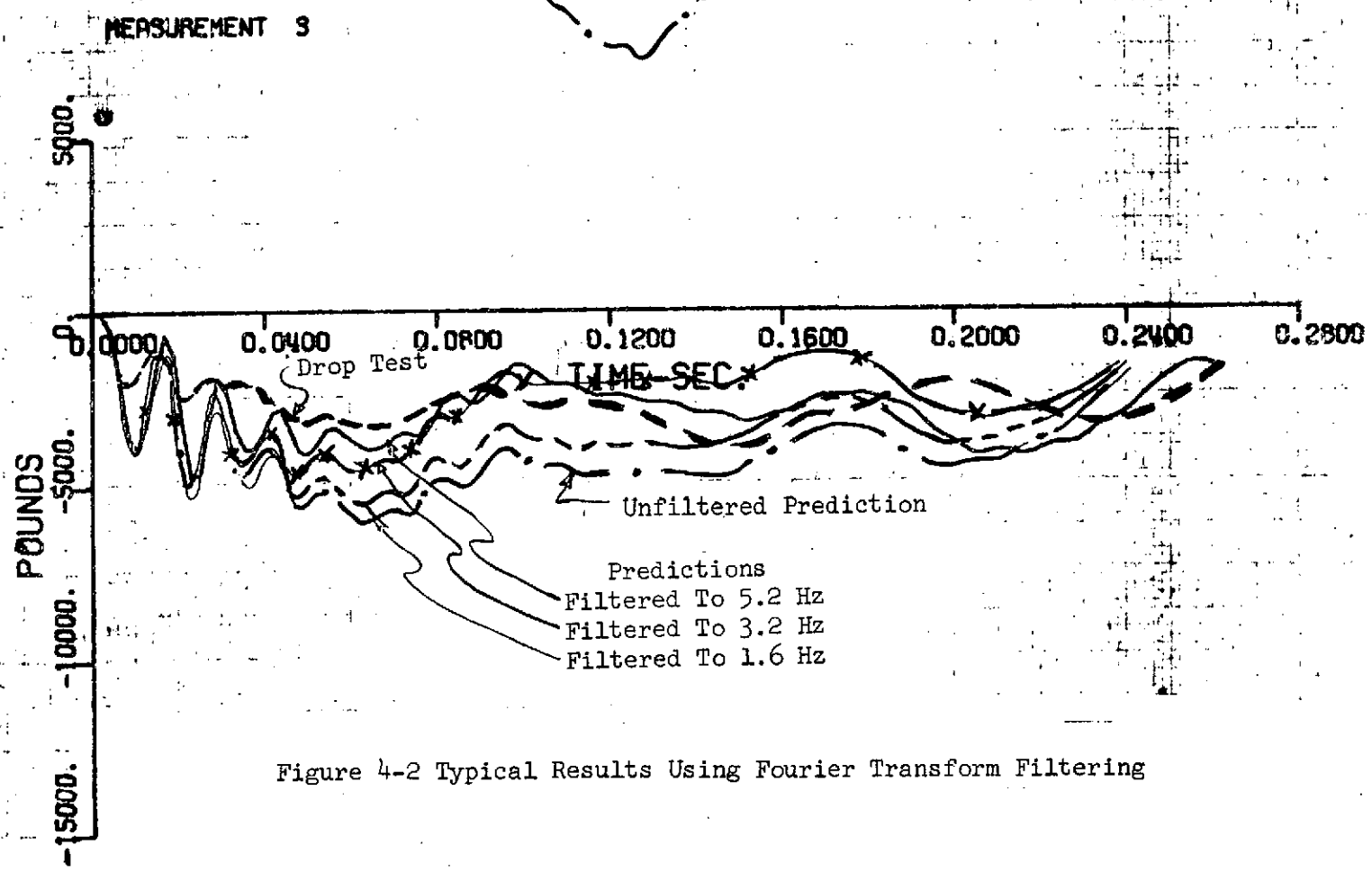
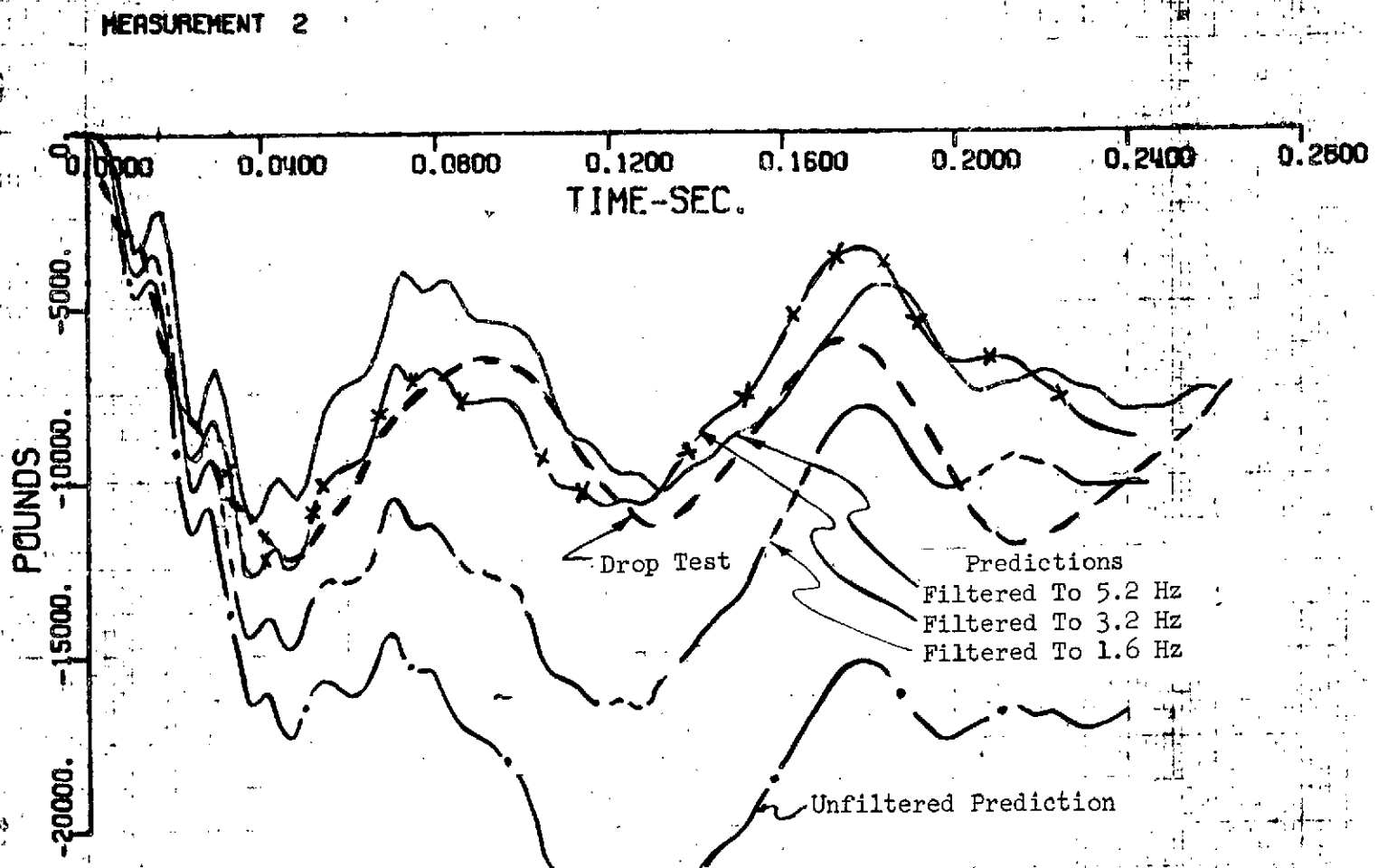


Figure 4-2 Typical Results Using Fourier Transform Filtering

#### 4a - Comparison of Drop Test Results with Predictions Using ITF Data

All of the ITF predictions shown on the pages which follow were computed using the Grumman data processing system with Fourier Transform filtering. A comparison is shown for every response channel that was common to the drop test and to the ITF testing. Responses include strains, both axial and shear, as well as accelerations and forces. Measurements indicated by number on the graphs are further described in Appendix B. In the plots, the drop test result is shown dashed while the ITF prediction is shown as a solid curve. Each curve is annotated with remarks; explanations for discrepancies are given when appropriate.

The following thoughts are offered to aid the reader in reviewing the results:

- Measurements which should display similar time histories due to structural symmetry are so marked. It should be noted that the ITF method as applied in this study, does not take advantage of any symmetry consideration; each prediction is made independent of any other.
- When an explanation for an inaccurate result is given, checks were made into the raw data in an effort to justify the opinion stated. Since both the drop tests and the ITF tests were conducted anywhere from a year to two years prior to the correlation study, few firm conclusions could be reached. Thus, when a scale factor error was suspected, a review of the test engineer's records was made to insure that a transcription error was not made, but checks further than this were not possible.
- The results frequently indicate that the ITF method will accurately predict high frequency response. Consistently, however, the ITF prediction exhibits less damping than does the drop test result.

Grumman's conclusions on the accuracy indicated by these results, along with recommendations for improving results in a new project, are given in Section 6.

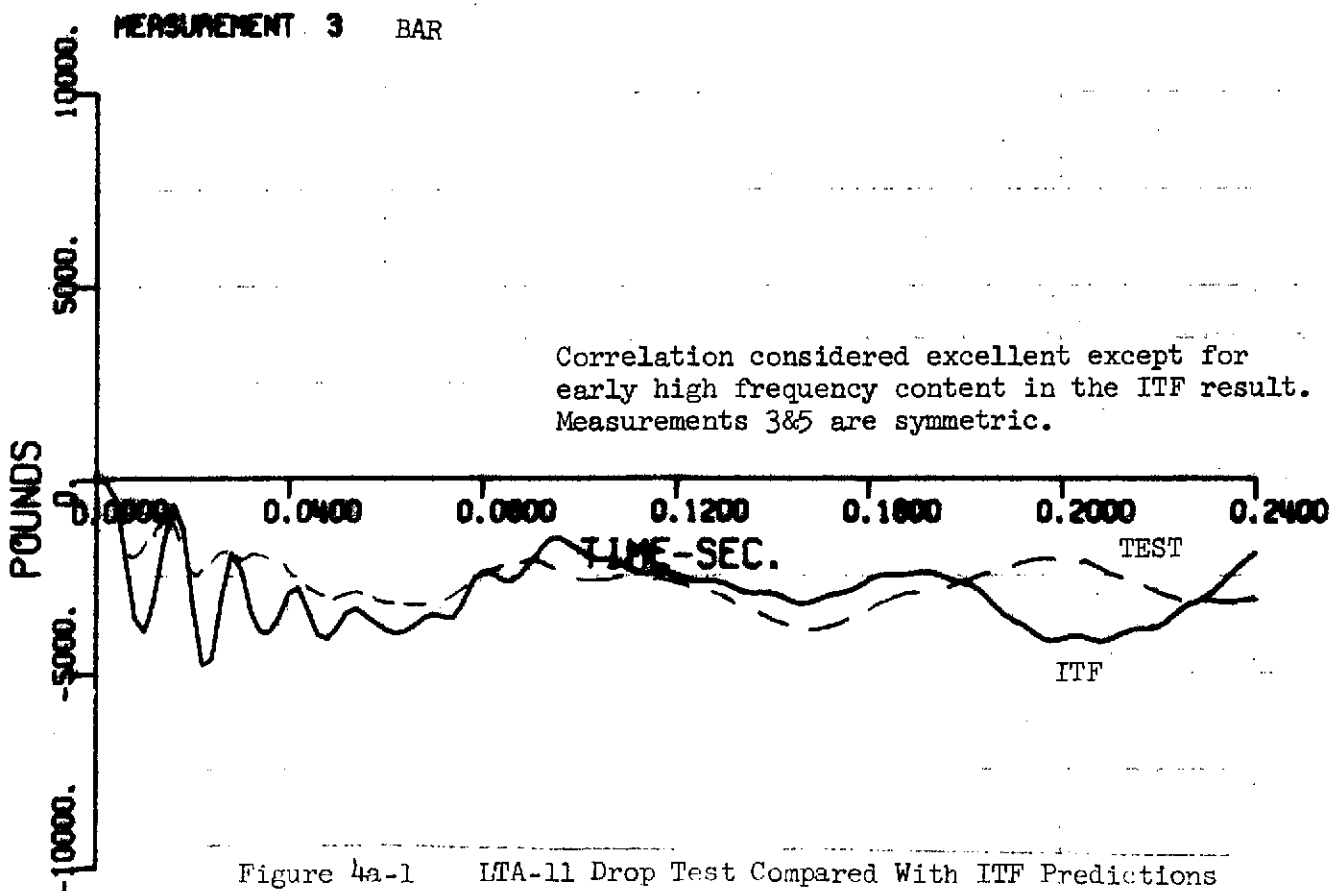
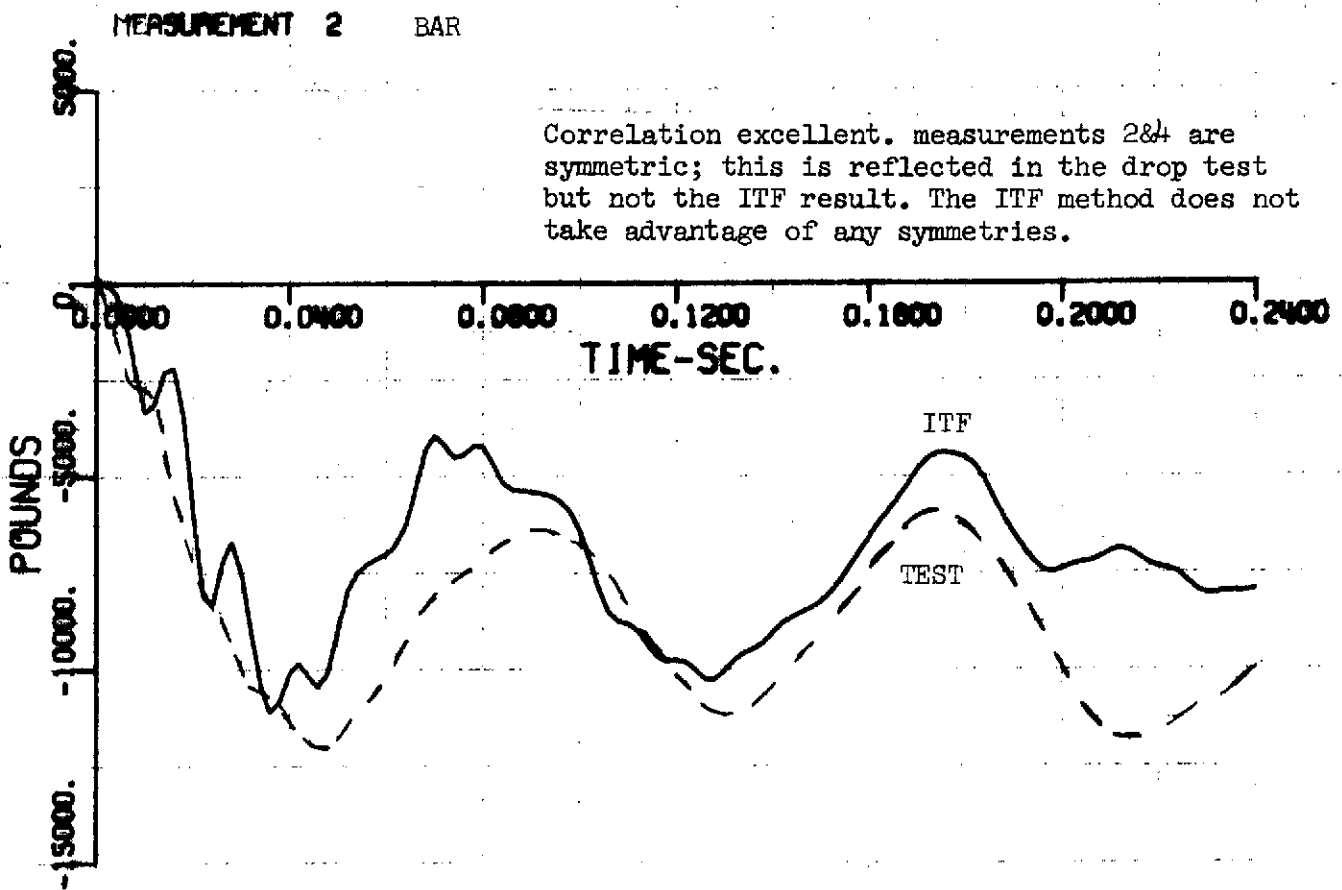


Figure 4a-1 LTA-11 Drop Test Compared With ITF Predictions

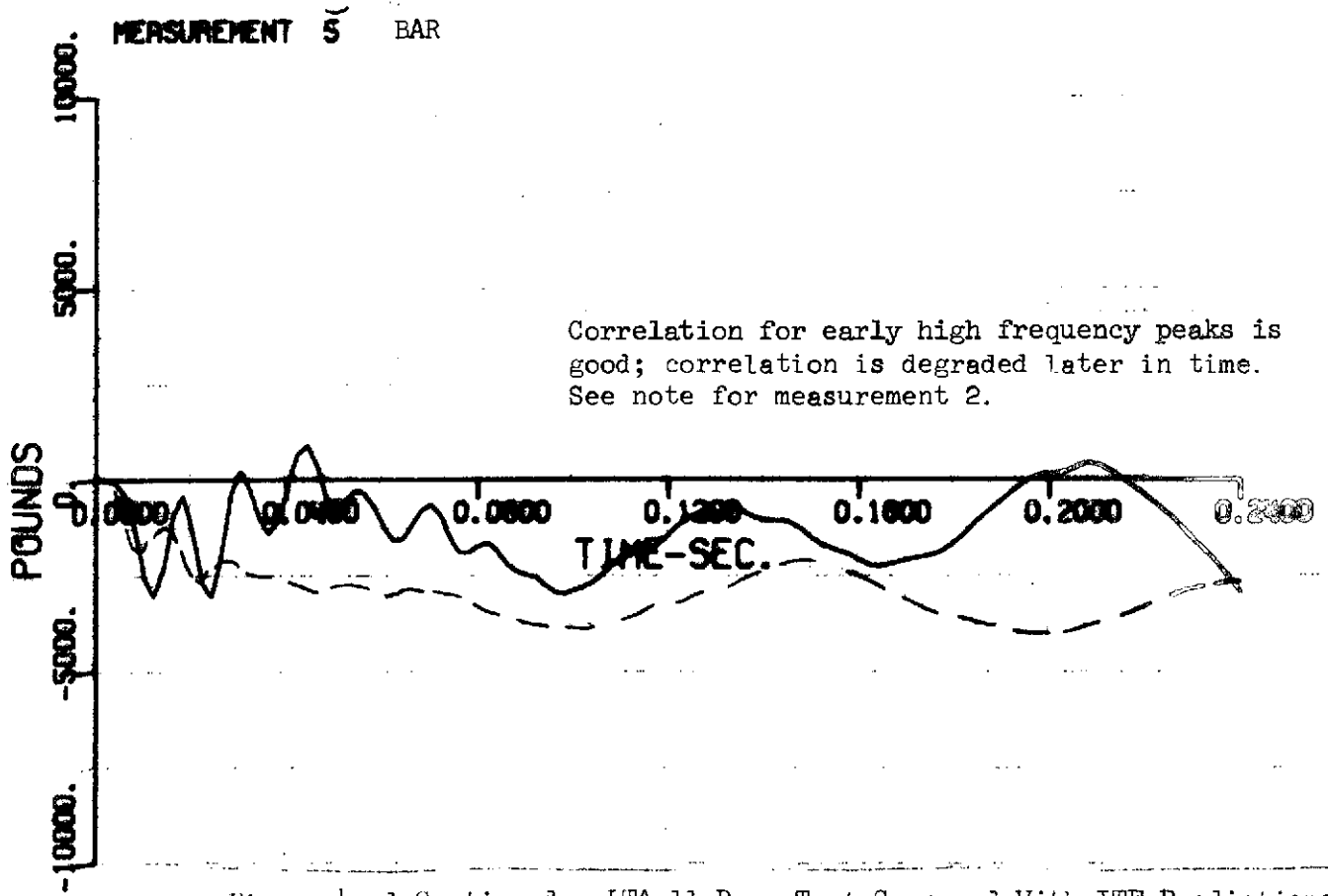
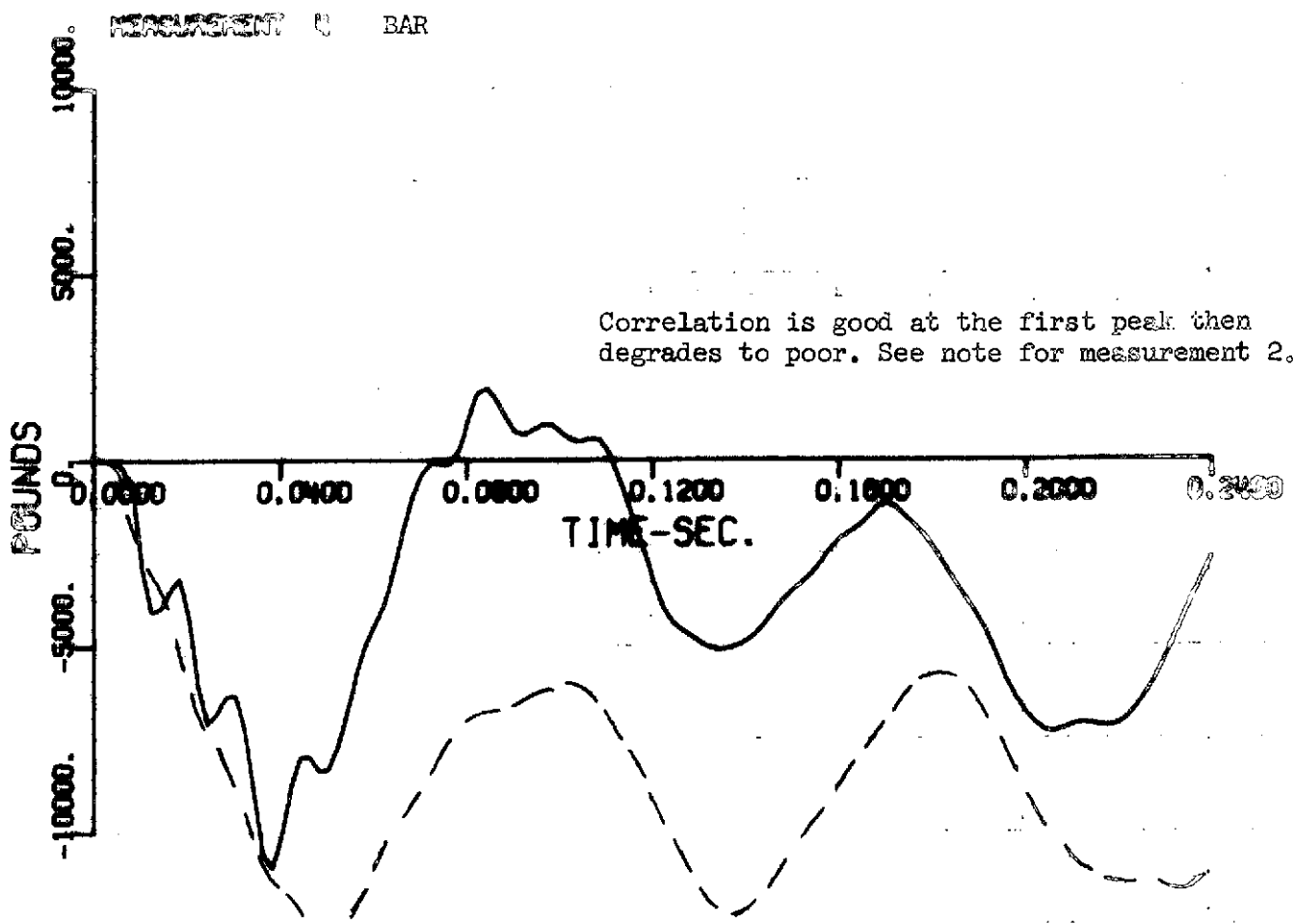


Figure 4a-1 Continued LFA-11 Drop Test Compared With ITF Predictions

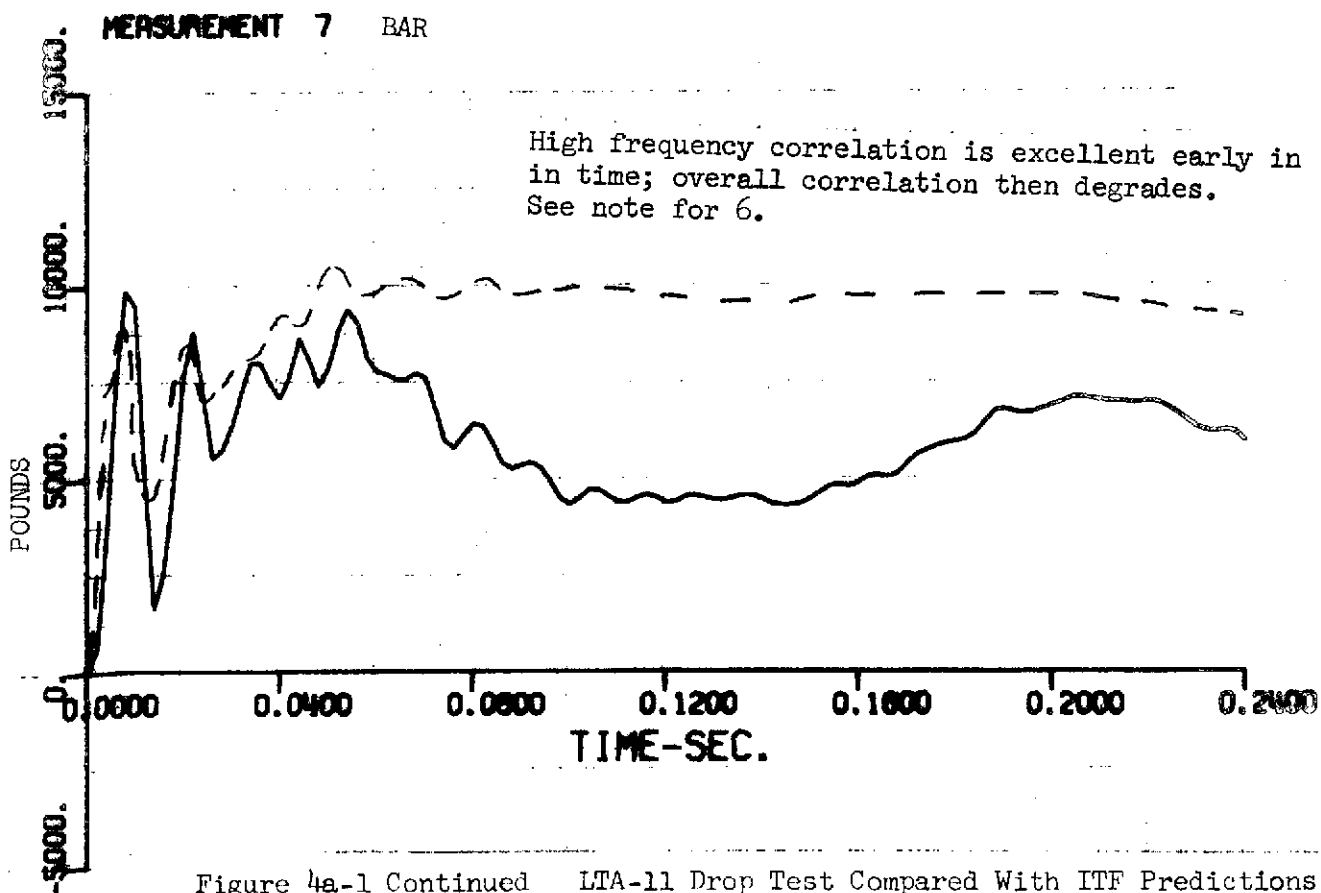
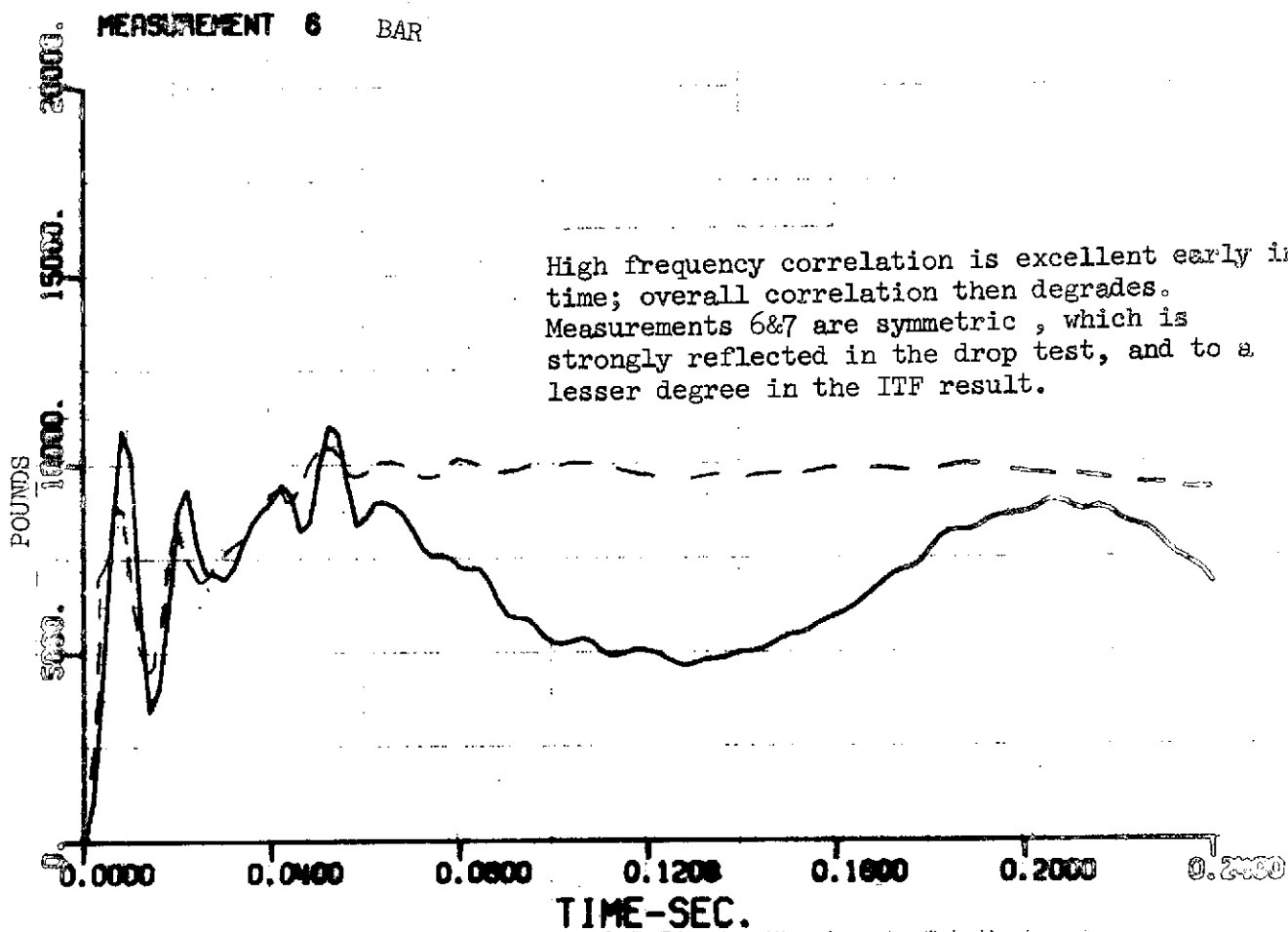


Figure 4a-1 Continued LTA-11 Drop Test Compared With ITF Predictions

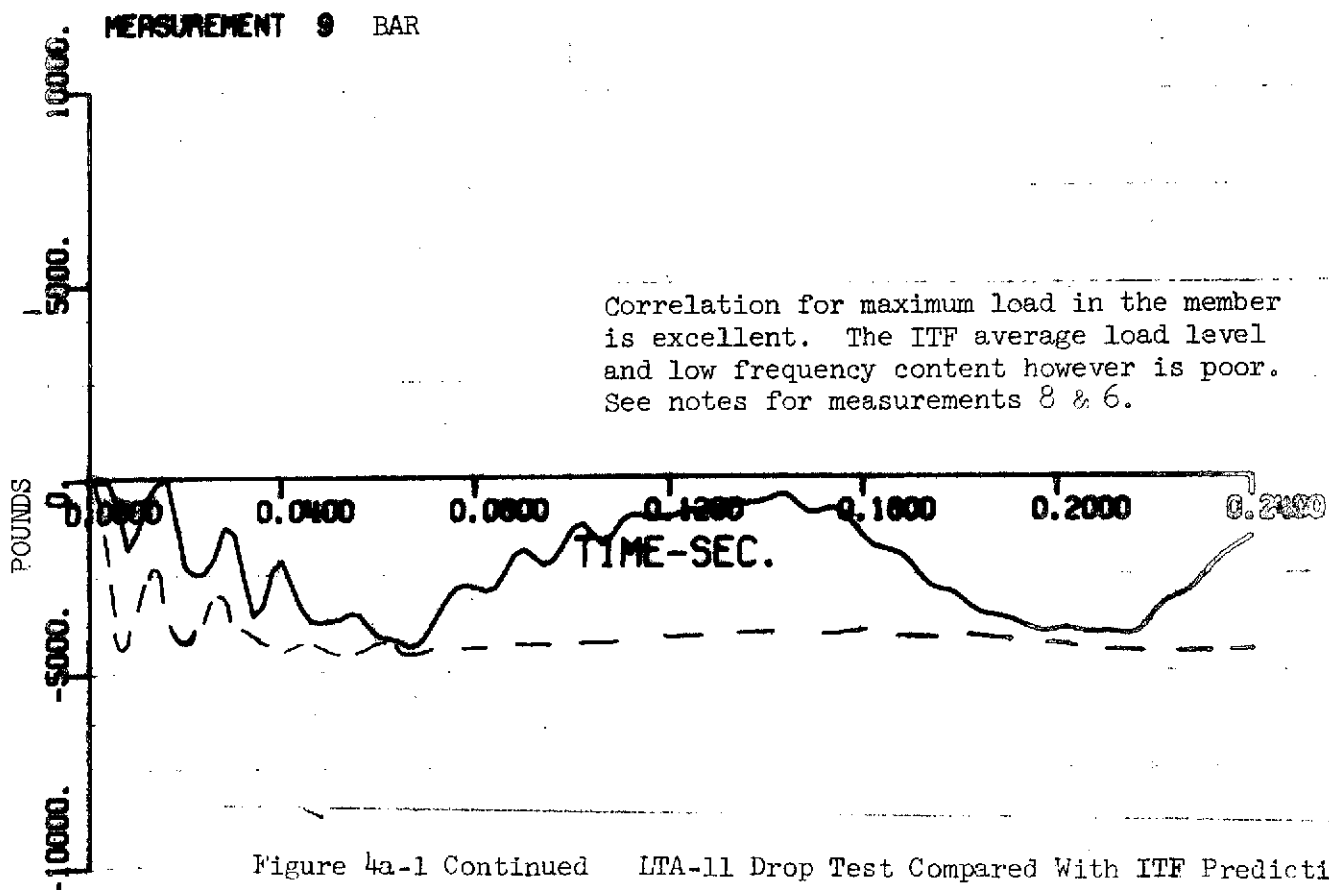
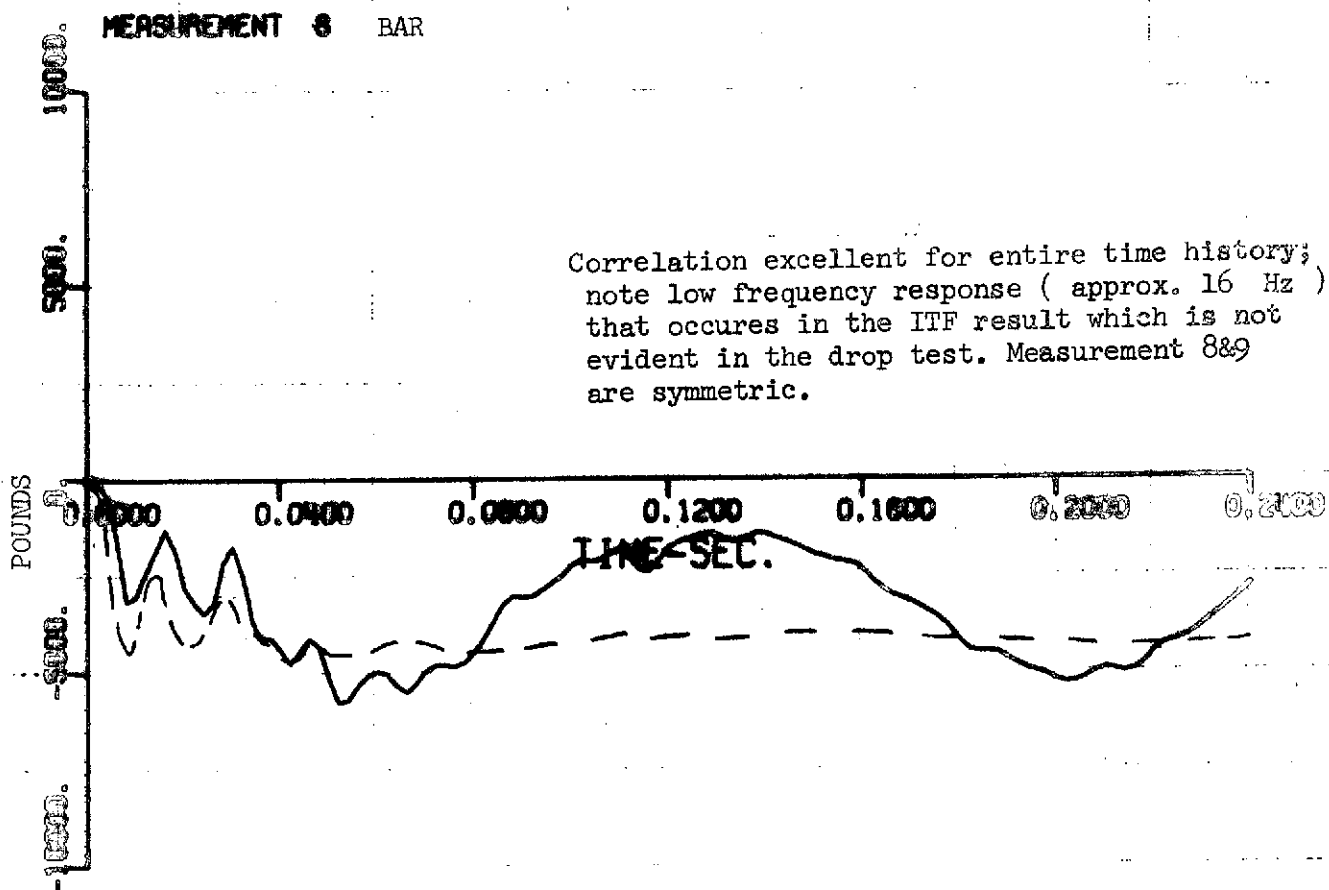
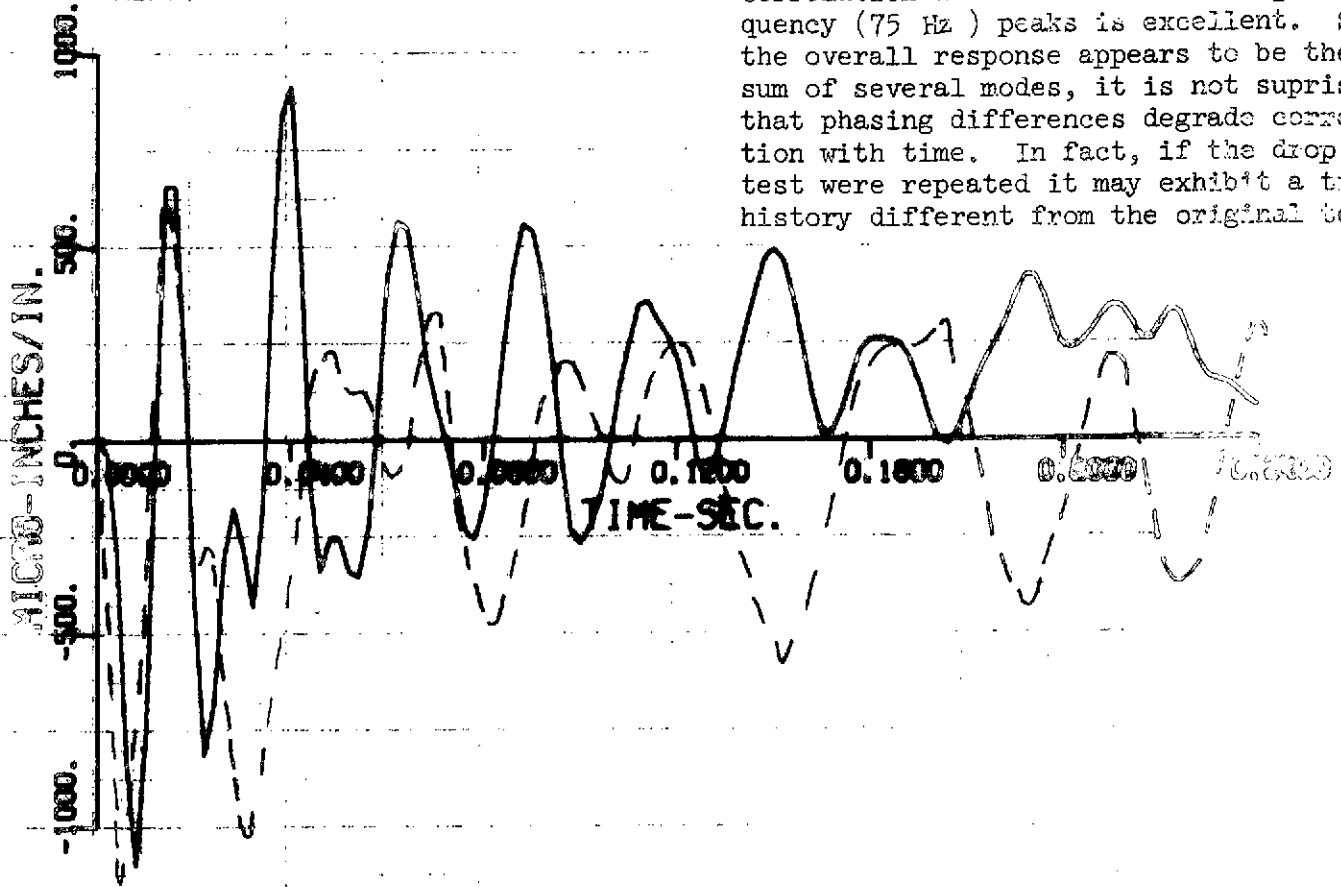


Figure 4a-1 Continued LTA-11 Drop Test Compared With ITF Predictions

MERSUREMENT 10 BAR-TENSION ONLY



MERSUREMENT 11 BAR-TENSION ONLY

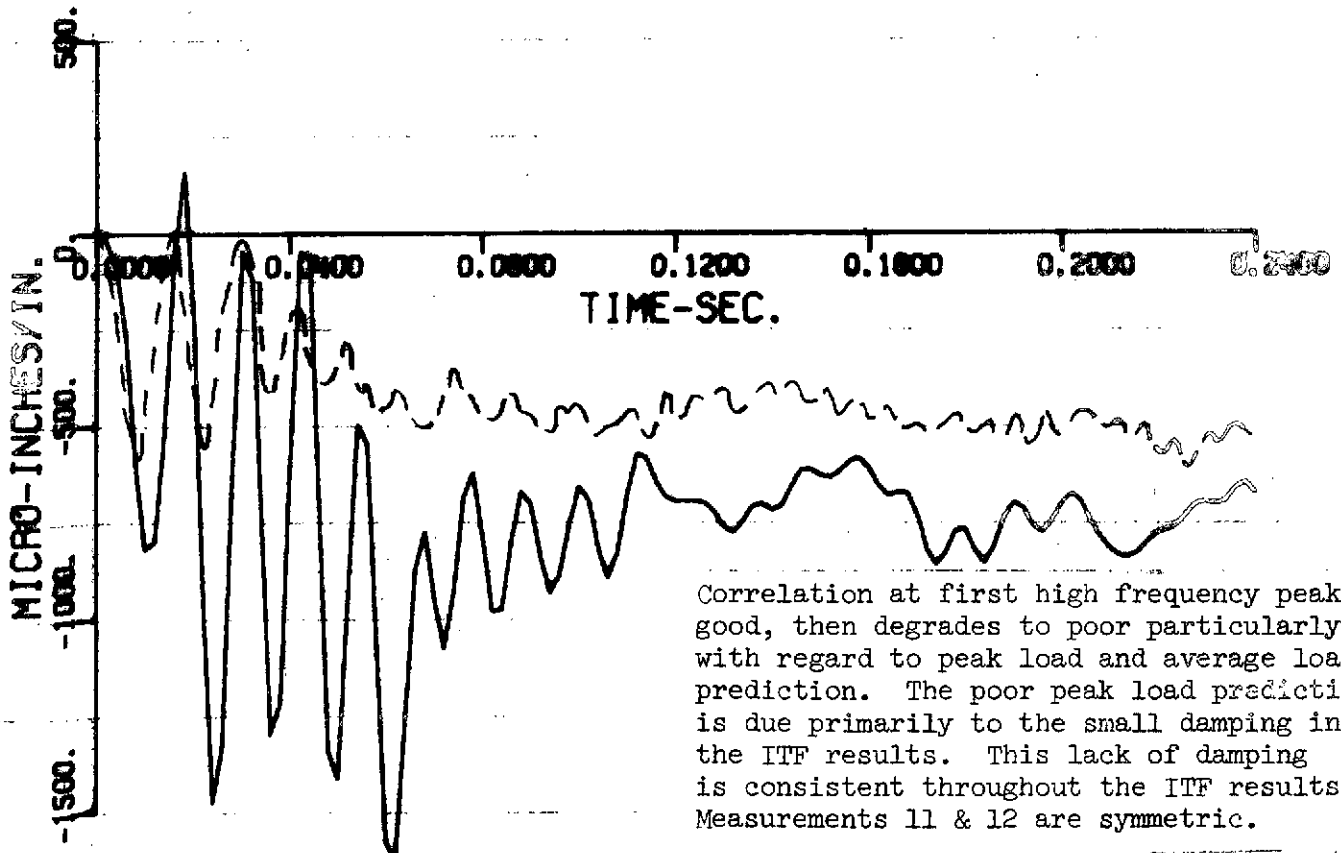


Figure 4a-1 Continued LTA-11 Drop Test Compared With ITF Predictions

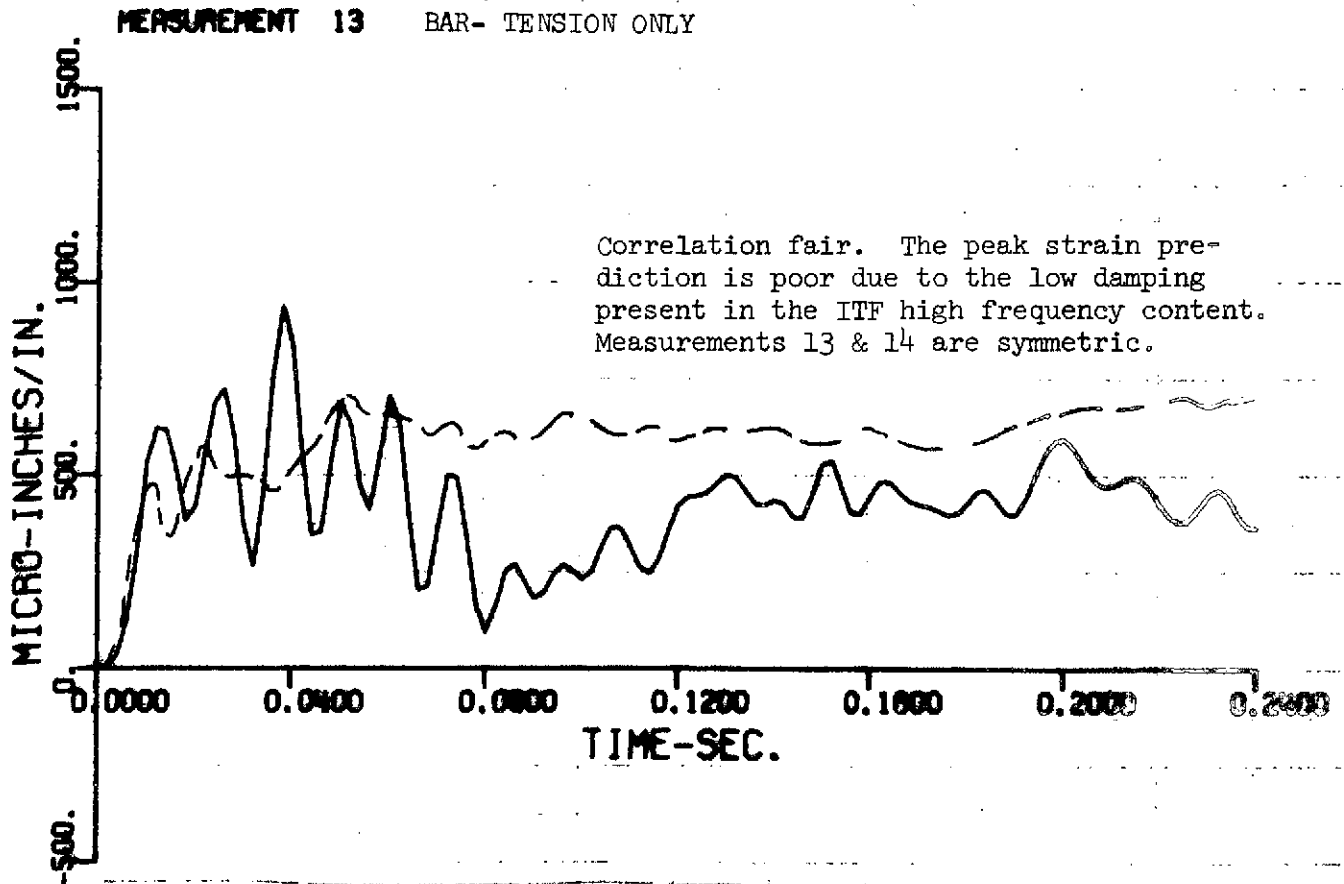
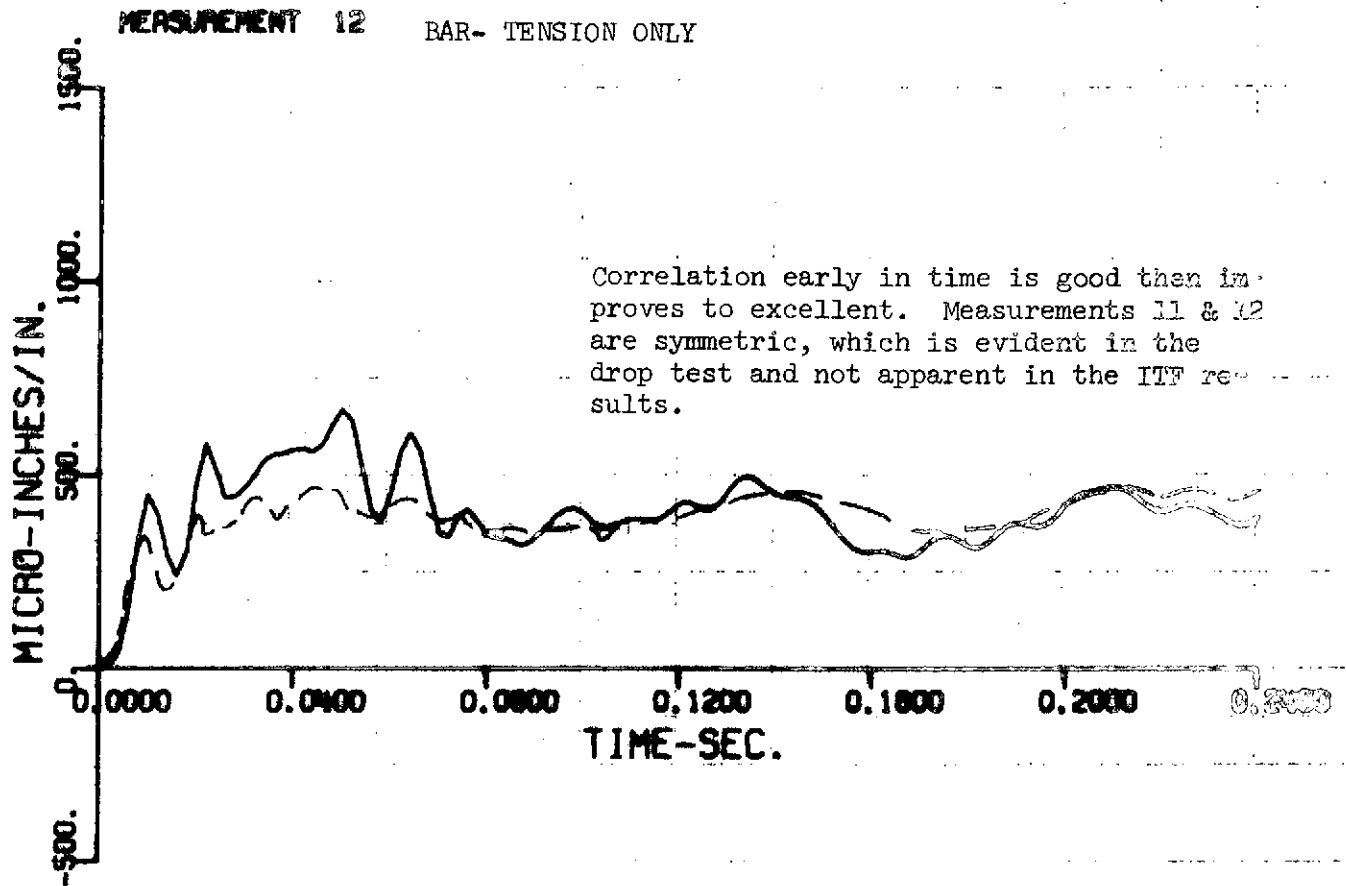
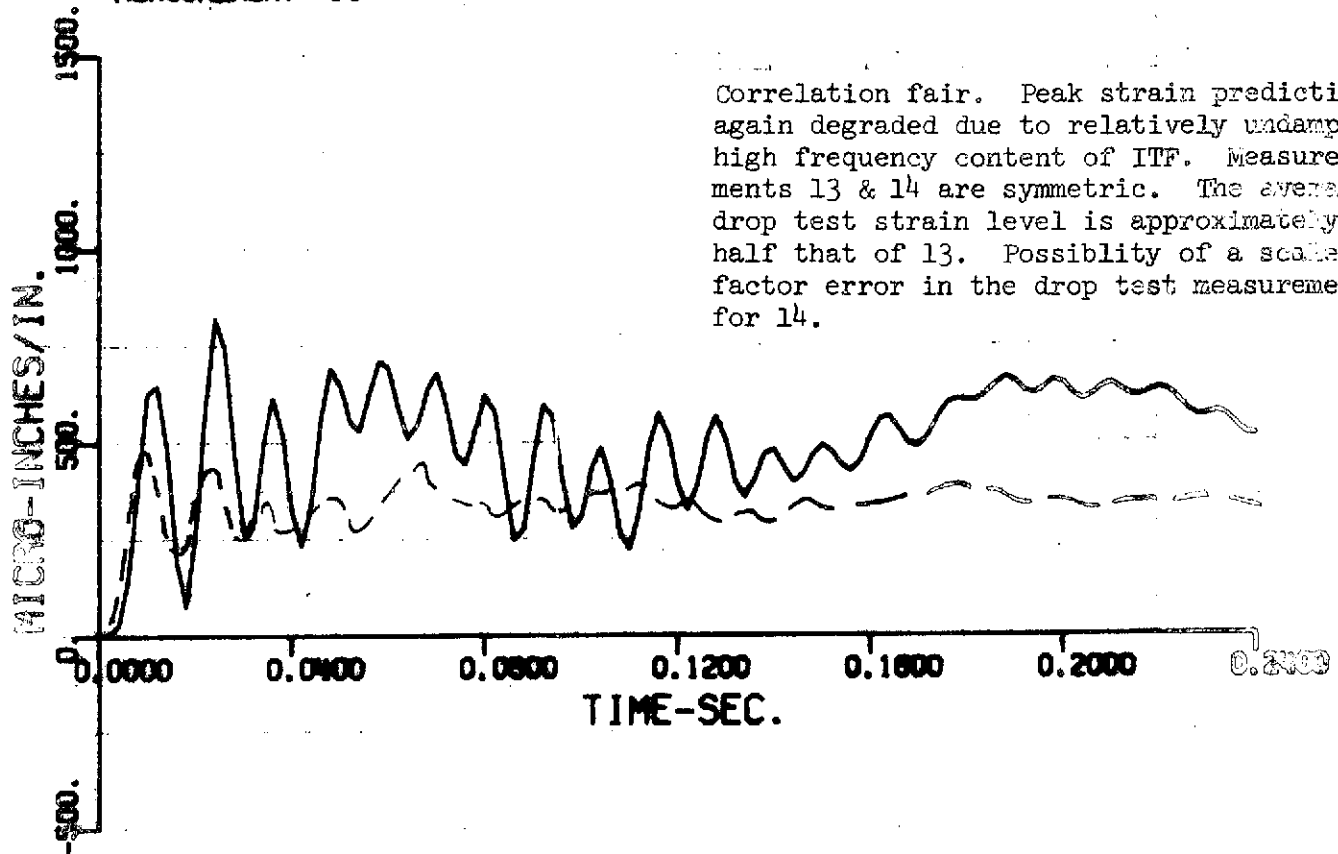


Figure 4a-1 Continued IMA-11 Drop Test Compared With ITF Predictions

## MEASUREMENT 14 BAR- TENSION ONLY



## MEASUREMENT 15 SHEAR PANEL - TENSION FIELD

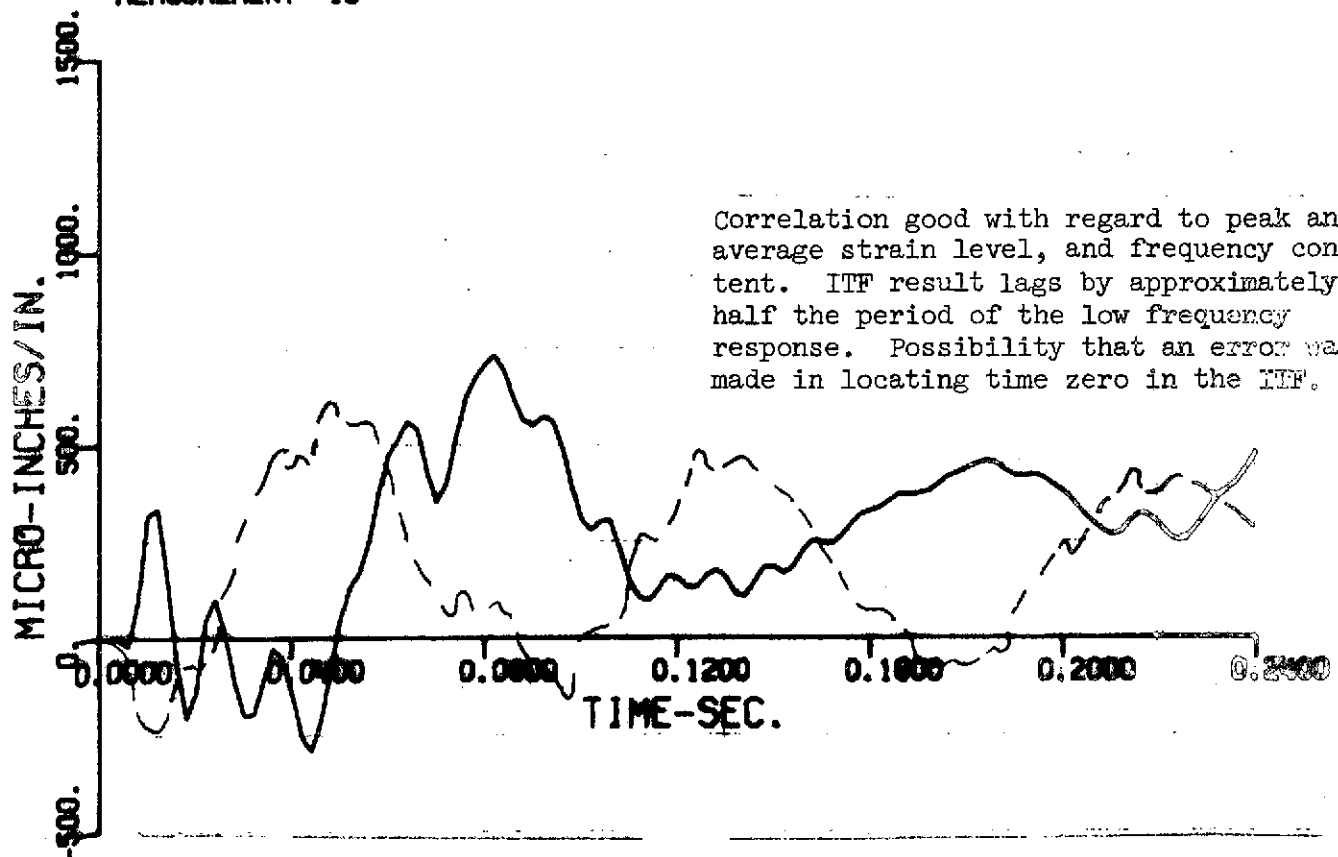
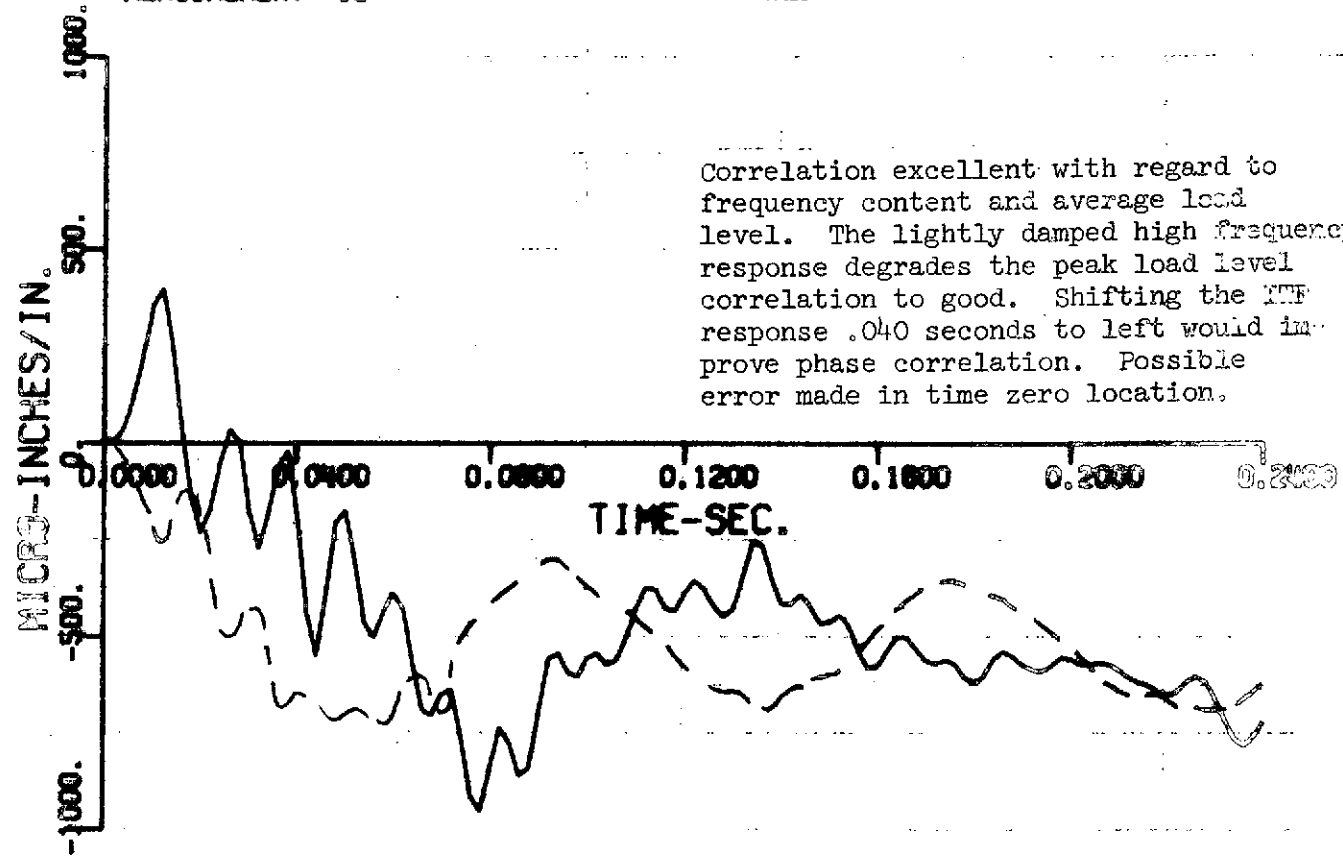


Figure 4a-1 Continued LTA-11 Drop Test Compared With ITF Predictions

MEASUREMENT 16 SHEAR PANEL- TENSION FIELD



MEASUREMENT 17 SHEAR PANEL- TENSION FIELD

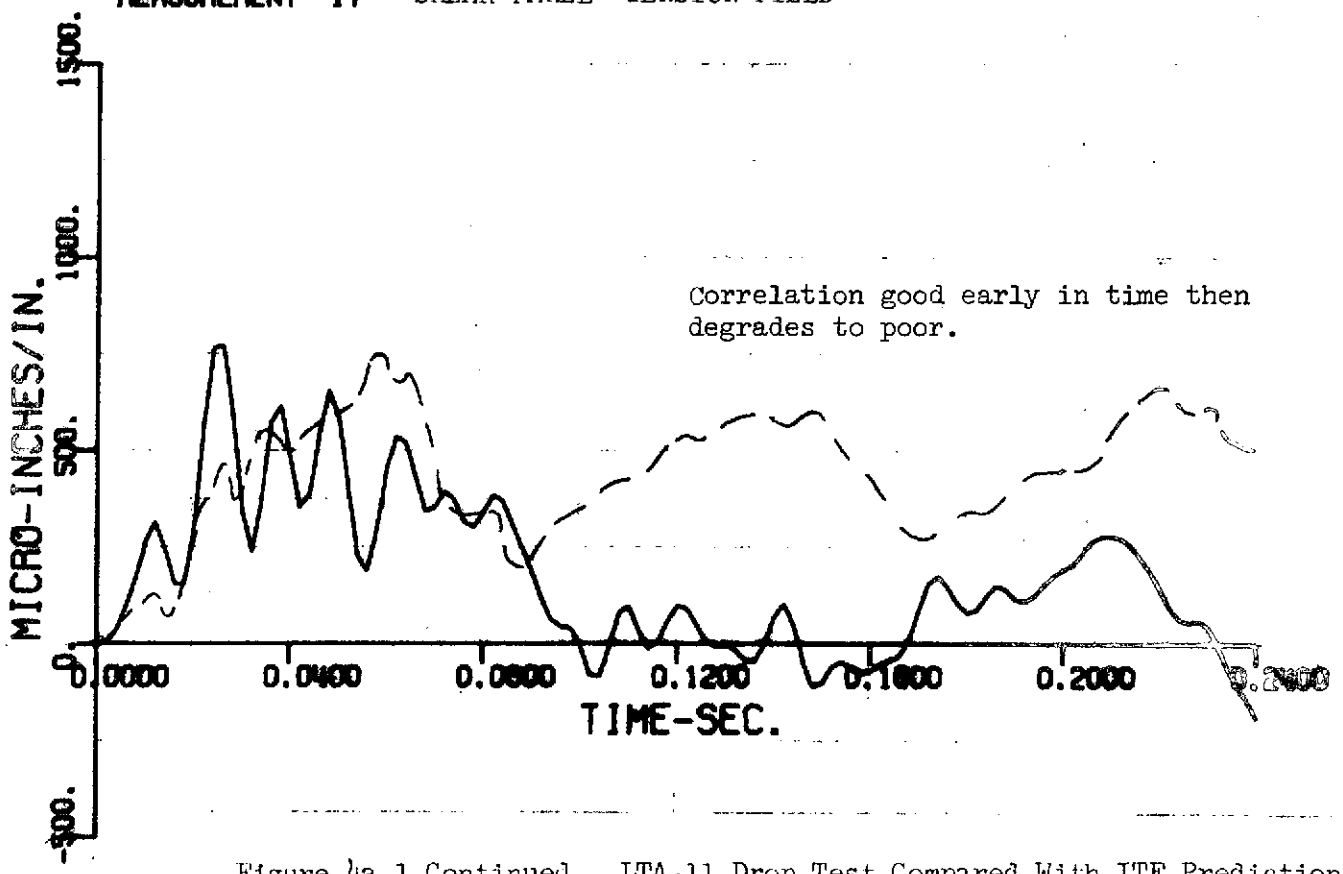
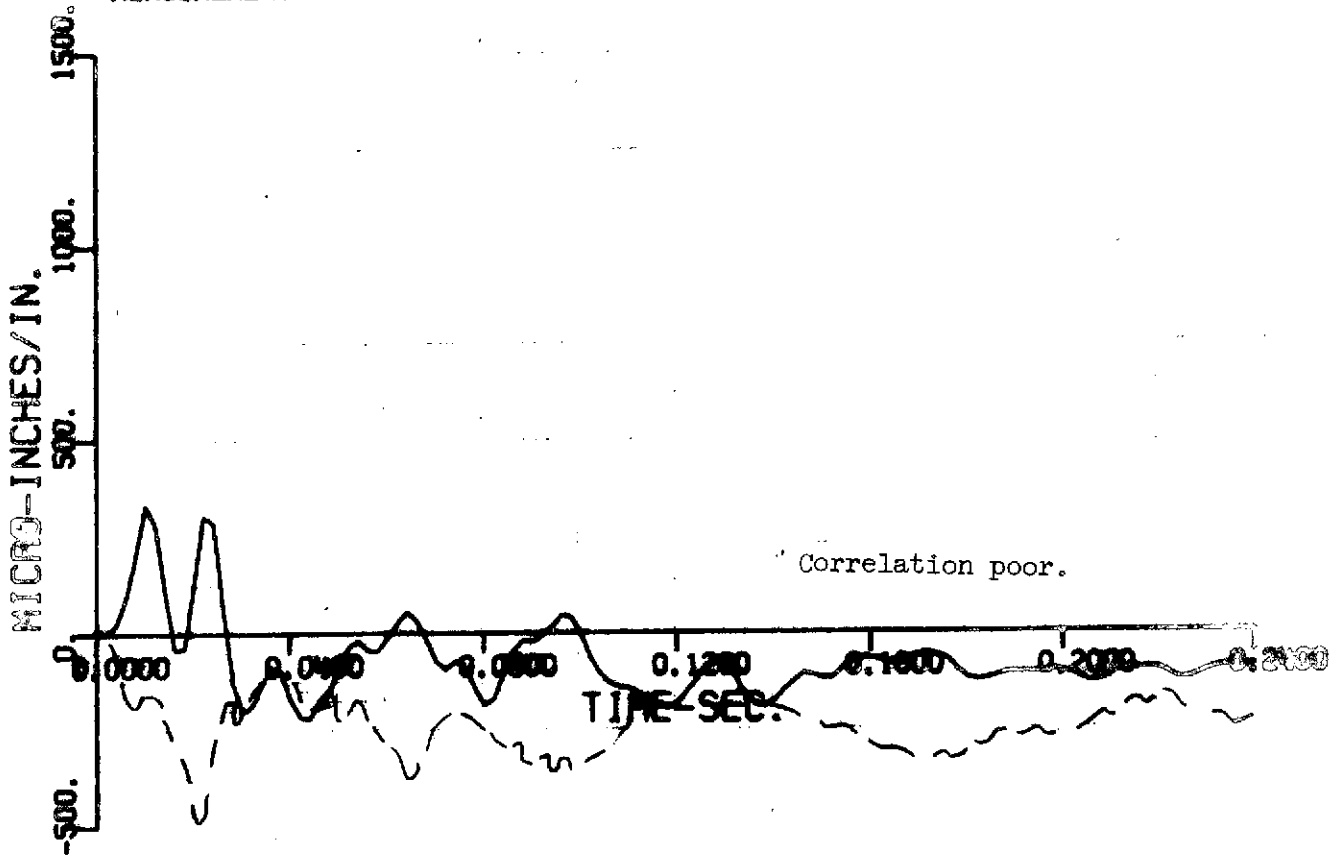


Figure 4a-1 Continued LTA-11 Drop Test Compared With ITF Predictions

## MEASUREMENT 18 SHEAR PANEL - TENSION FIELD



## MEASUREMENT 19 BAR

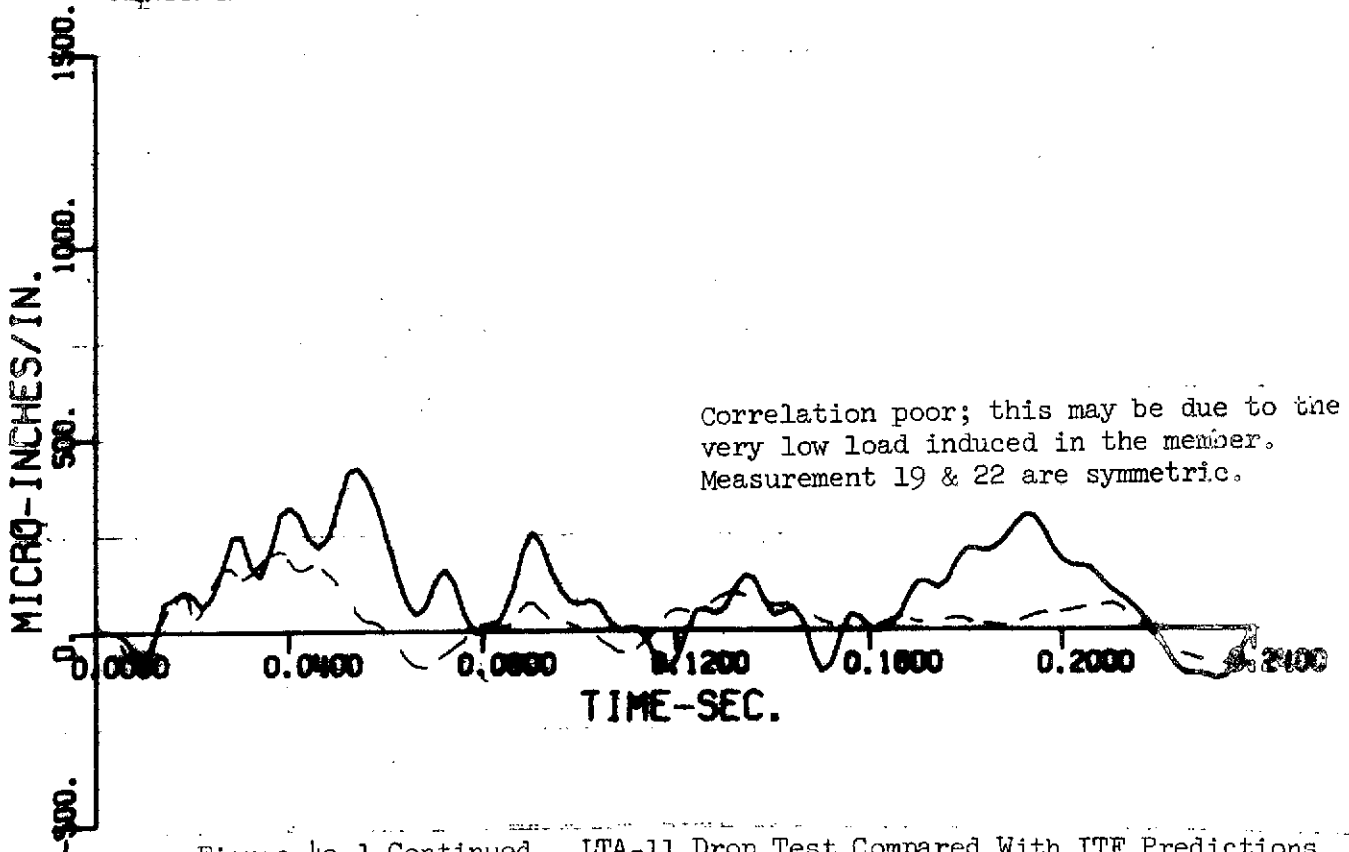


Figure 4a-1 Continued LTA-11 Drop Test Compared With ITF Predictions

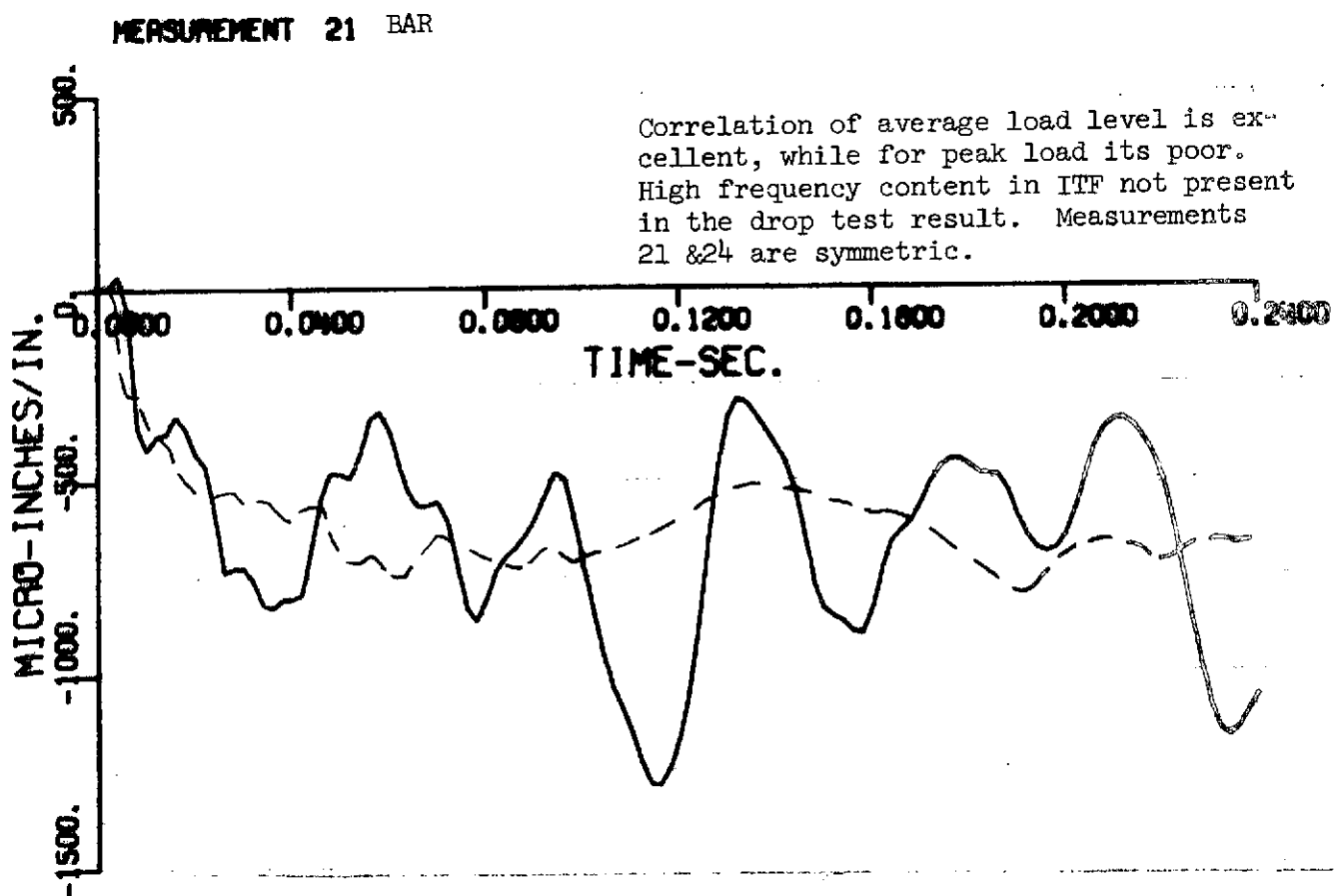
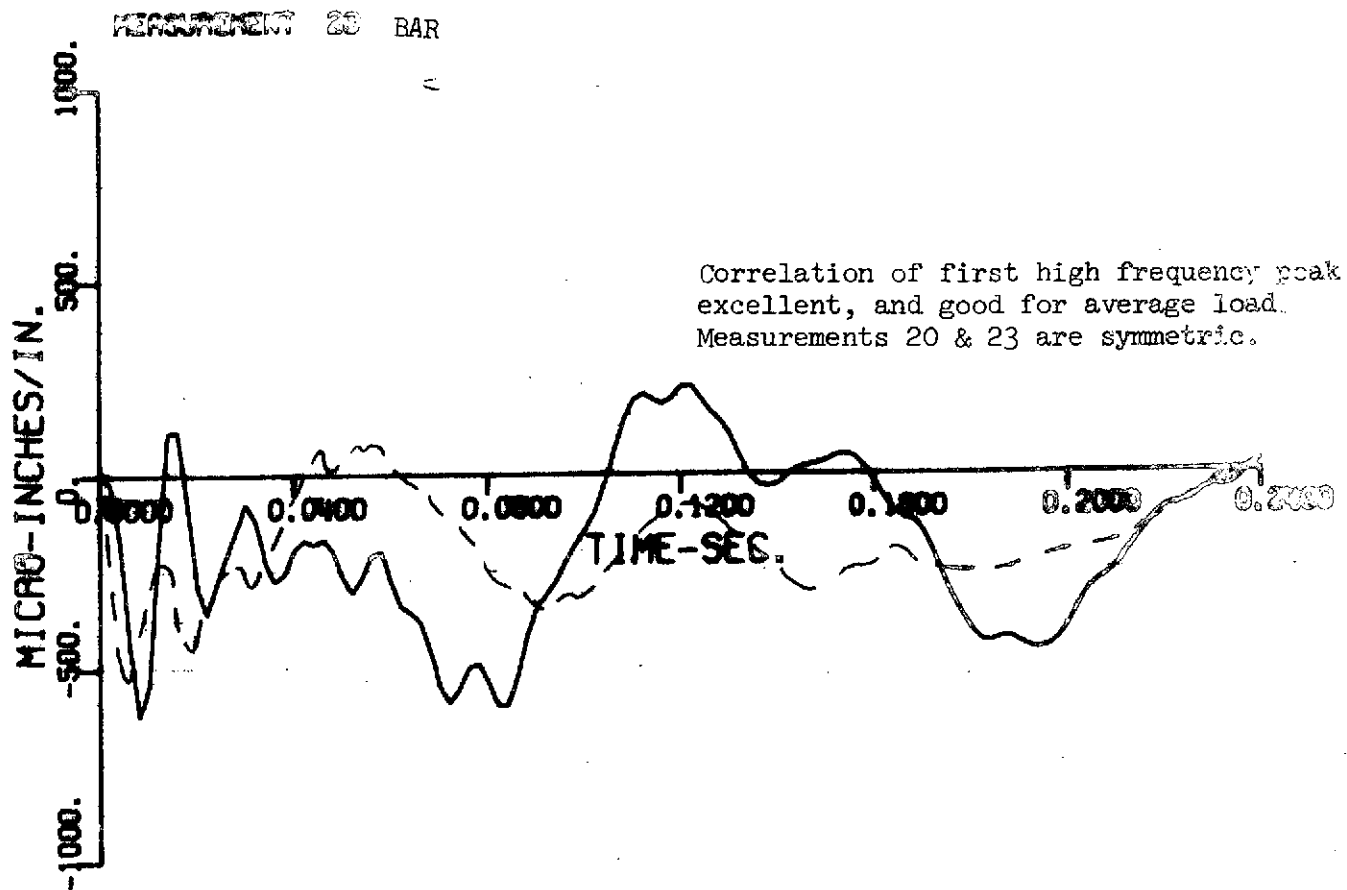
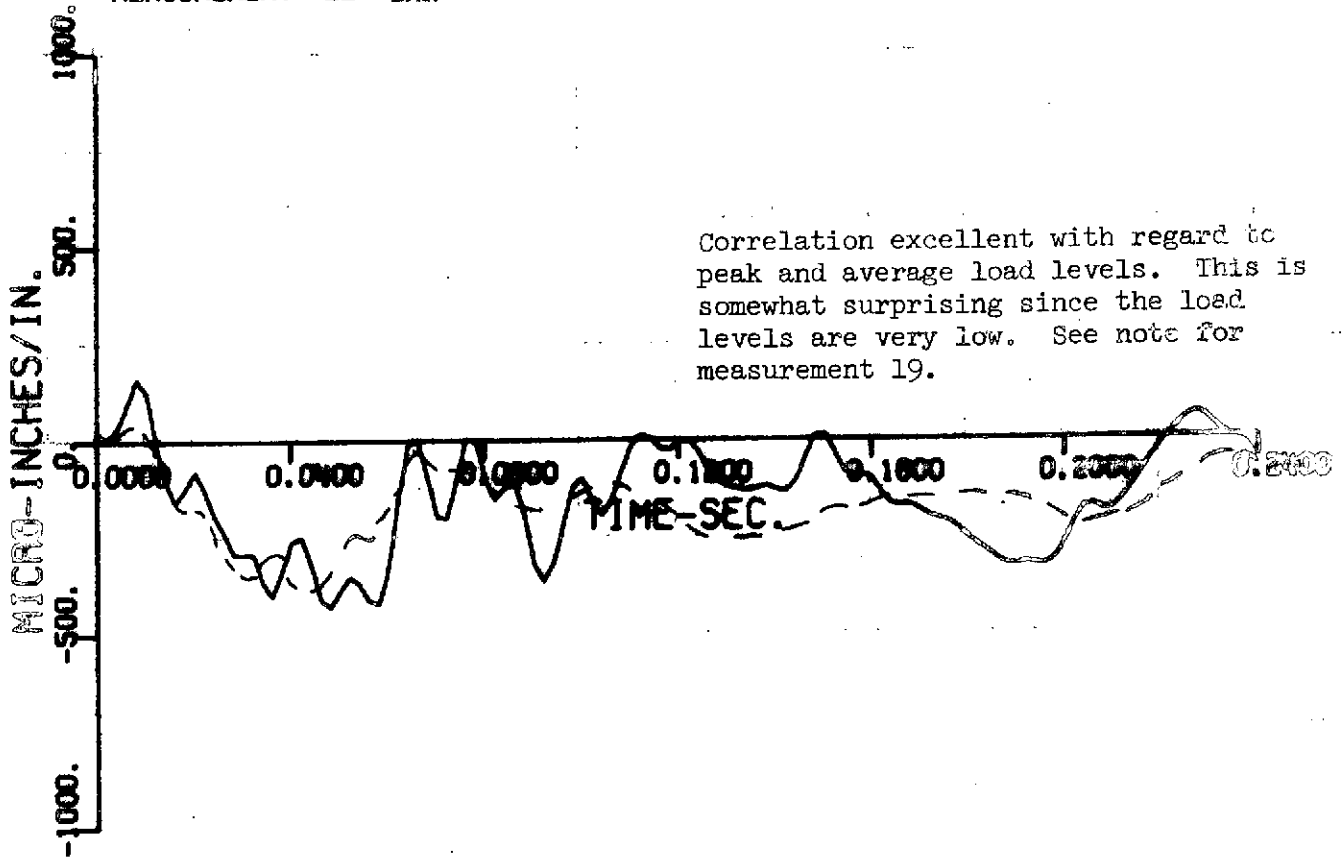


Figure 4a-1 Continued LTA-11 Drop Test Compared With ITF Predictions

## MEASUREMENT 22 BAR



## MEASUREMENT 23 BAR

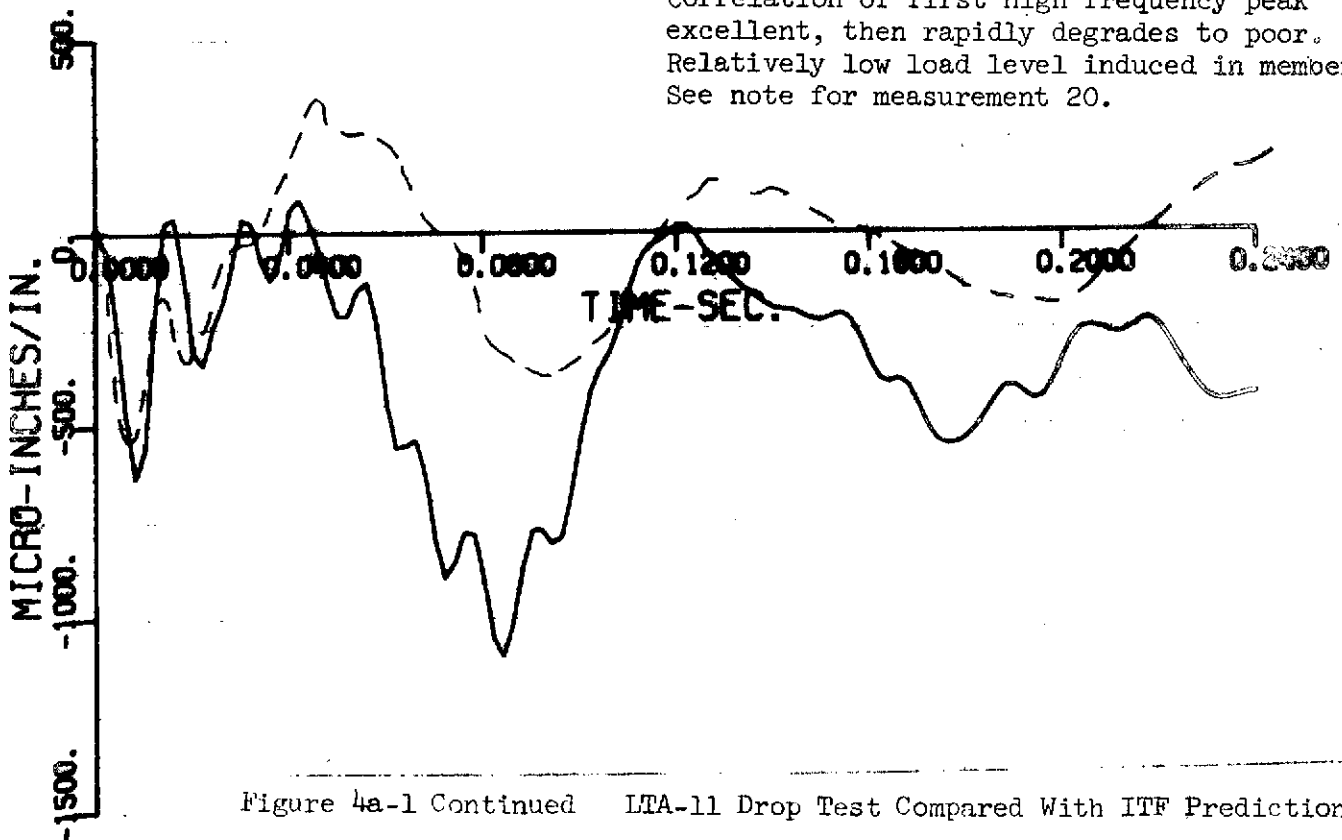
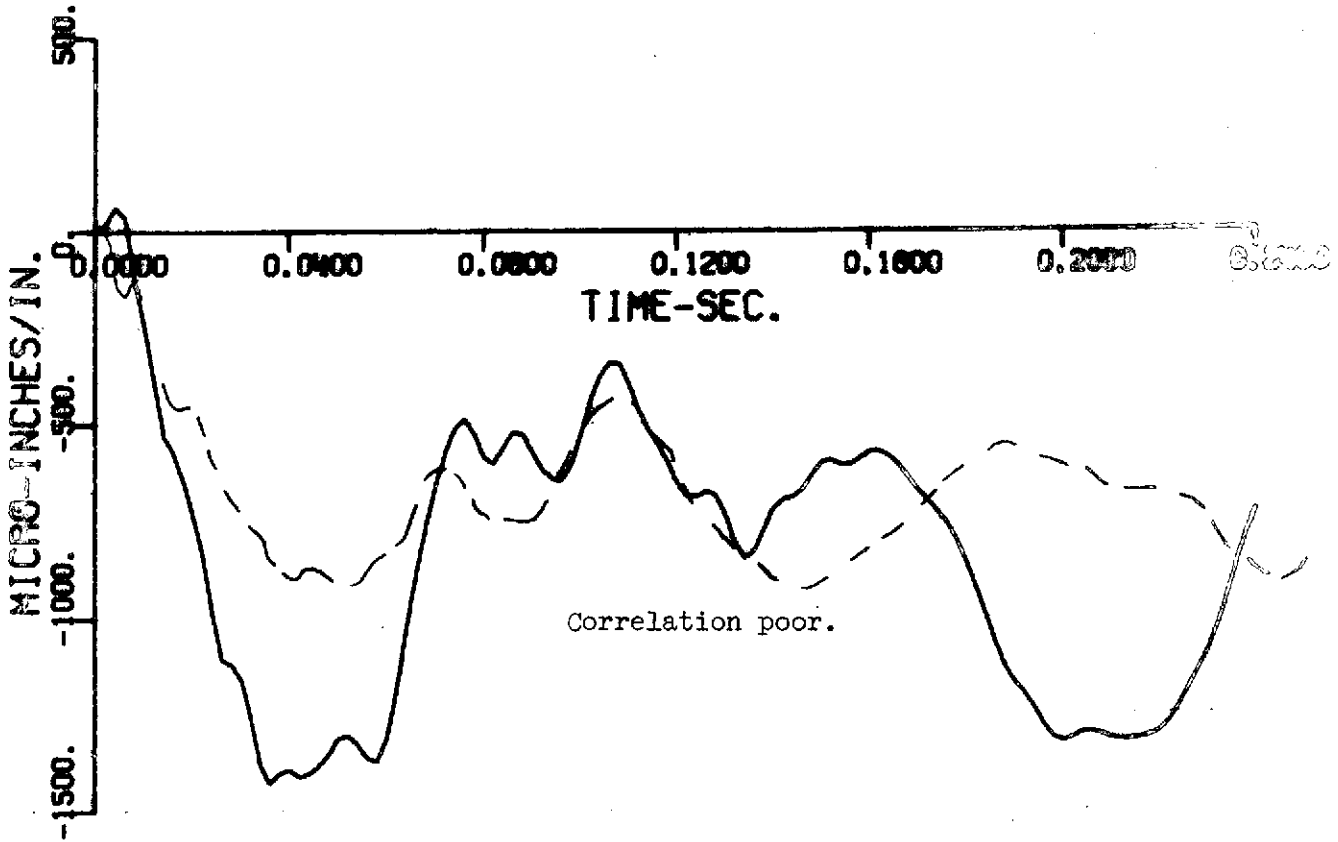


Figure 4a-1 Continued LTA-11 Drop Test Compared With ITF Predictions

MERSUREMENT 24 BAR



MERSUREMENT 25 BAR

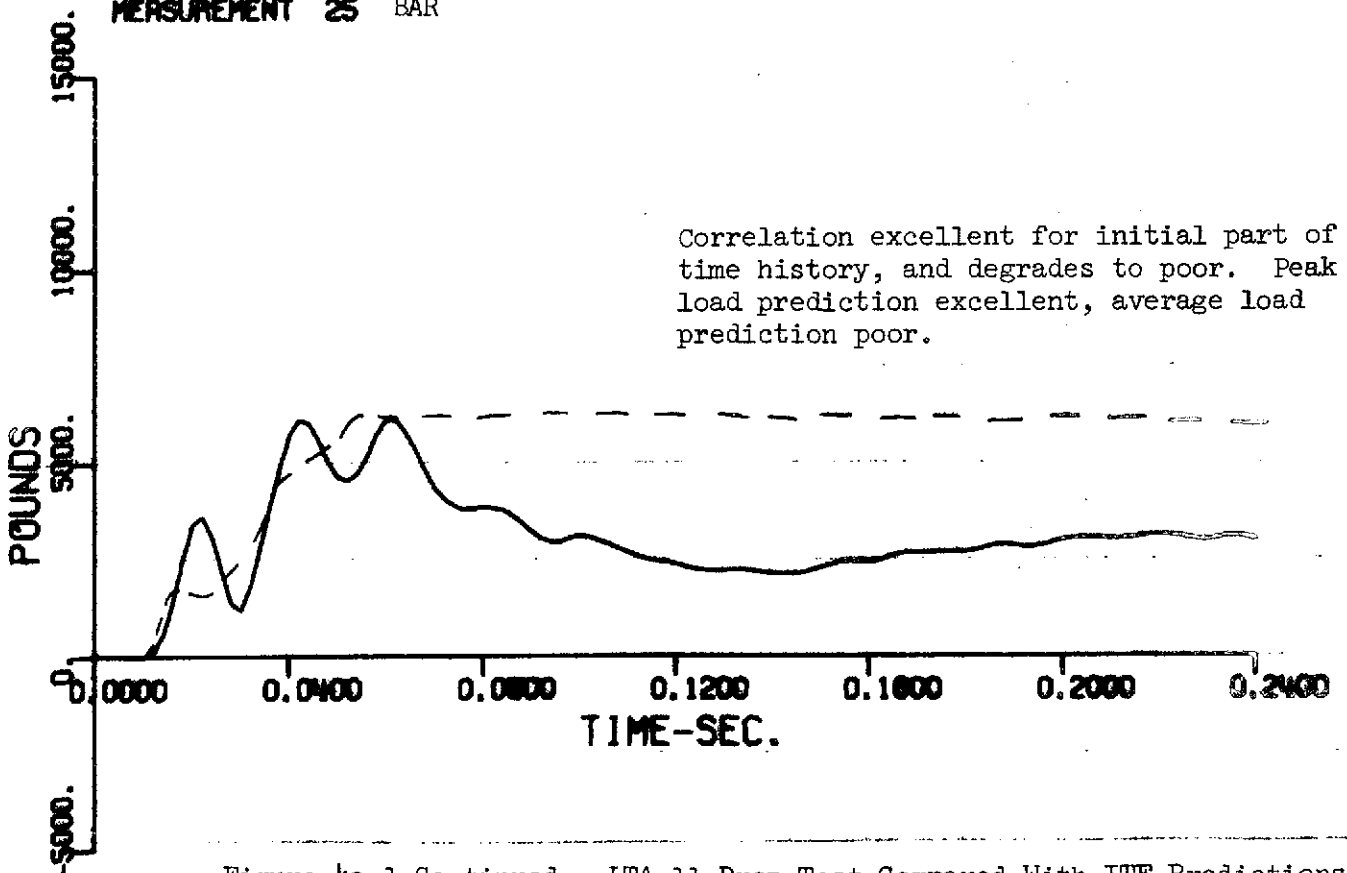


Figure 4a-1 Continued LTA-11 Drop Test Compared With IITF Predictions

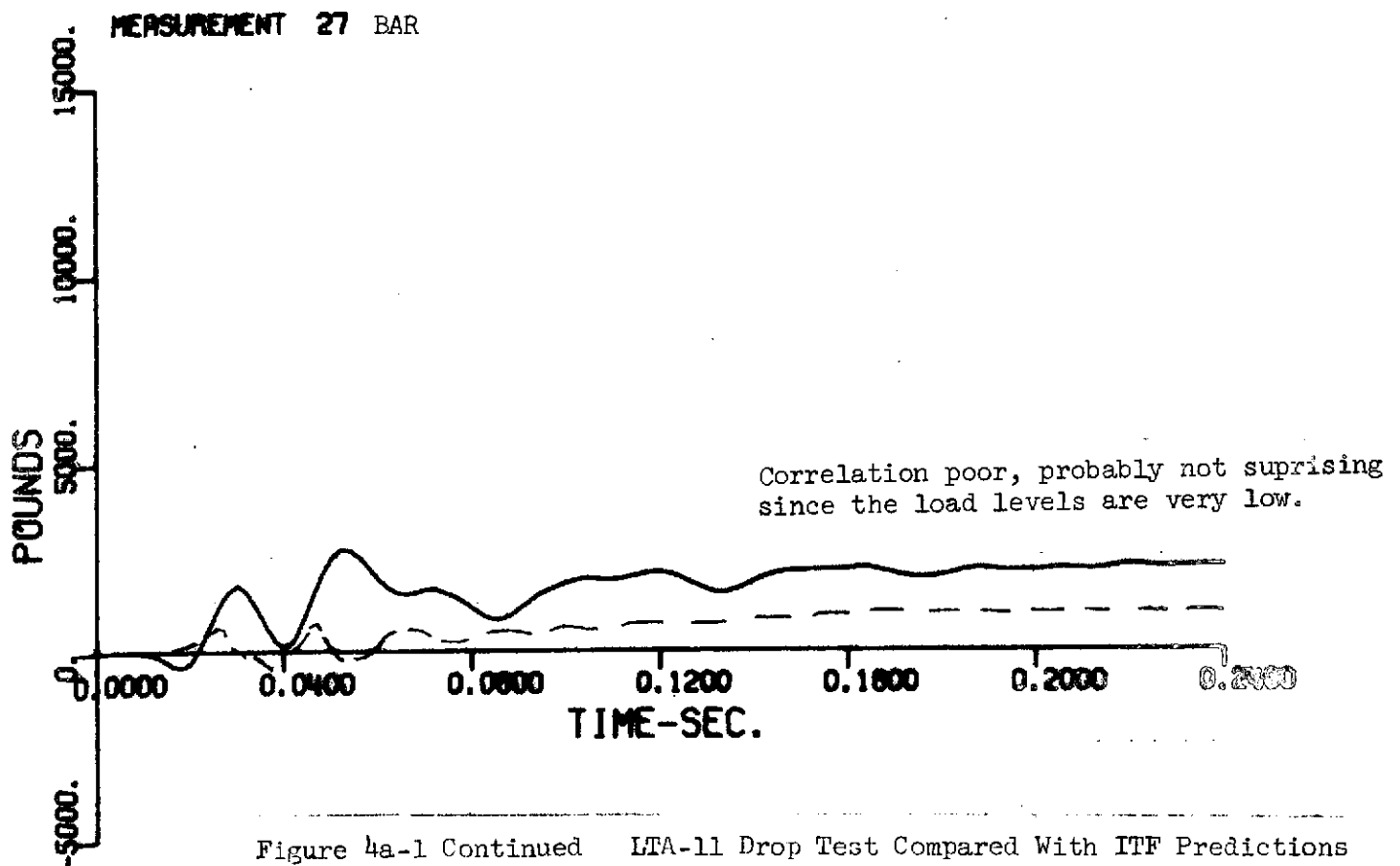
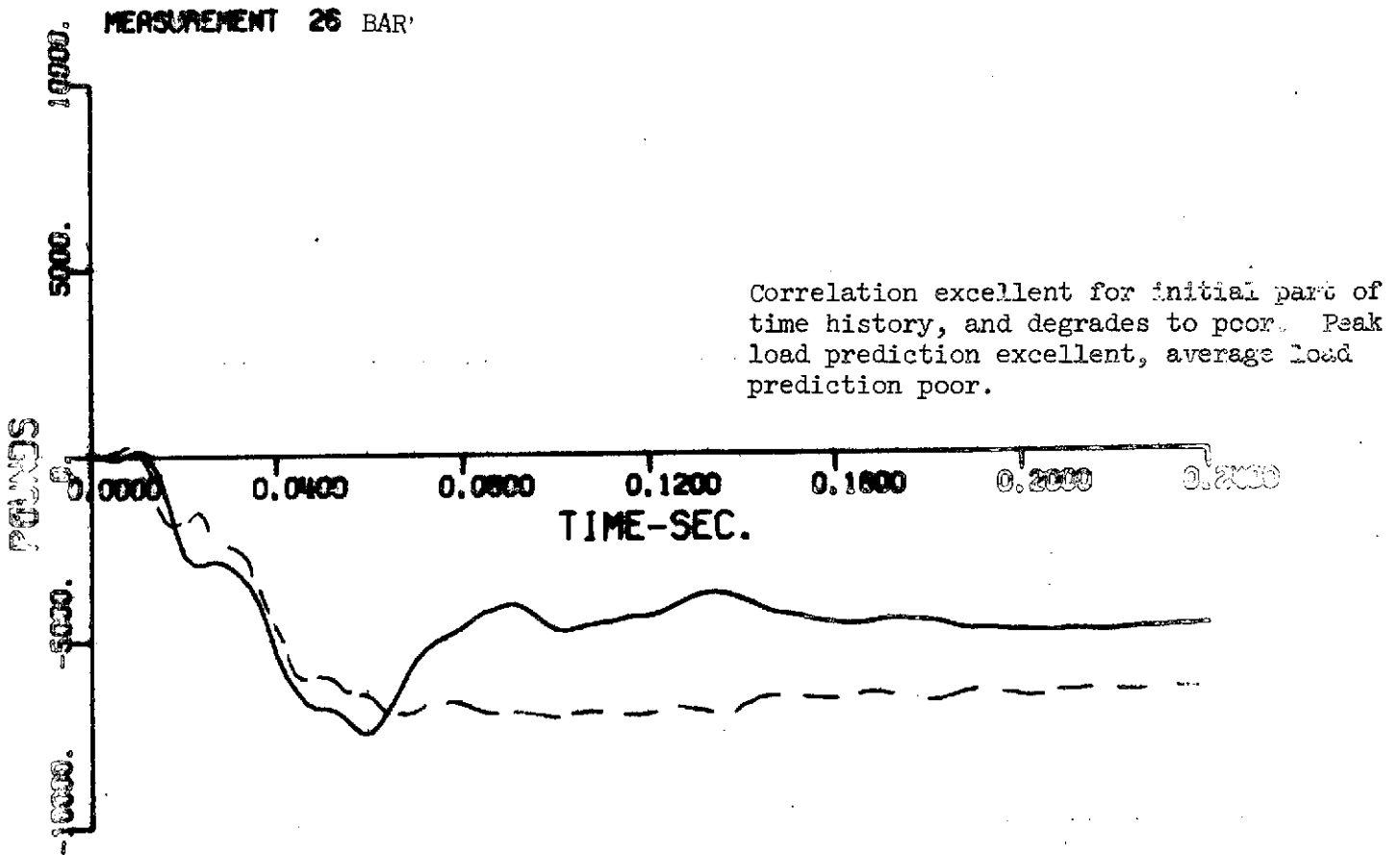
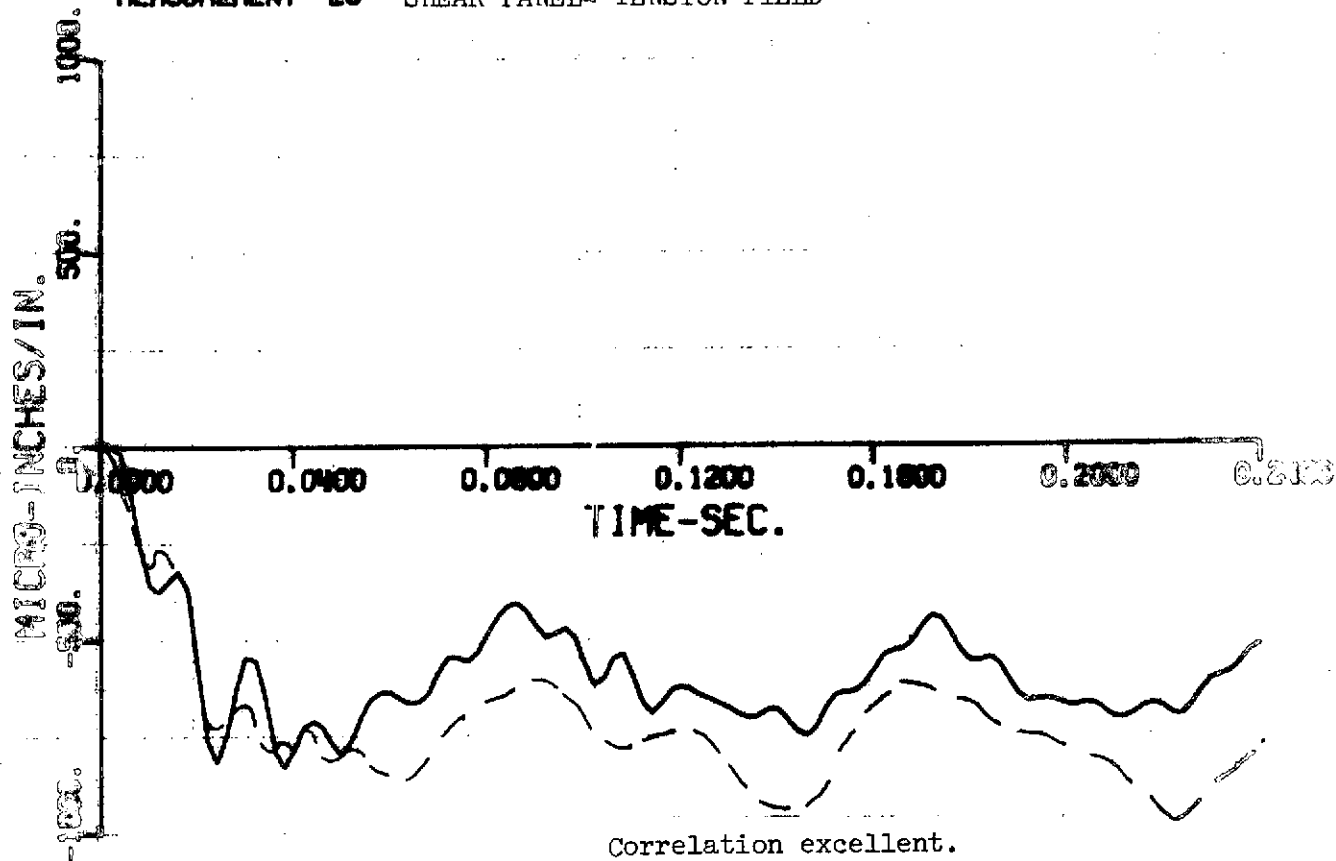


Figure 4a-1 Continued LTA-11 Drop Test Compared With ITF Predictions

MEASUREMENT 28 SHEAR PANEL- TENSION FIELD



MEASUREMENT 29 SHEAR PANEL- TENSION FIELD

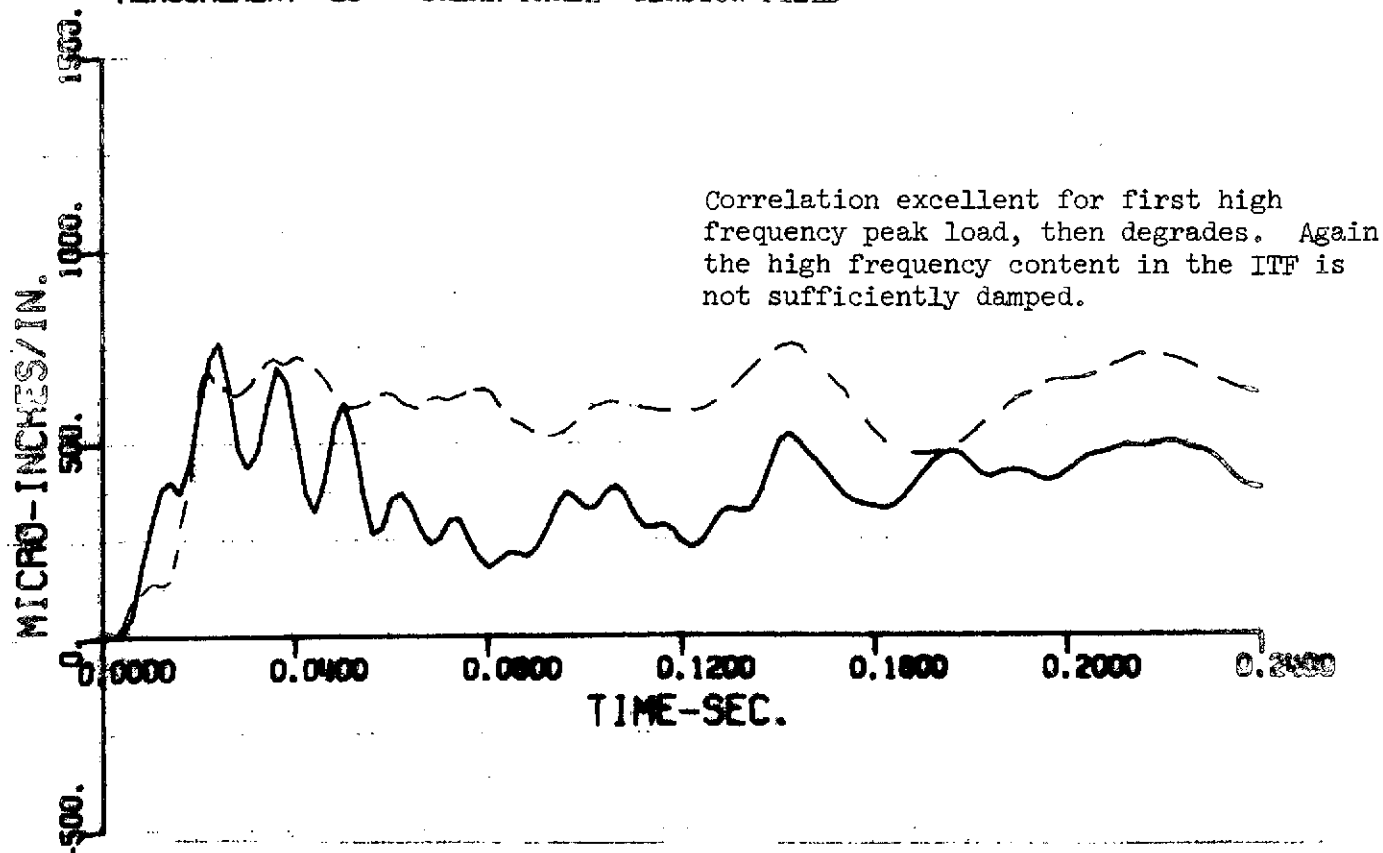
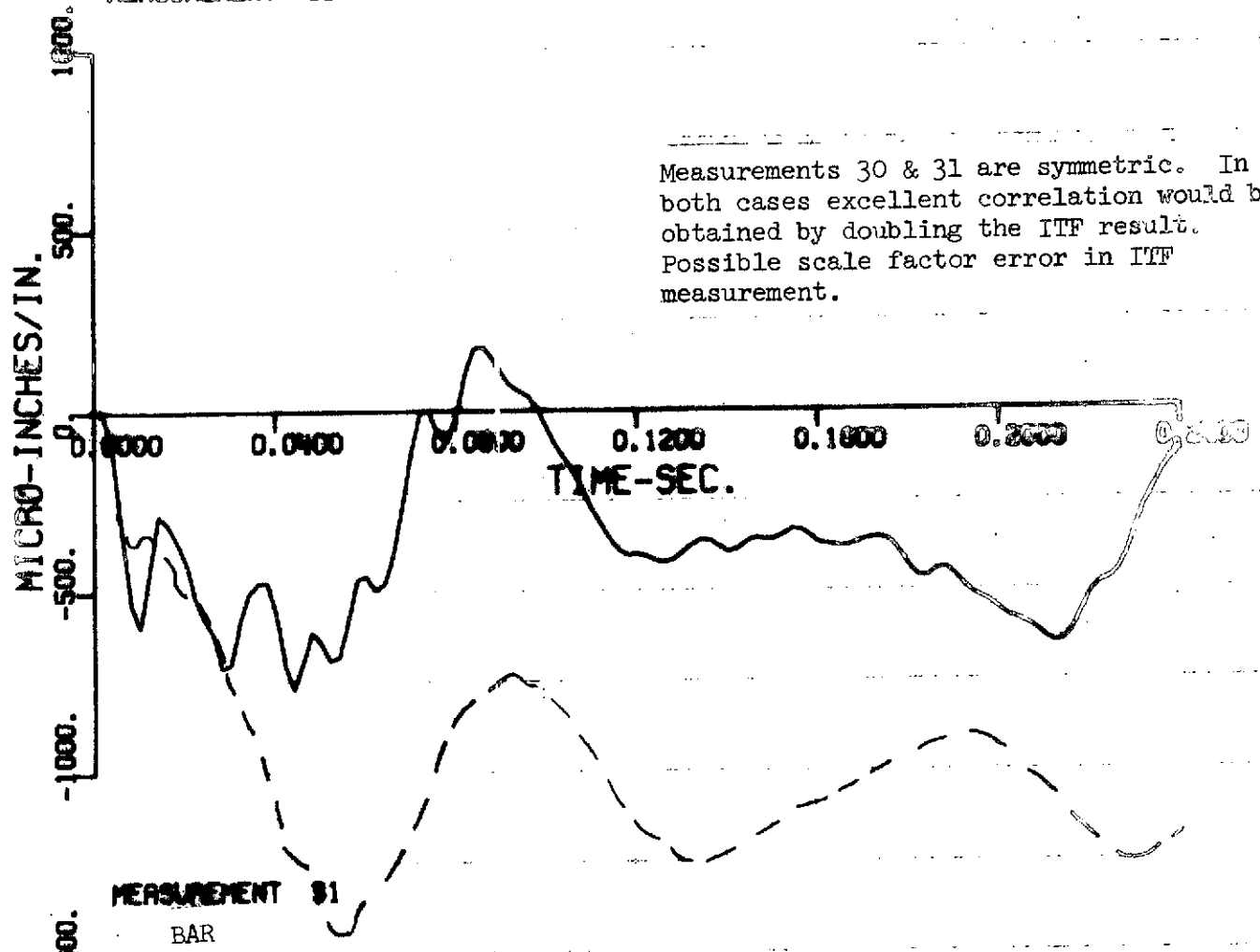
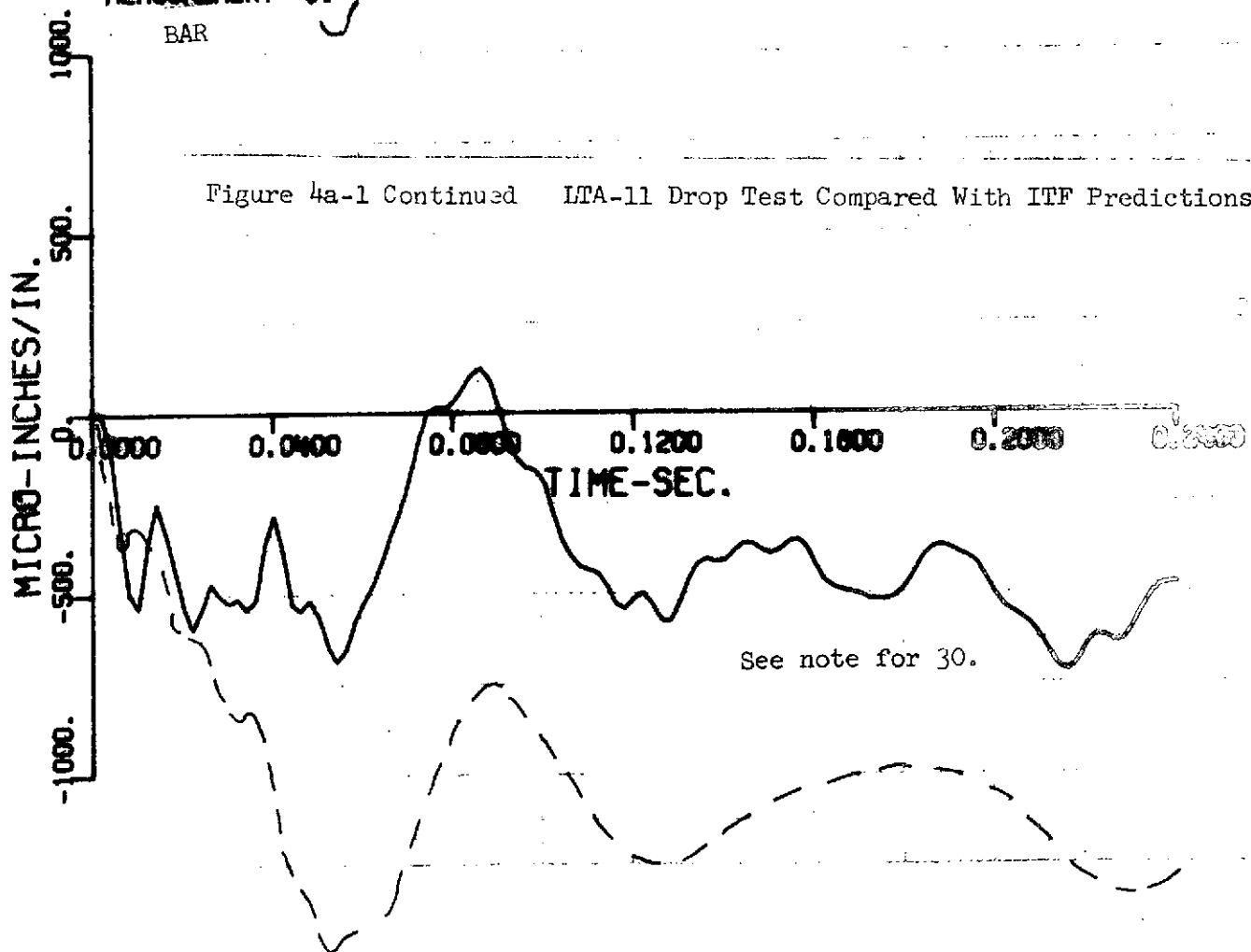


Figure 4a-1 Continued LTA-11 Drop Test Compared With ITF Predictions



MEASUREMENT 31  
BAR

Figure 4a-1 Continued LTA-11 Drop Test Compared With ITF Predictions



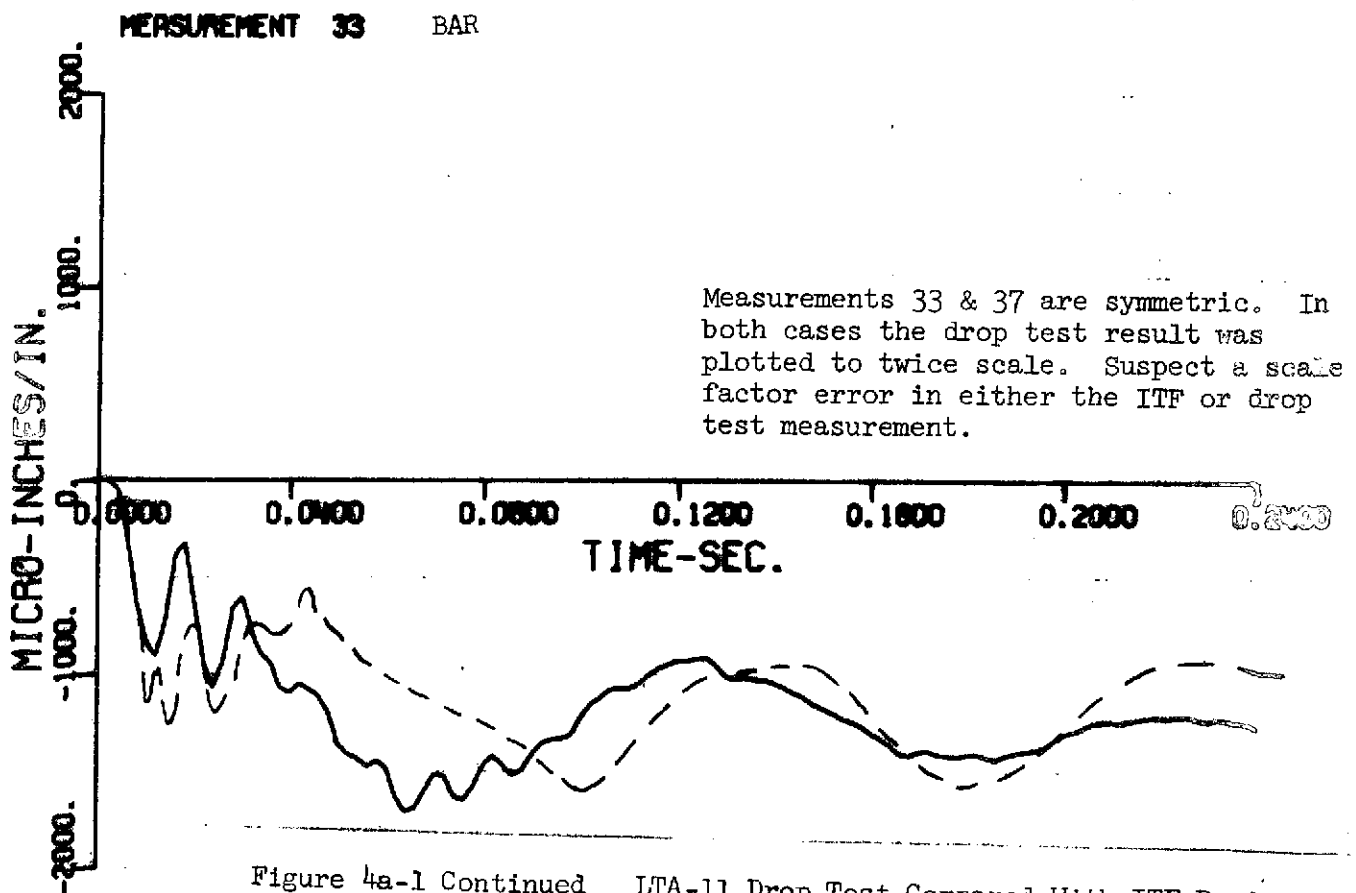
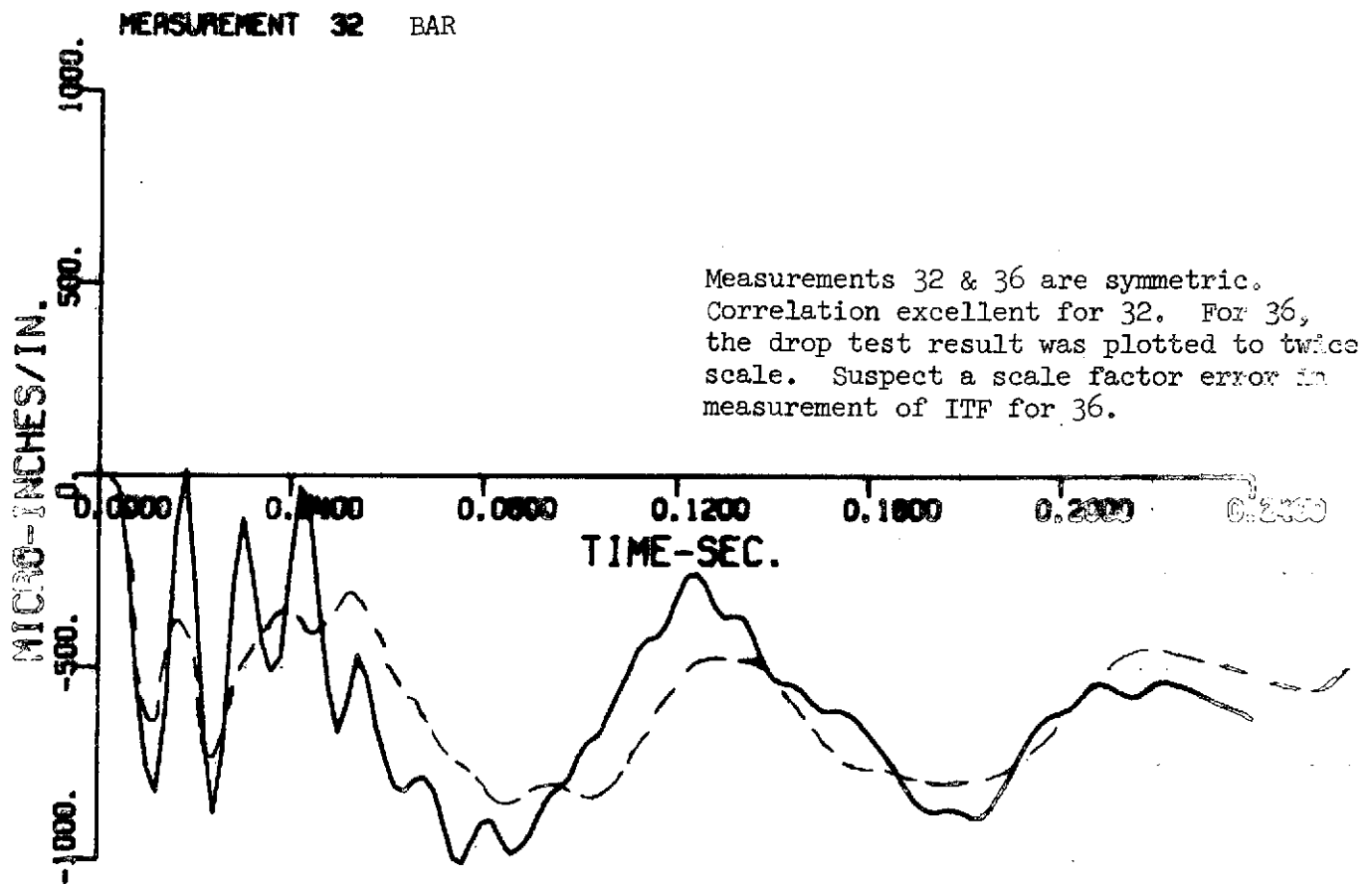
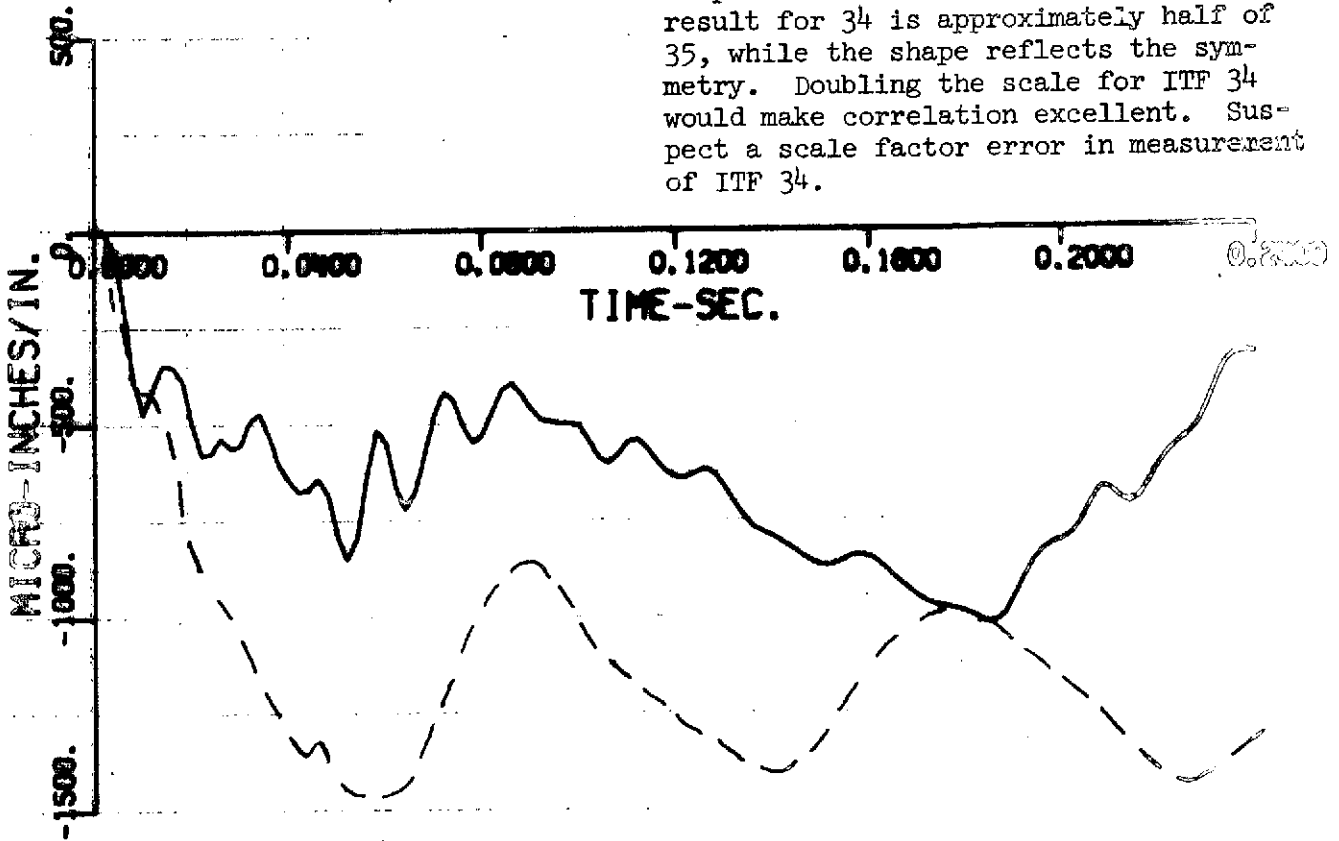


Figure 4a-1 Continued LTA-11 Drop Test Compared With ITF Predictions

MEASUREMENT 34 BAR

Measurements 34 & 35 are symmetric. The drop test results are symmetric, the ITF result for 34 is approximately half of 35, while the shape reflects the symmetry. Doubling the scale for ITF 34 would make correlation excellent. Suspect a scale factor error in measurement of ITF 34.



MEASUREMENT 35 BAR

Correlation excellent. See note for 34.

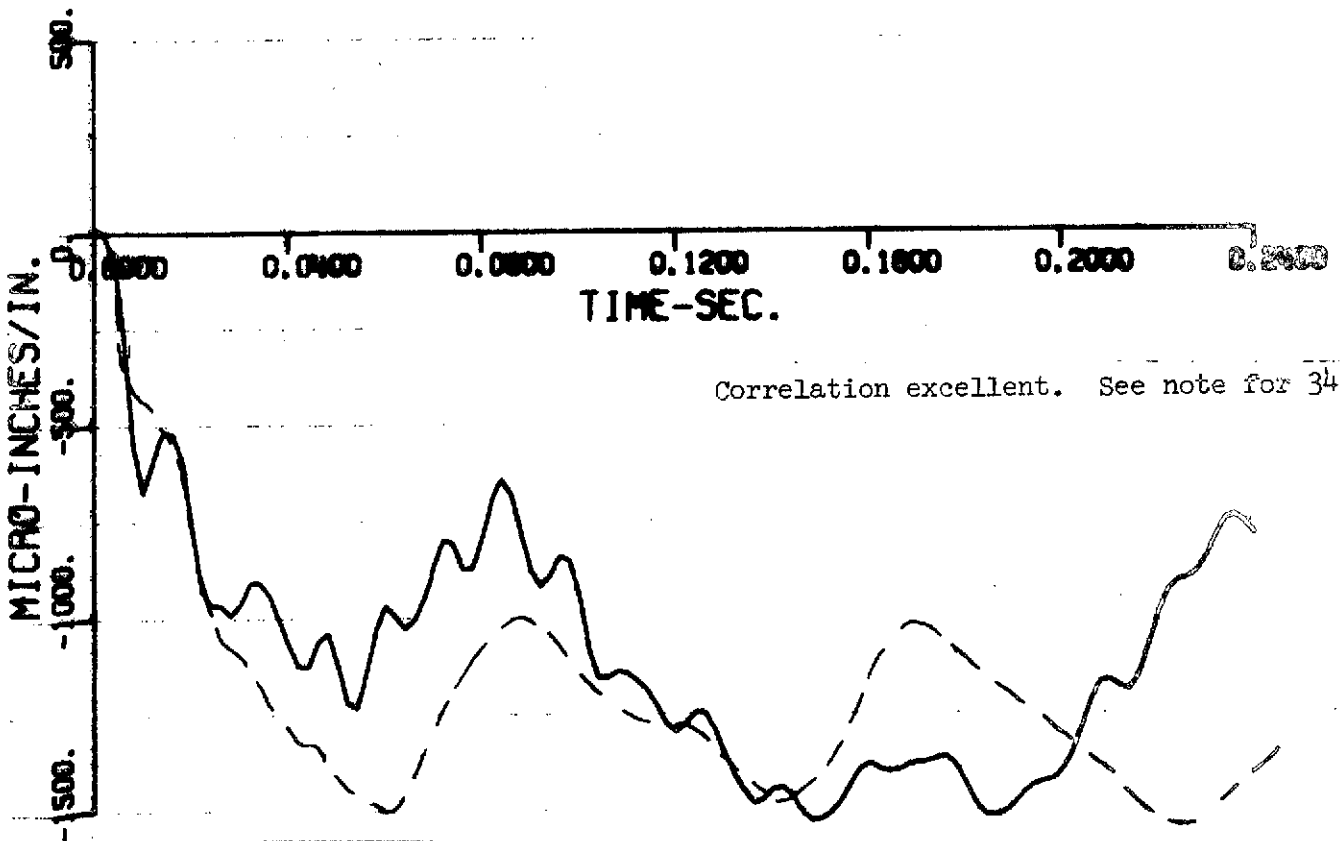
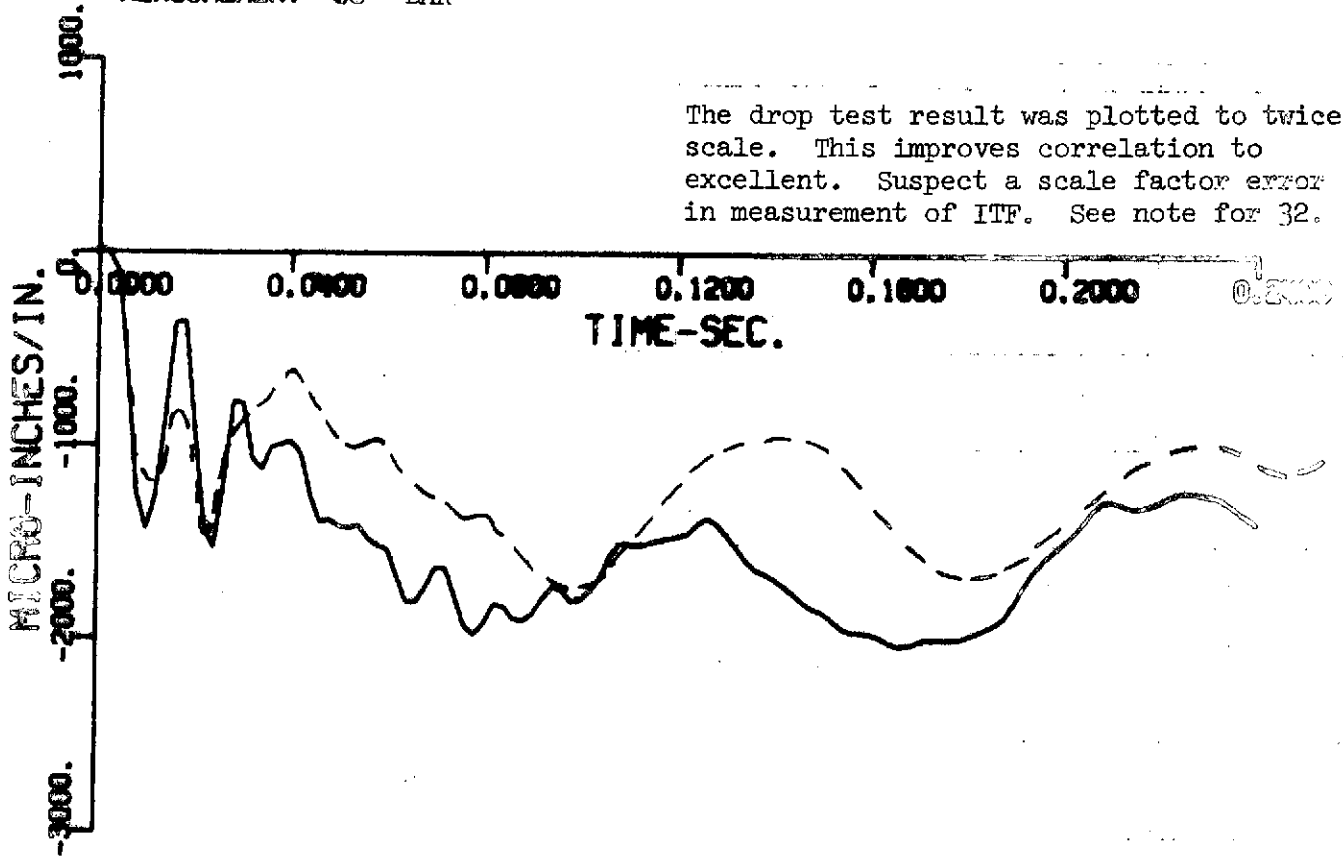


Figure 4a-1 Continued LTA-11 Drop Test Compared With ITF Predictions

MEASUREMENT 30 BAR



MEASUREMENT 37 BAR

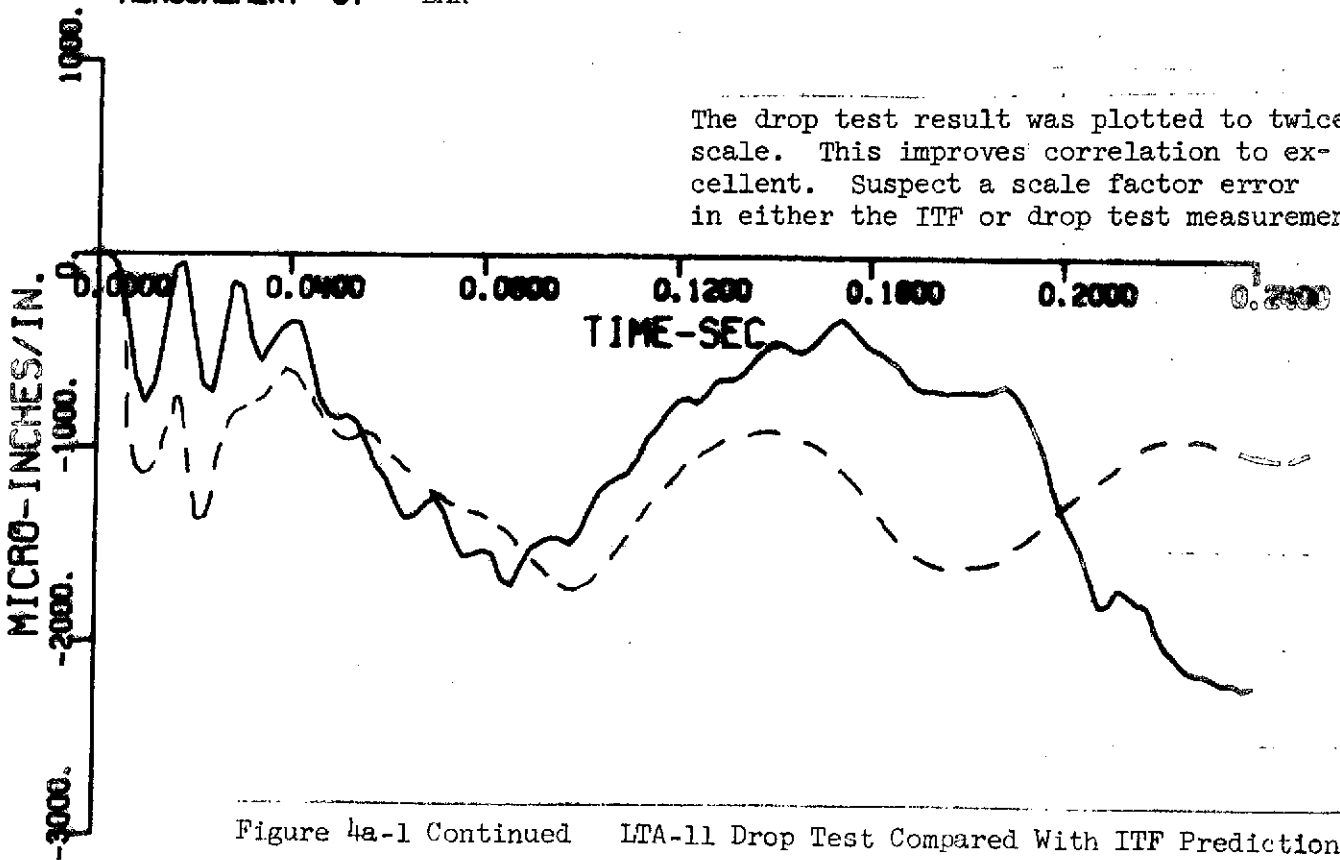


Figure 4a-1 Continued LTA-11 Drop Test Compared With ITF Predictions

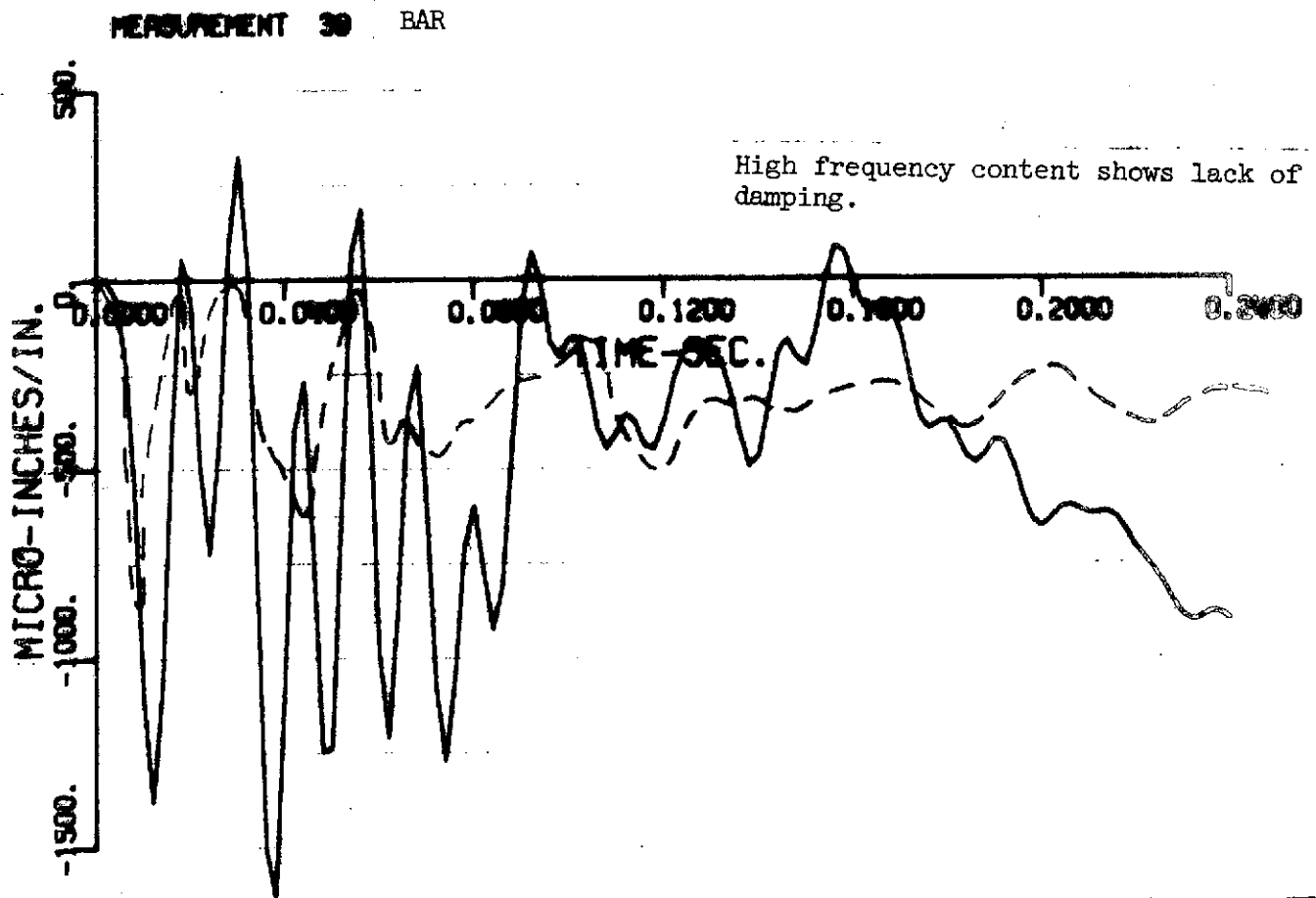
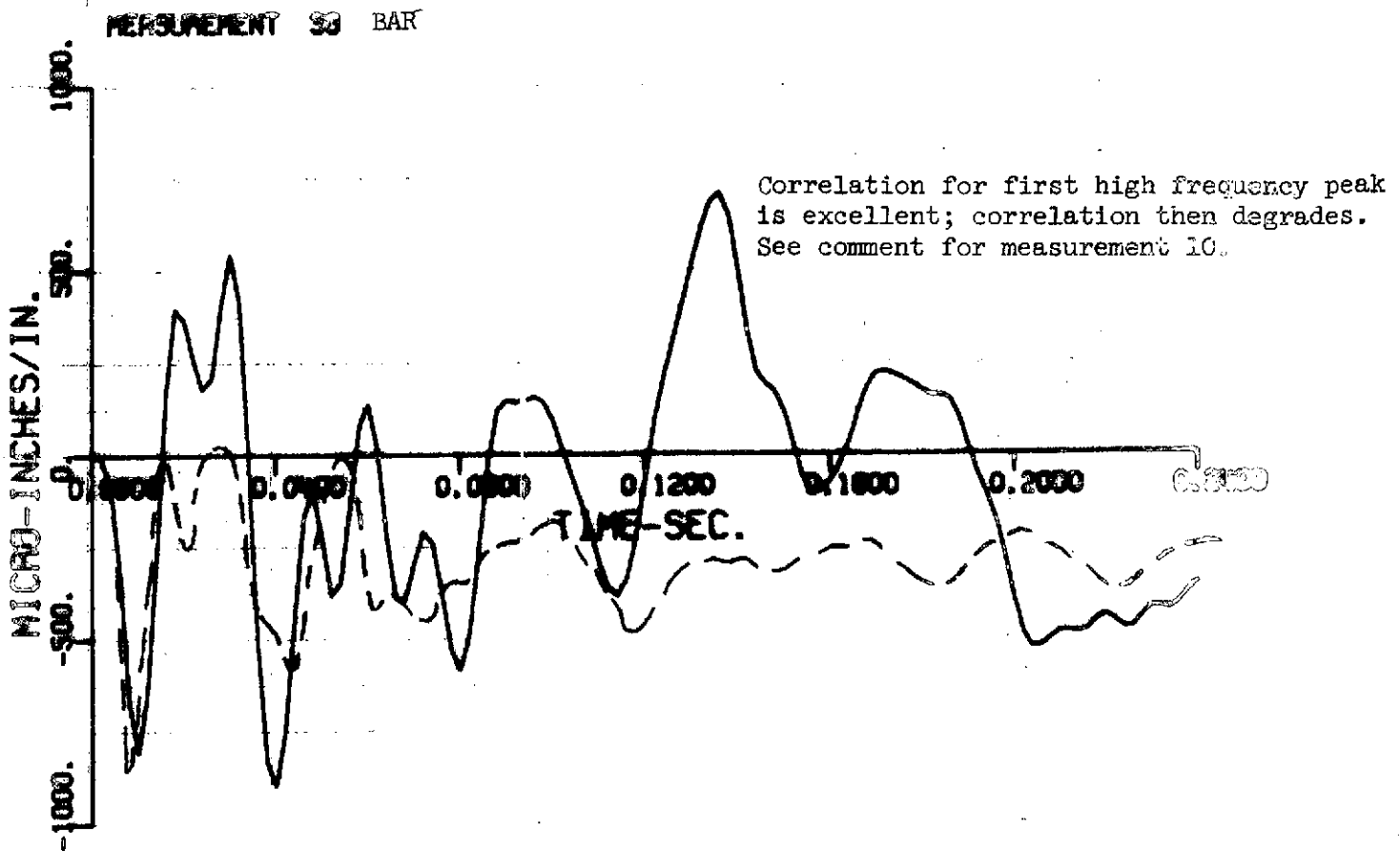


Figure 4a-1 Continued LTA-11 Drop Test Compared With ITF Predictions

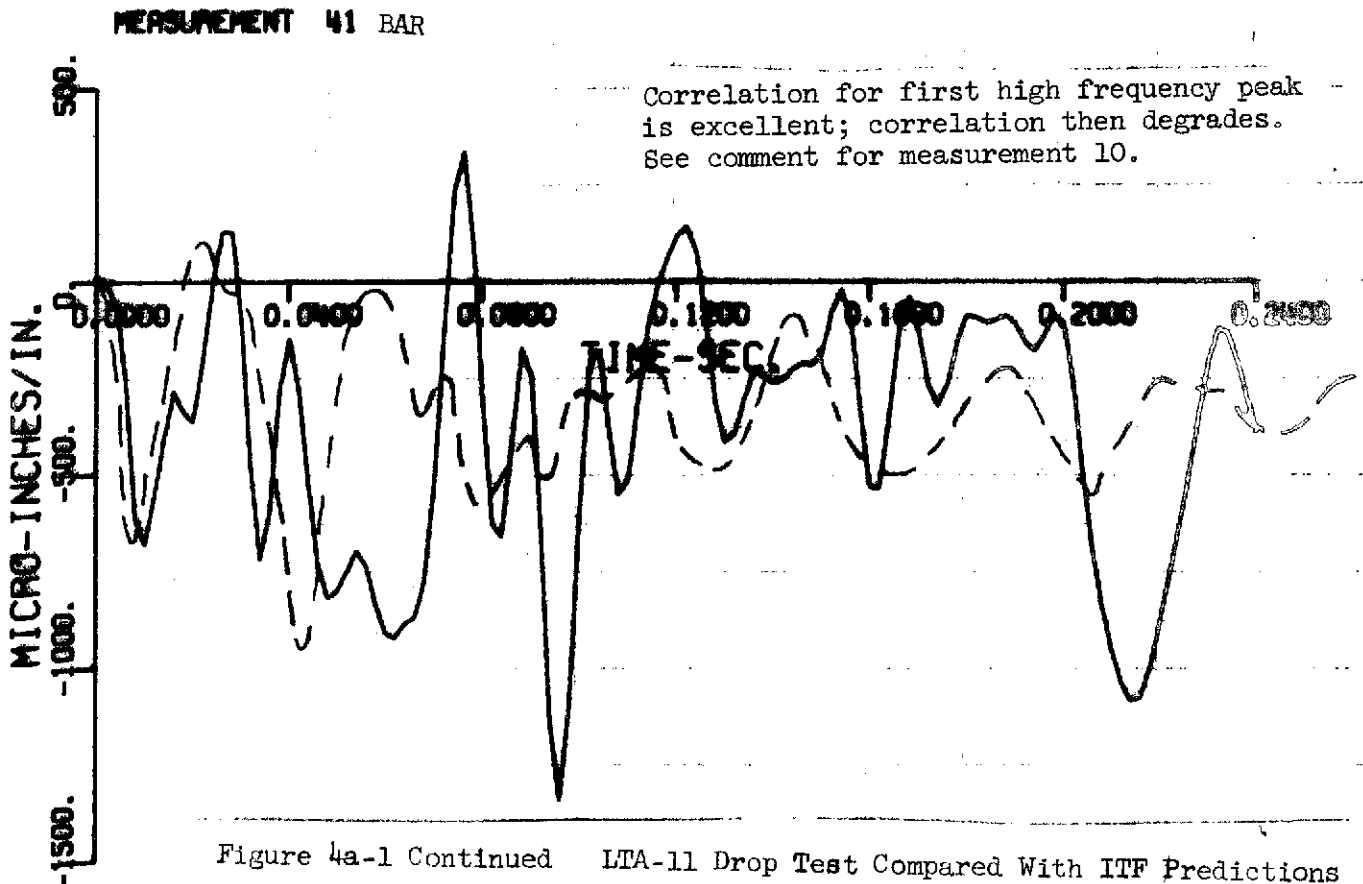
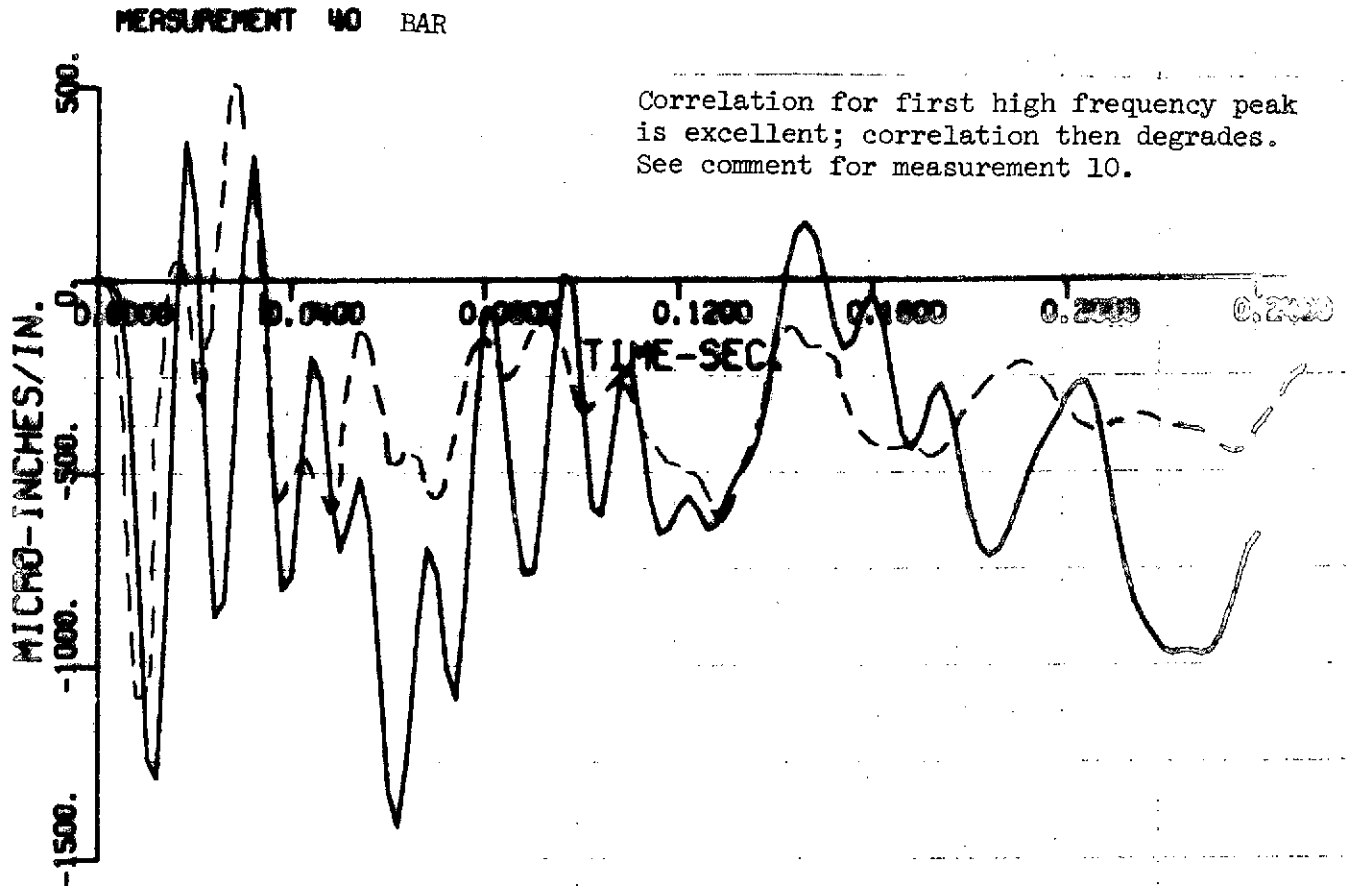
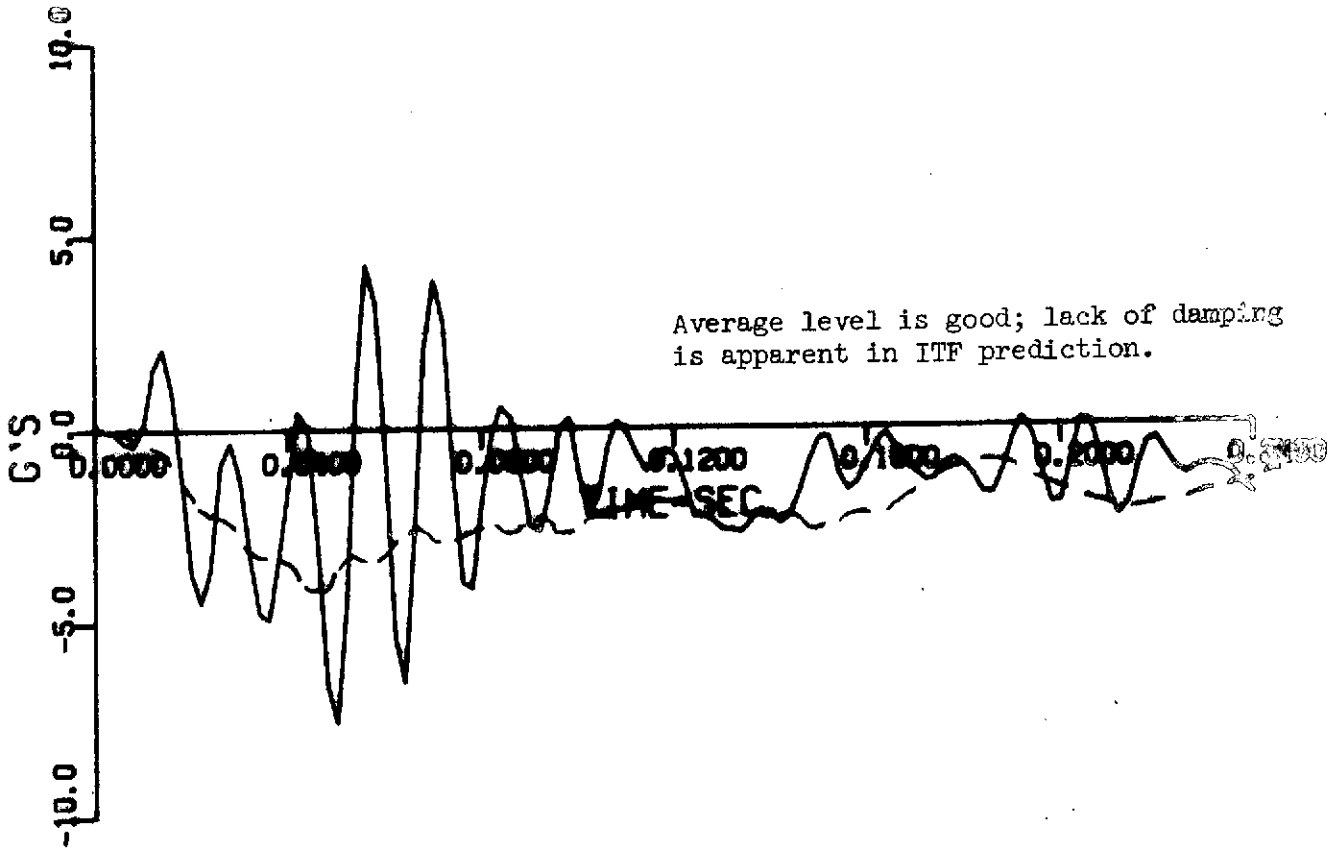


Figure 4a-1 Continued LTA-11 Drop Test Compared With ITF Predictions

MERSUREMENT 60 ACCELEROMETER X DIRECTION



MERSUREMENT 61 ACCELEROMETER Z DIRECTION

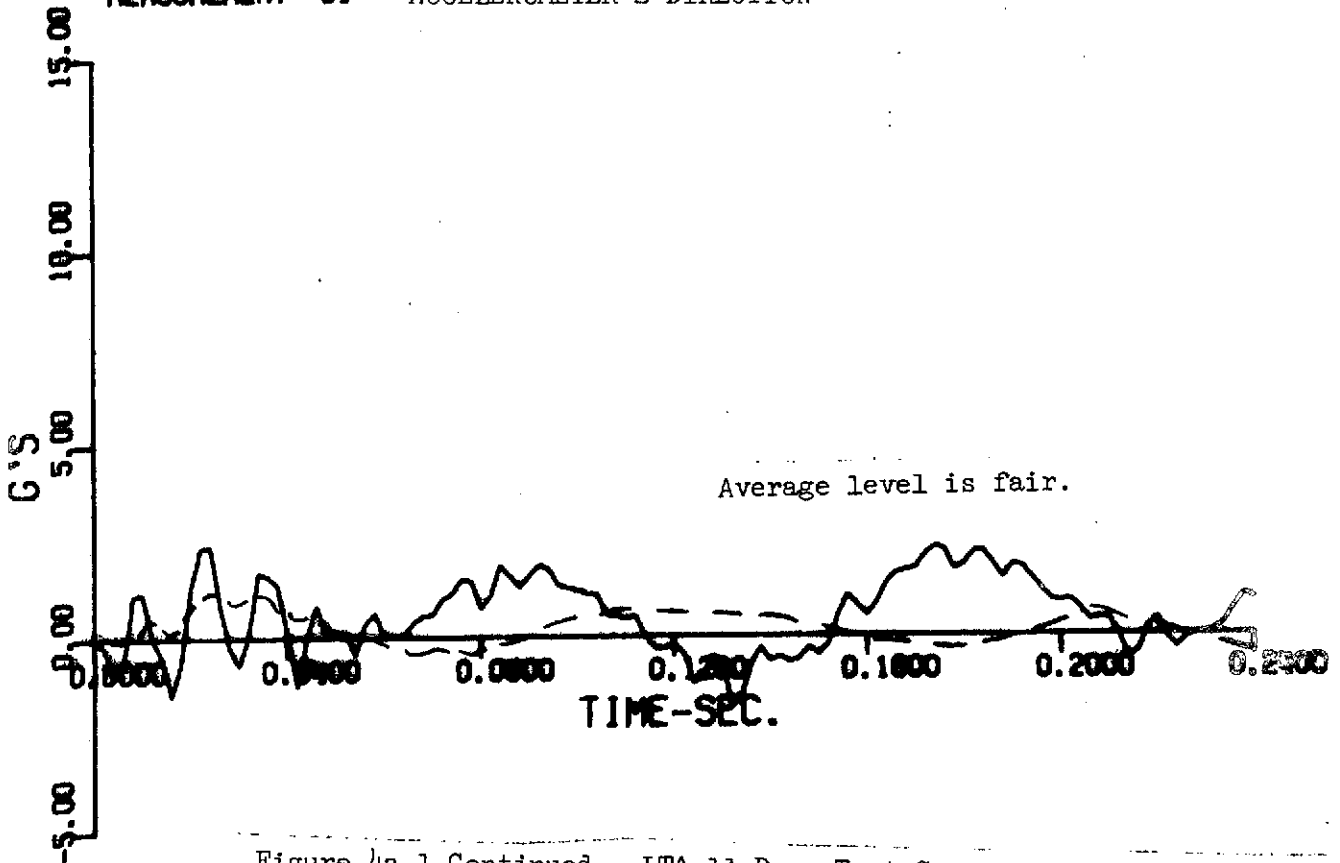


Figure 4a-1 Continued LTA-11 Drop Test Compared With ITF Predictions

4b - Comparison of Drop Test Results, Predictions Using ITF's, and Predictions From Modal Analysis

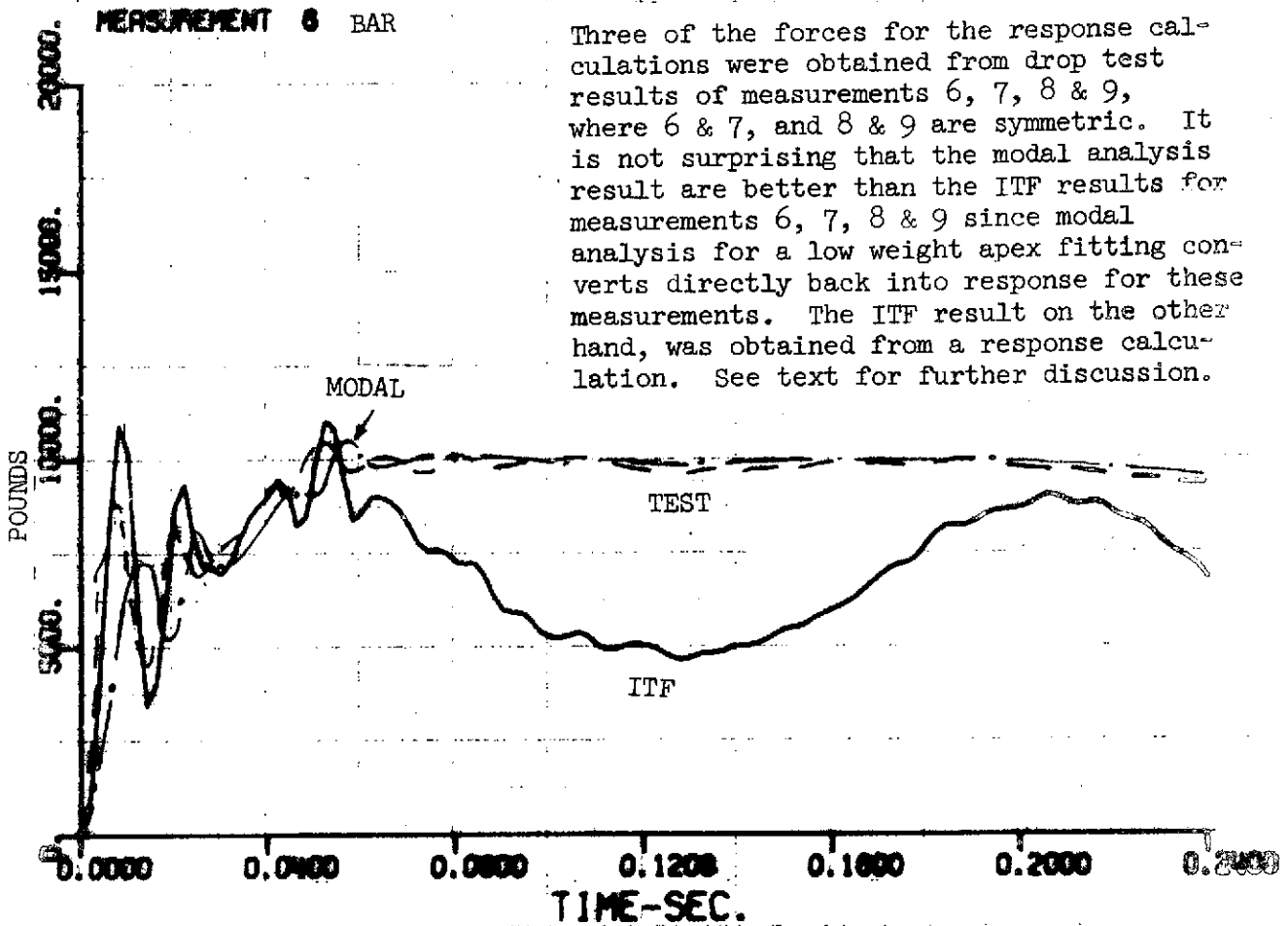
The work reported in this section was performed to provide an additional basis for evaluating the accuracy of the ITF method. The study consisted of predicting internal response of the LTA-11 for the drop test condition under investigation using standard modal and transient response techniques. The finite element math model, identified as "Big Spring IV", was provided by LM project personnel; the sketches of Appendix E give some further insight into this model. The model was evolved through the years of LM development, using test data wherever possible to improve the idealization. Although not the most up-to-date analytic representation, it contained a load distribution matrix for computing internal responses that corresponded, in large measure, to the data recorded during impulse testing. The forcing functions used to excite the model were the same as those used for the ITF predictions, Figure 4-1; computation was accomplished using the Grumman transient response package, Reference 7.

The time history results that follow are for all channels common to the drop test, the ITF program, and the modal analysis. Note that drop test results are shown as dashed curves, ITF results as solid curves, and modal analysis as dashed-dot curves. Comments relevant to the comparison are amended to the graphs.

While the comparison is, in general, self-explanatory, a few remarks are pertinent to measurements 6, 7, 8 and 9. As mentioned at the beginning of this section, the forcing functions were computed from outrigger and deployment truss forces recorded during the drop test. Among these forces are measurements 6 through 9. Since the mass at the apex fittings is very small in the modal analysis, the load distribution matrix essentially takes the applied forces and statically distributes them back into the truss members. Thus, it is only reasonable to expect that the results from the modal analysis would compare very well with drop test results. This accurate comparison is evident in the graphs. On the other hand, the ITF approach predicts these responses

as it does all the others in the system. Any spurious effects are as likely to introduce errors into measurements 6 through 9 as they are to degrade other channels of data.

Conclusions and recommendations with regard to the comparison shown here are presented in Section 6. When conclusions are drawn (Section 6) as to the accuracy of the ITF method as compared to modal analysis, results for measurements 6 through 9 are not weighted as heavily as are those for the other channels.



Three of the forces for the response calculations were obtained from drop test results of measurements 6, 7, 8 & 9, where 6 & 7, and 8 & 9 are symmetric. It is not surprising that the modal analysis result are better than the ITF results for measurements 6, 7, 8 & 9 since modal analysis for a low weight apex fitting converts directly back into response for these measurements. The ITF result on the other hand, was obtained from a response calculation. See text for further discussion.

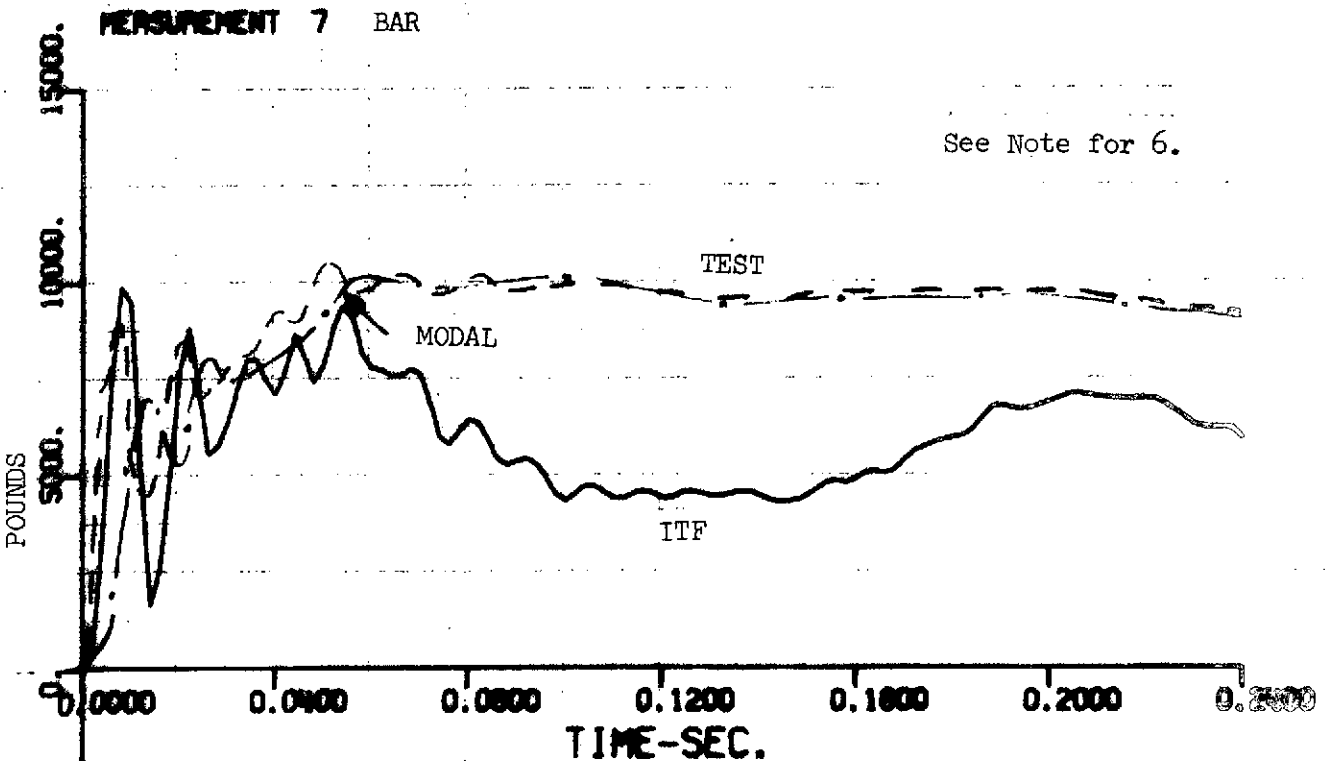


Figure 4b-1 LTA-11 Drop Test Compared With ITF and Modal Analysis Predictions

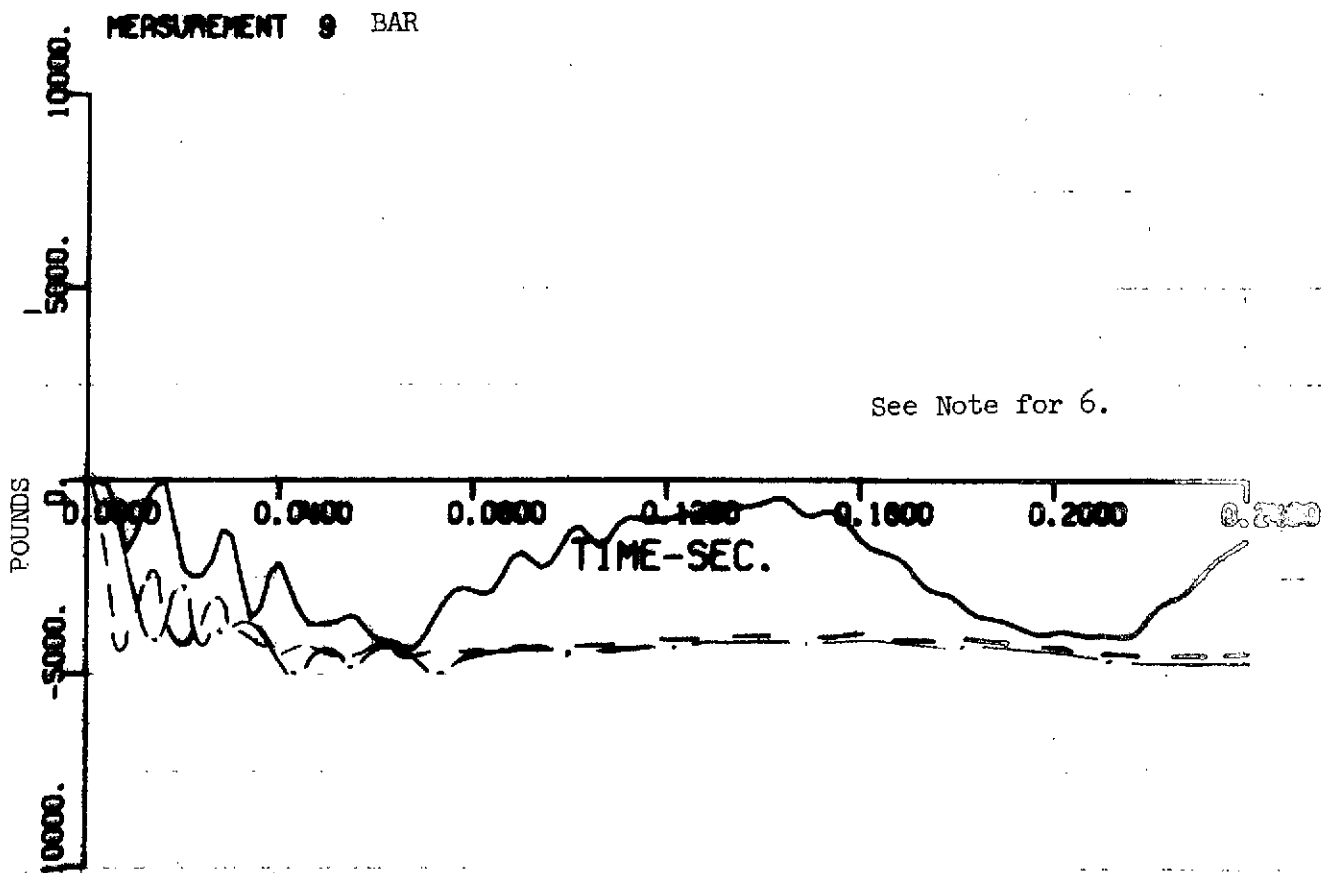
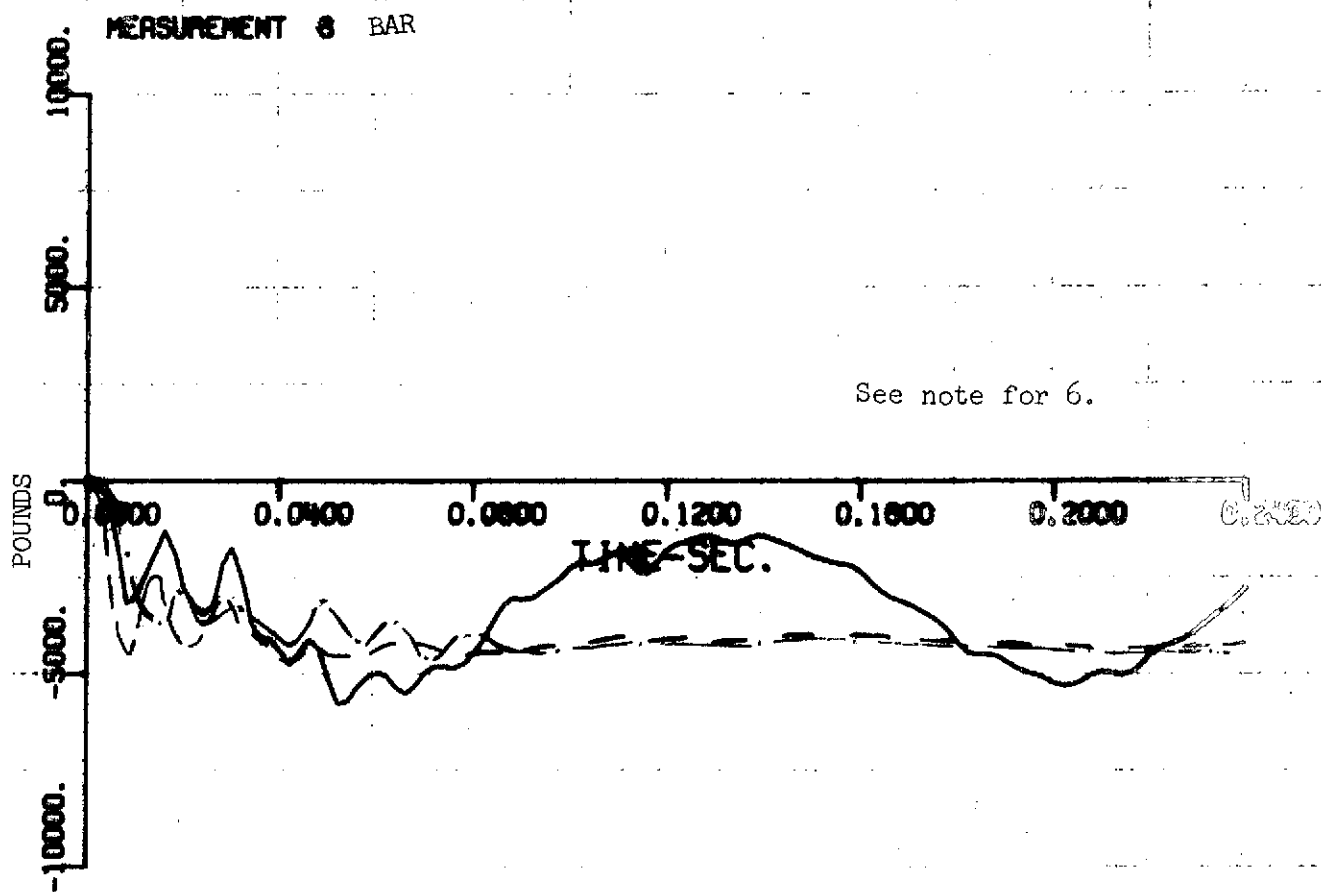
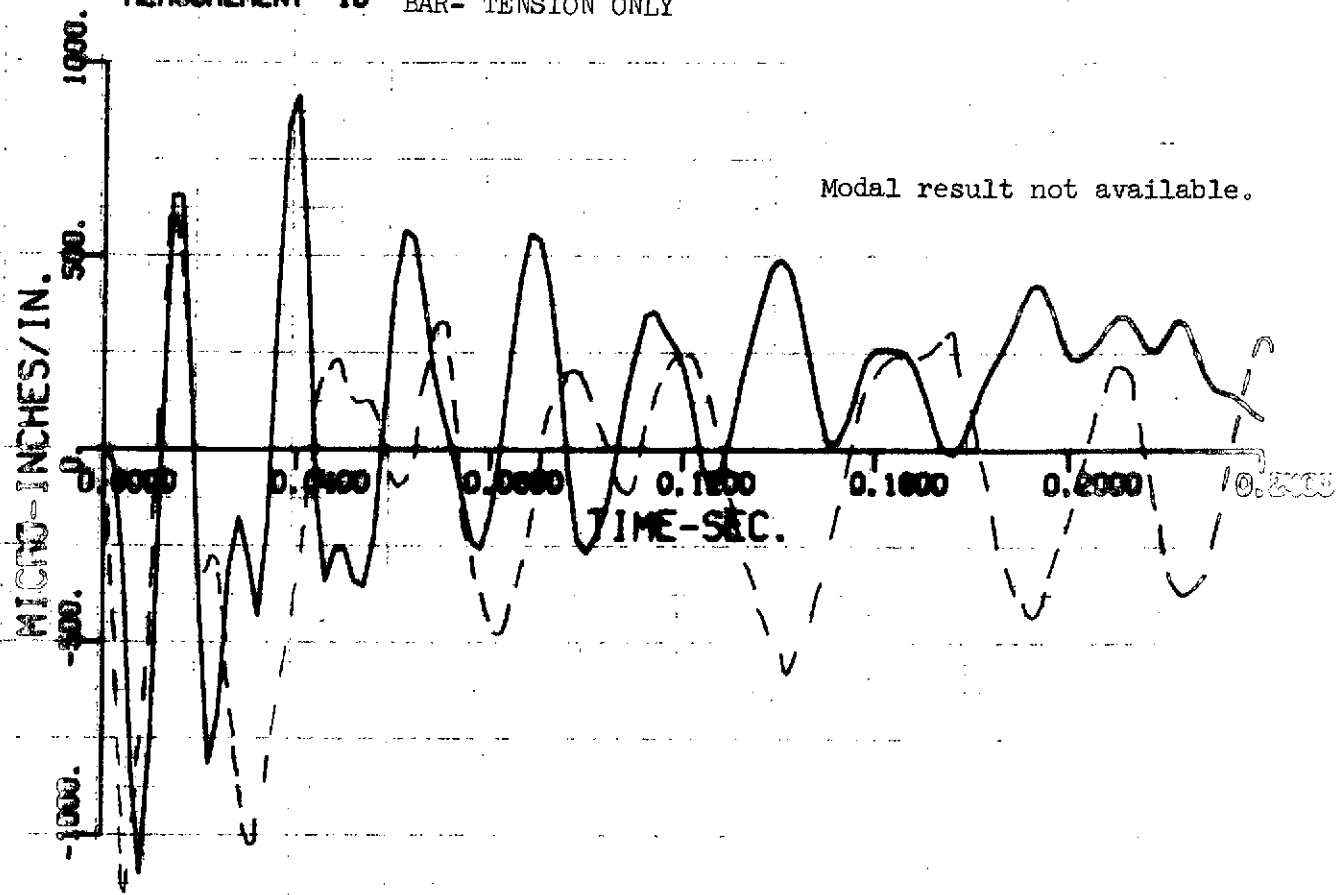


Figure 4b-1 Continued LTA-11 Drop Test Compared With ITF and Modal Analysis Predictions

MERSUREMENT 10 BAR- TENSION ONLY



MERSUREMENT 11 BAR- TENSION ONLY

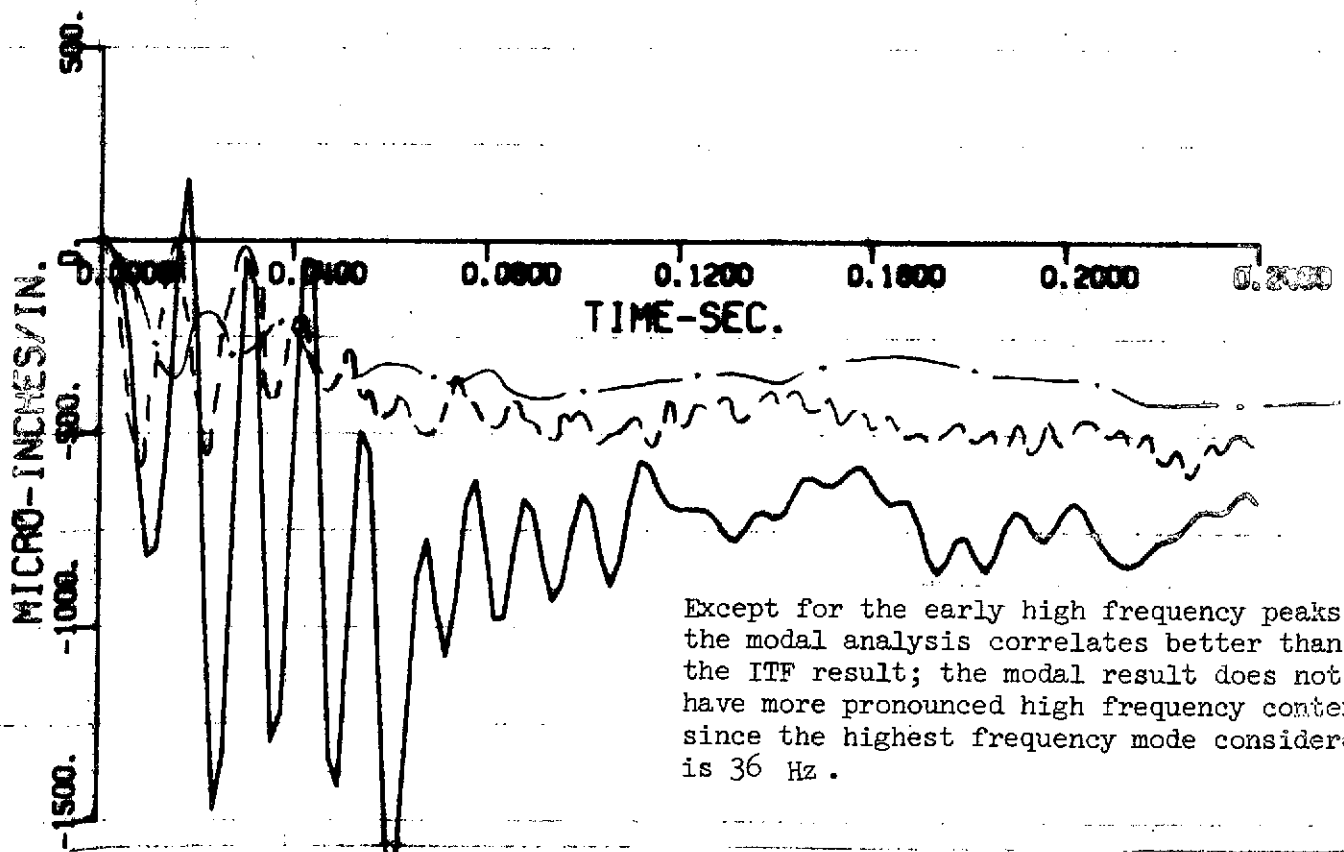


Figure 4b-1 Continued LTA-11 Drop Test Compared With ITF and Modal Analysis Predictions

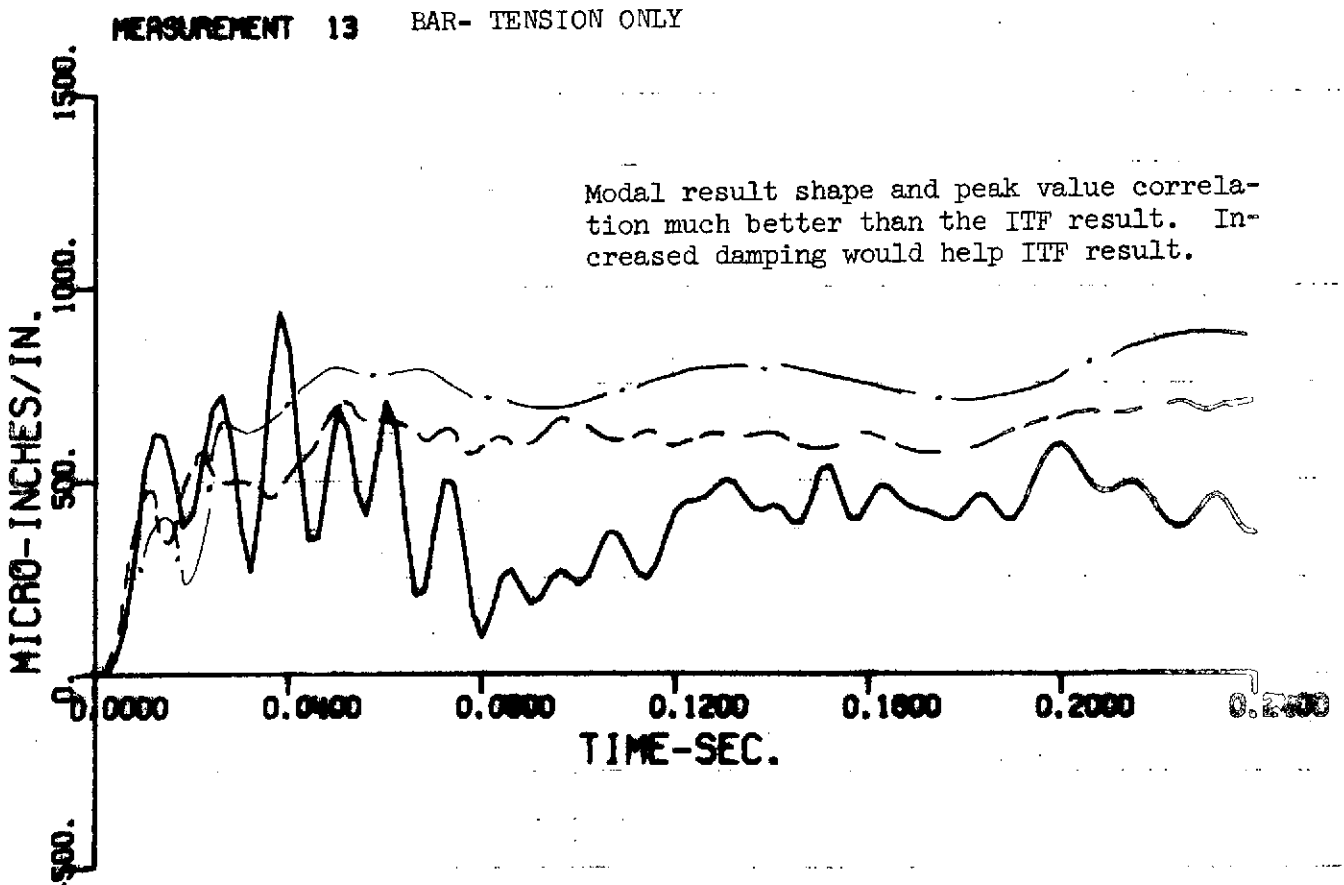
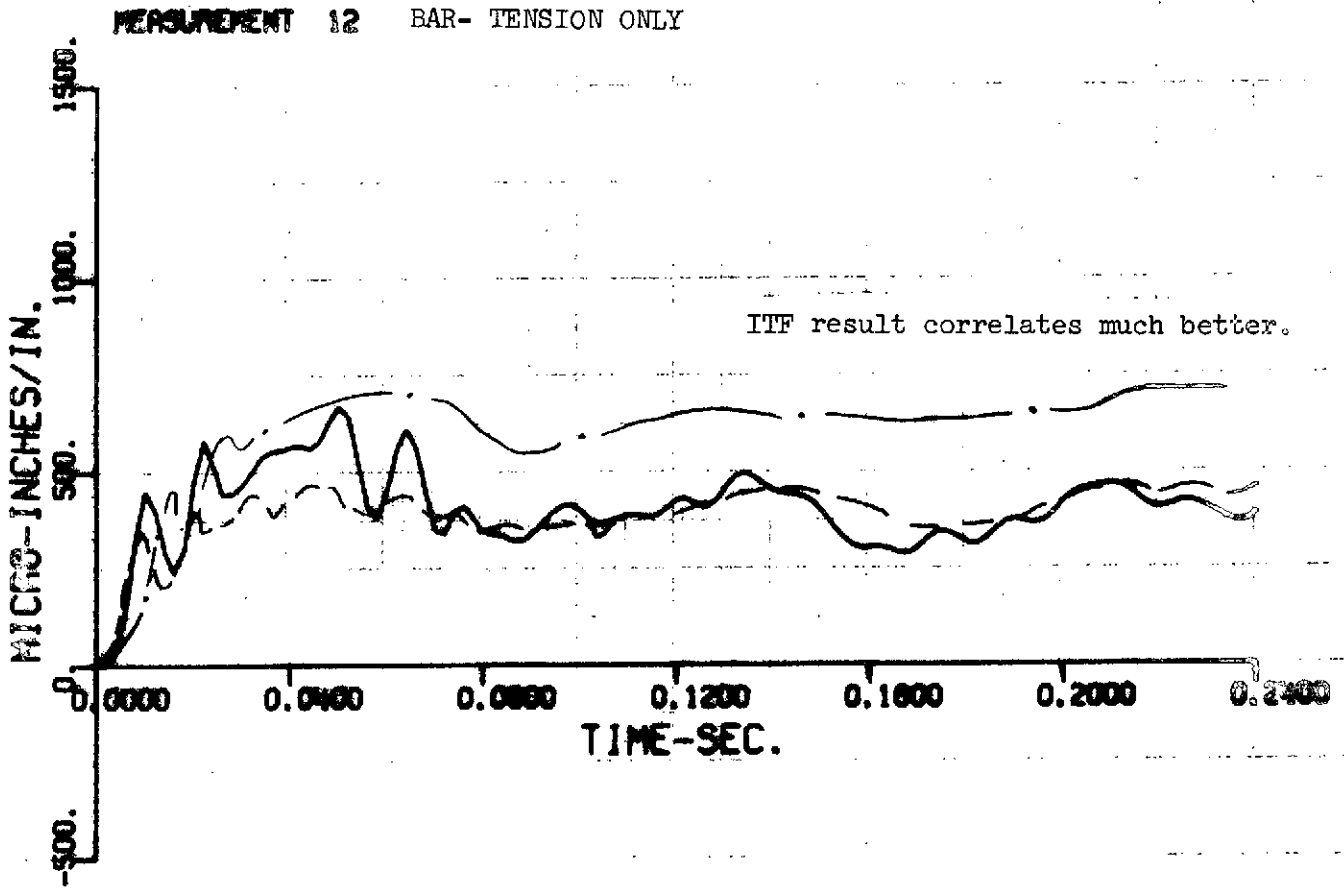


Figure 4b-1 Continued LTA-11 Drop Test Compared With ITF and Modal Analysis Predictions

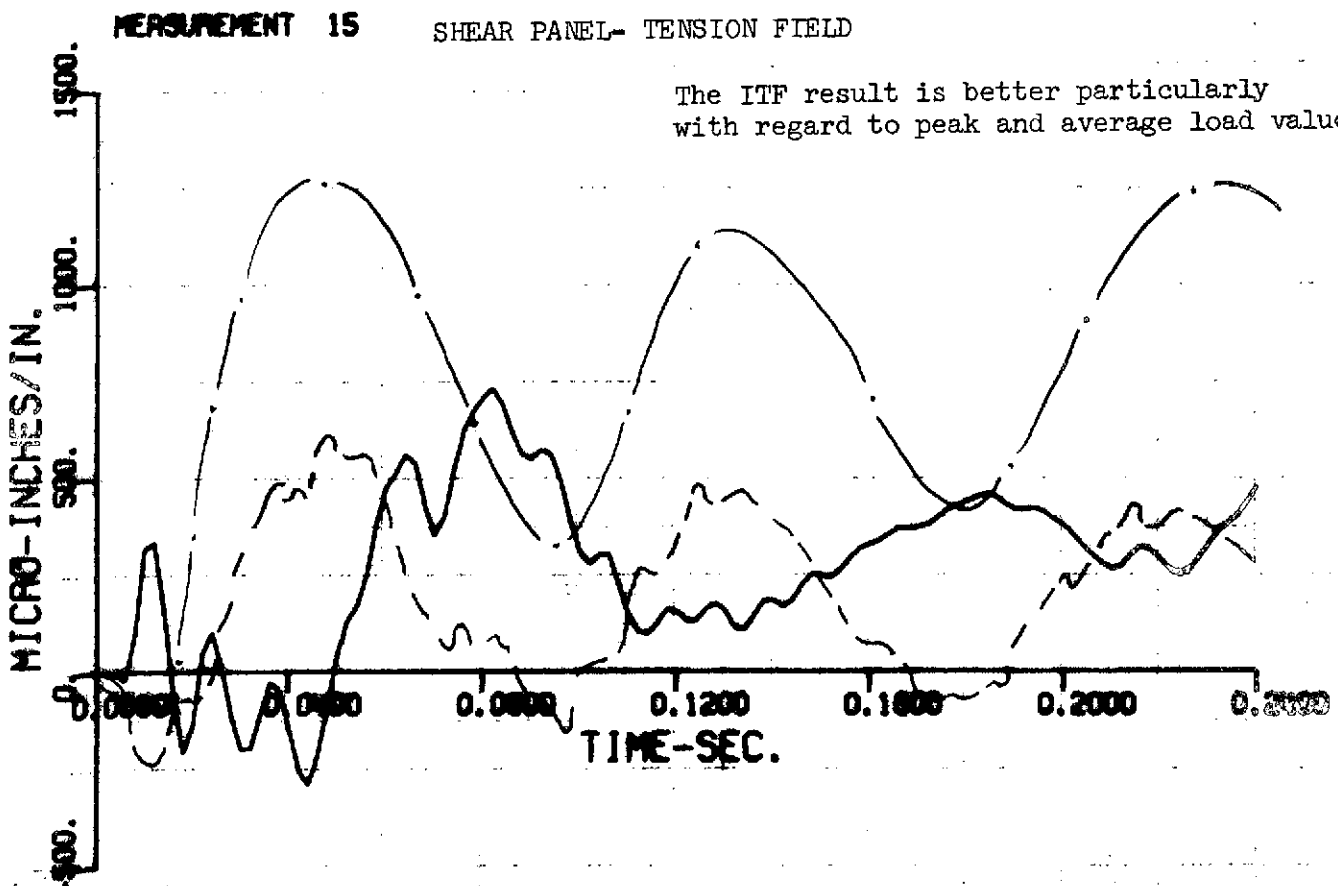
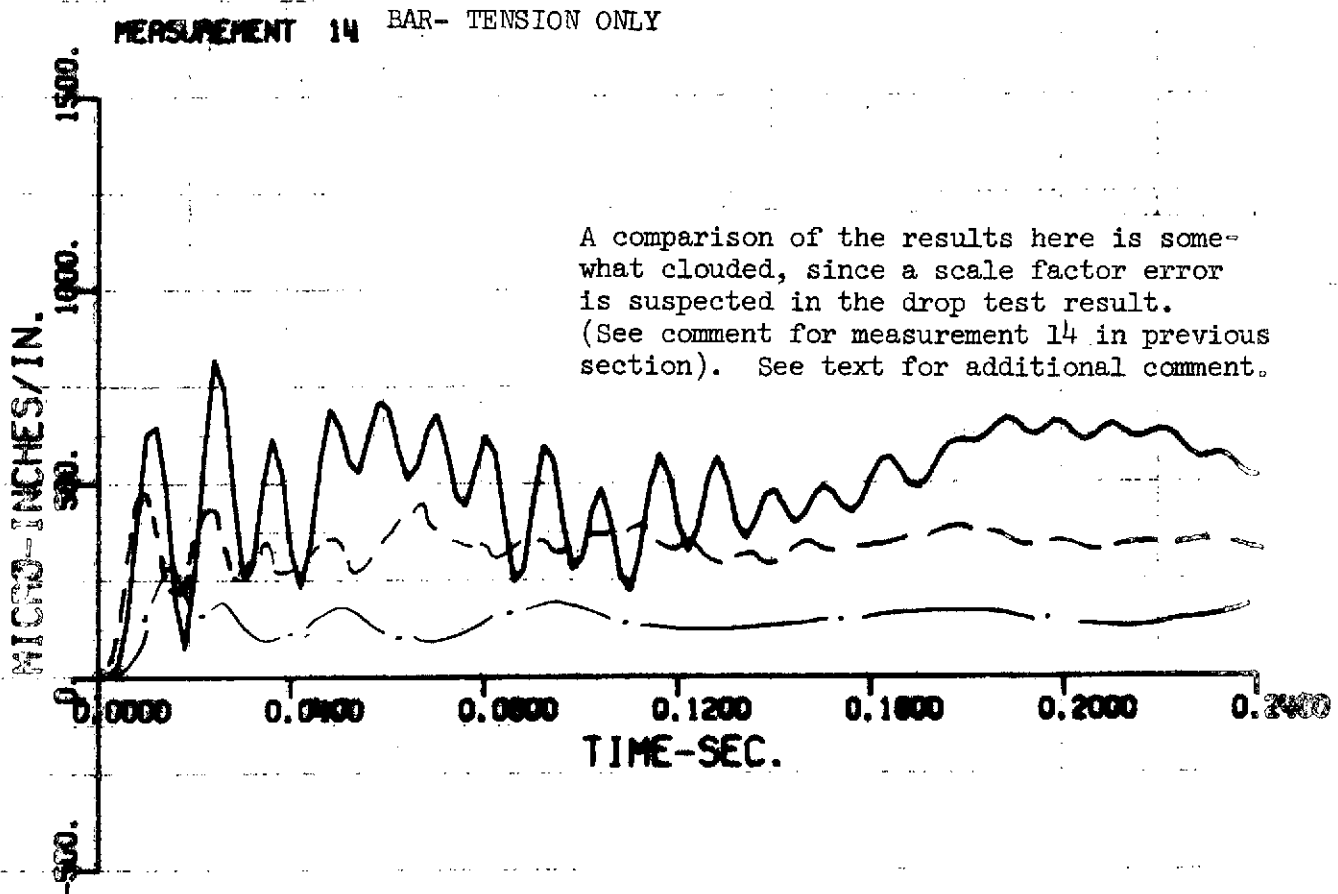


Figure 4b-1 Continued LTA-11 Drop Test Compared With ITF and Modal Analysis Predictions

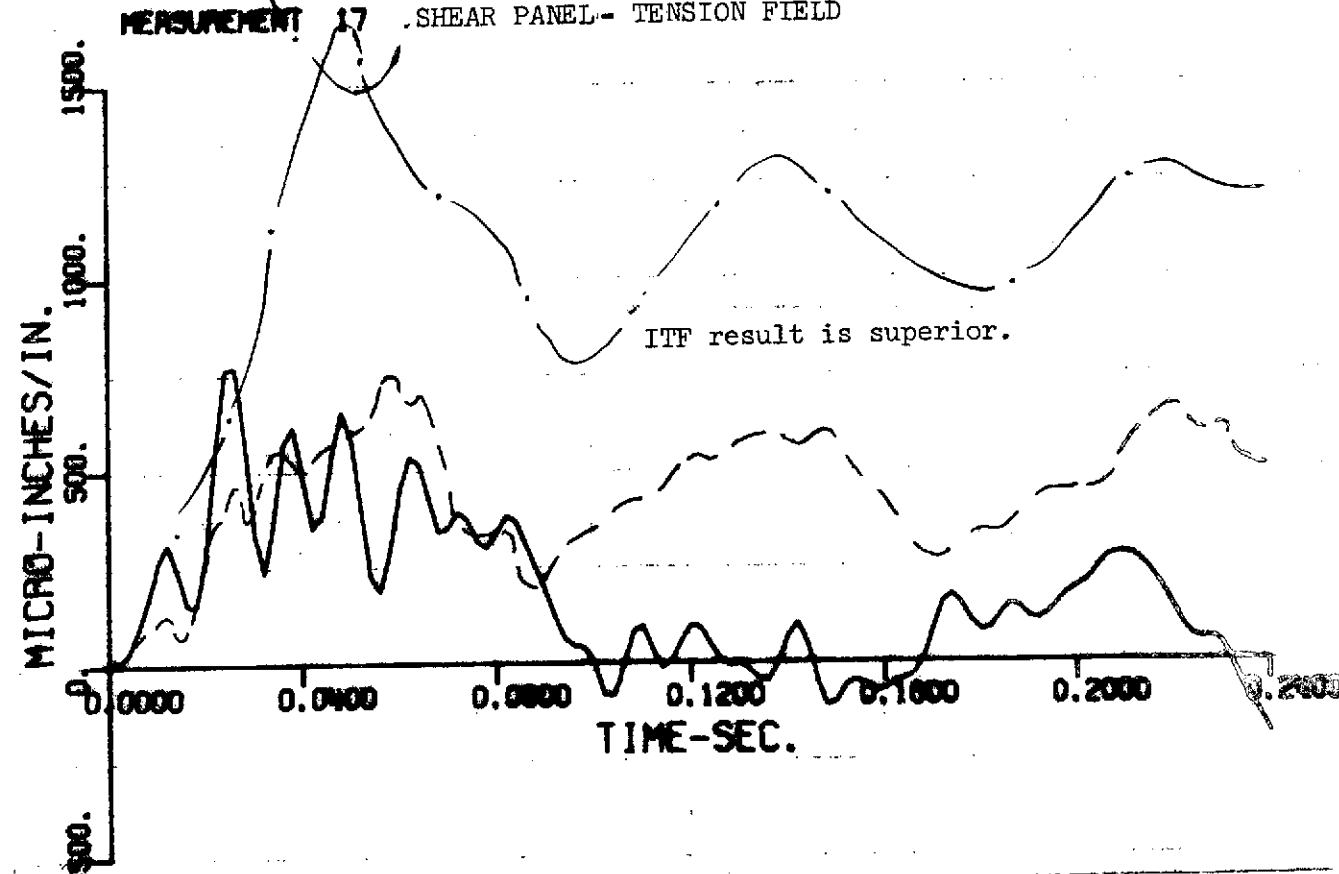
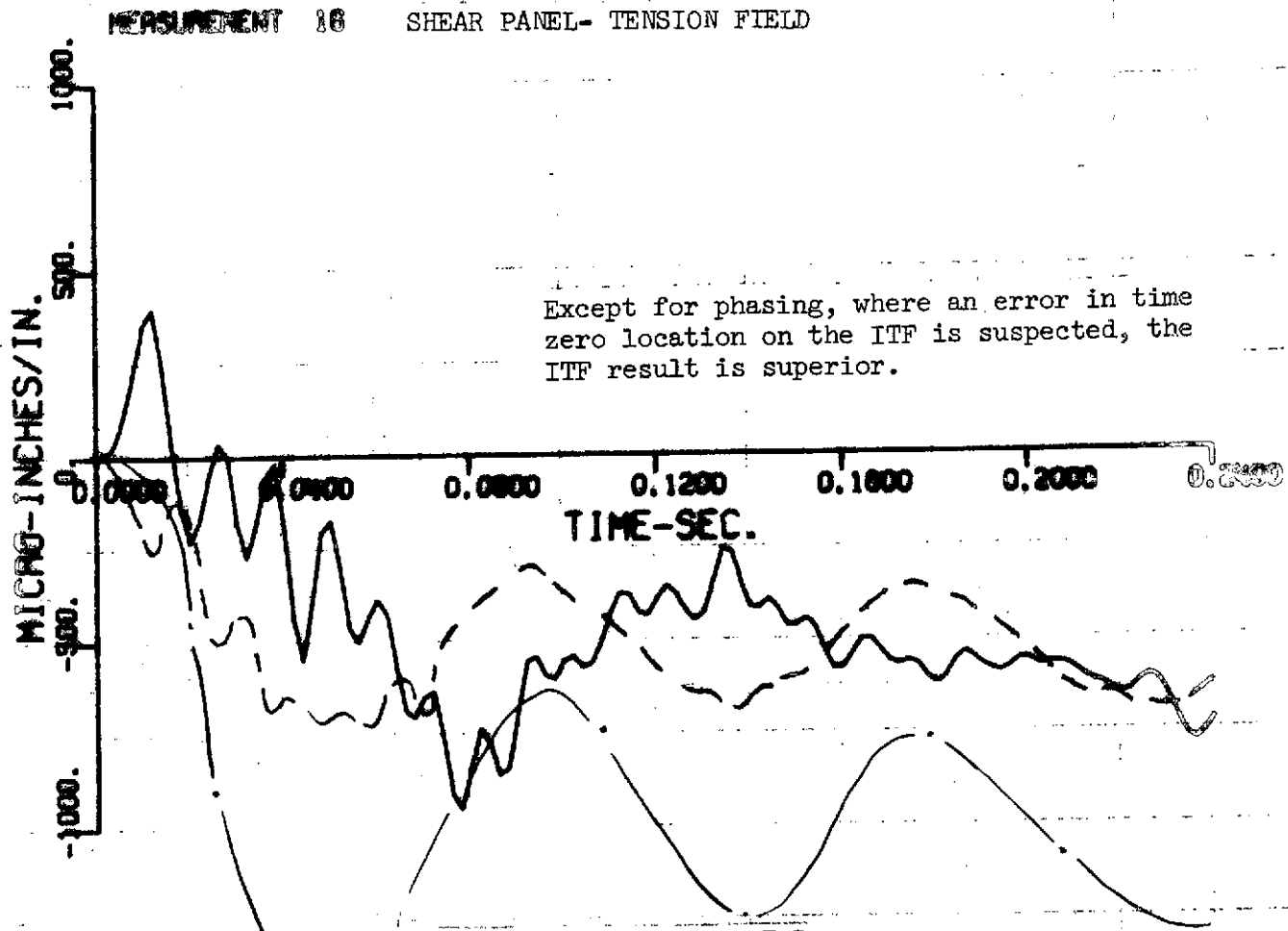
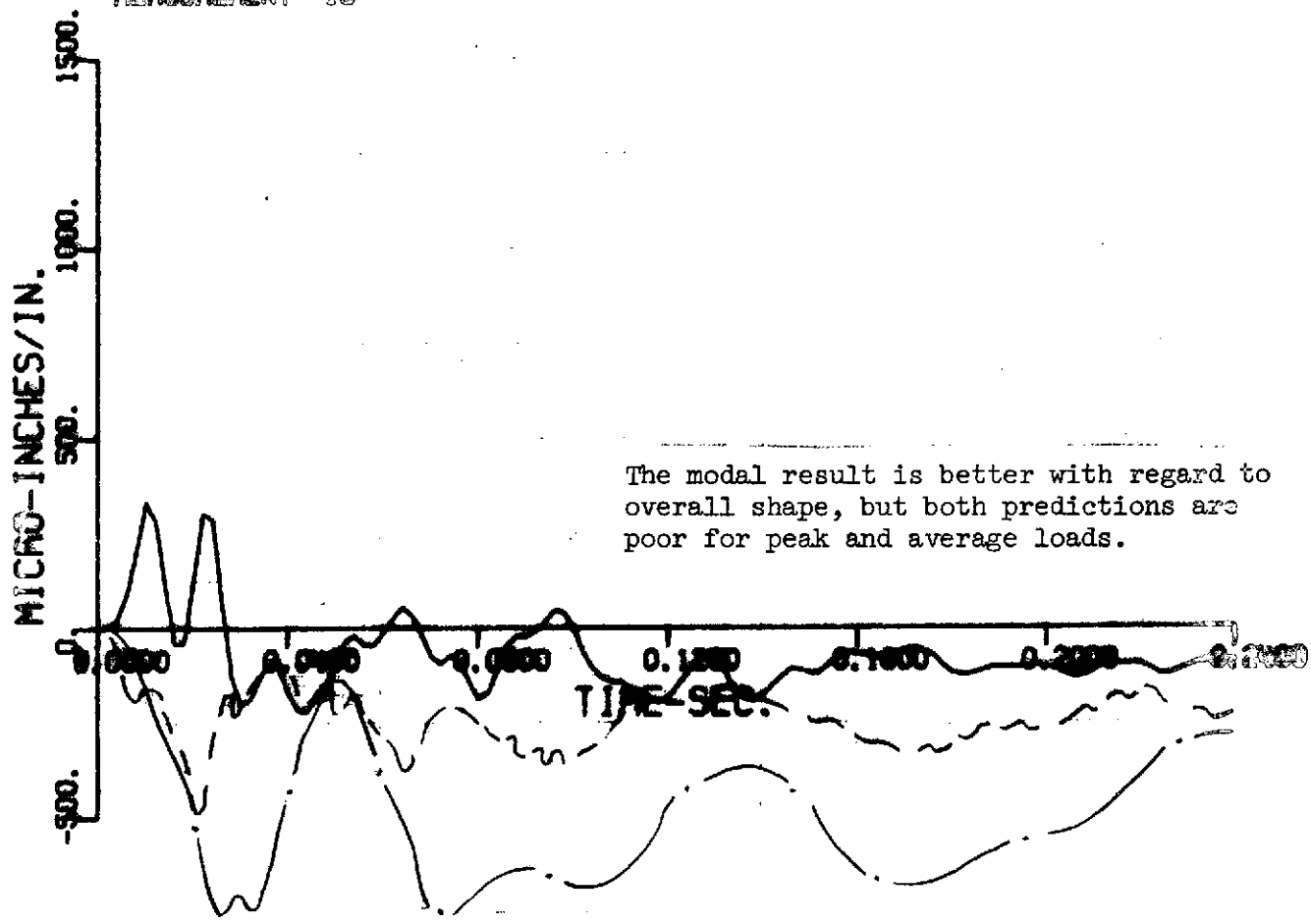


Figure 4b-1 Continued LTA-11 Drop Test Compared With ITF and Modal Analysis Predictions

MEASUREMENT 18 SHEAR PANEL- TENSION FIELD



MEASUREMENT 19 BAR

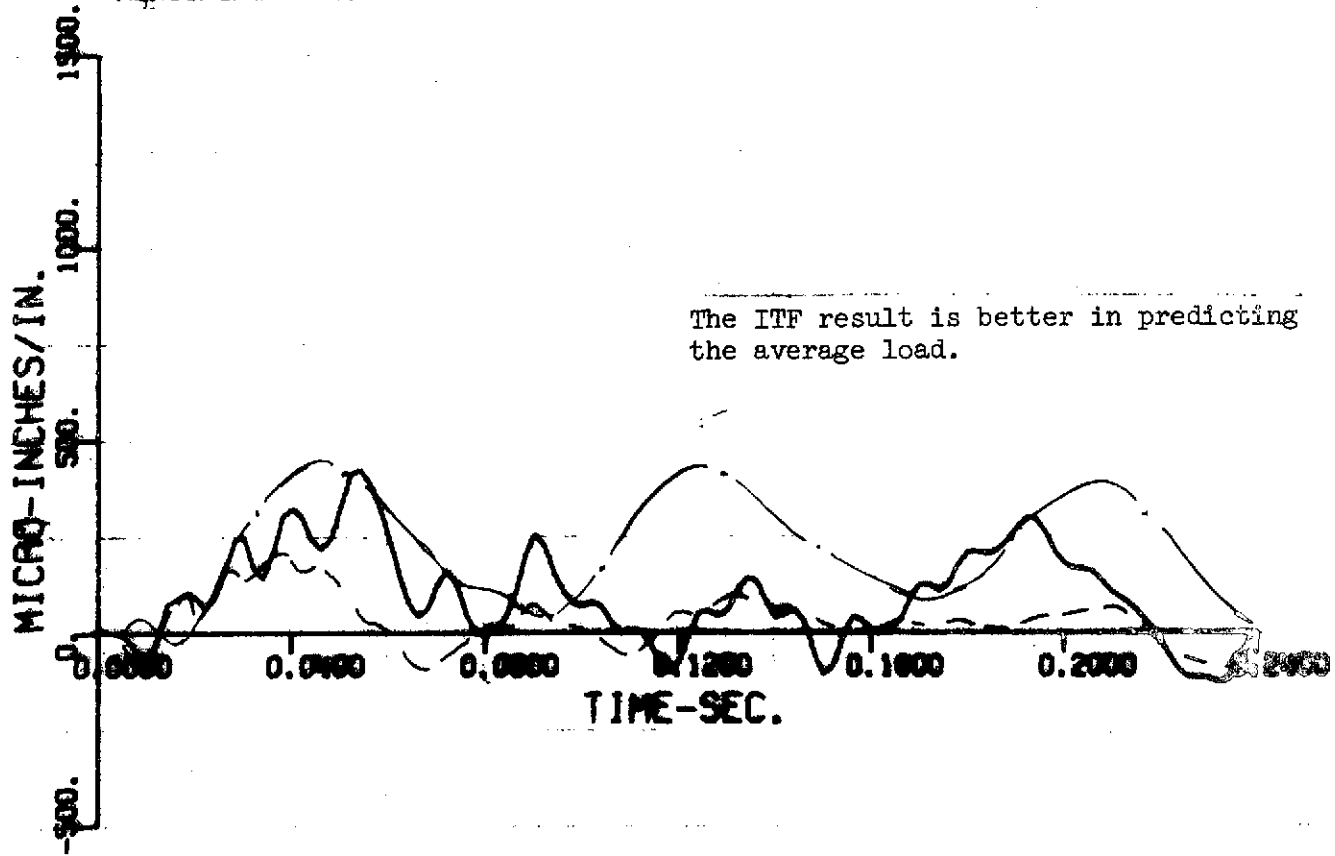
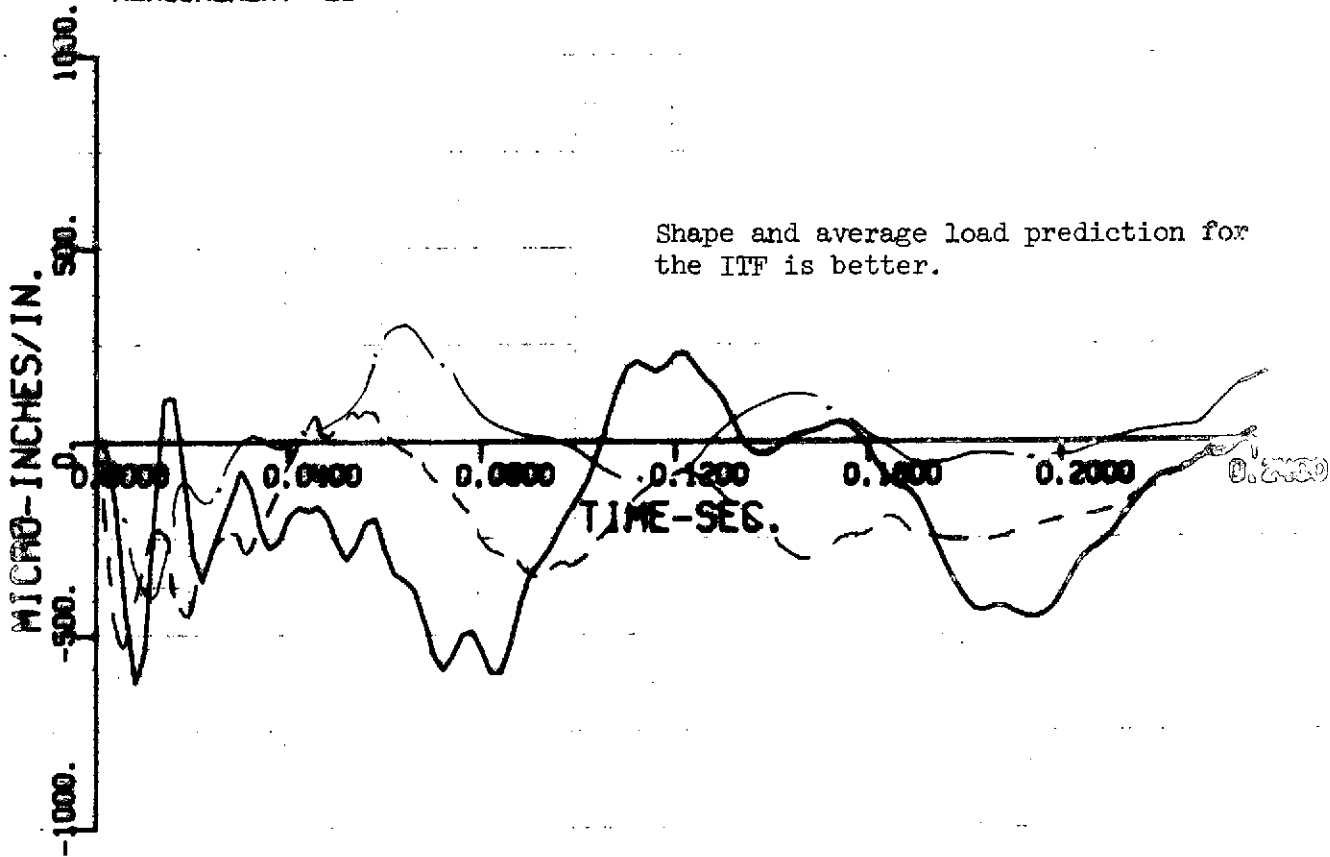


Figure 4b-1 Continued LTA-11 Drop 1

MEASUREMENT 20 BAR



MEASUREMENT 21 BAR

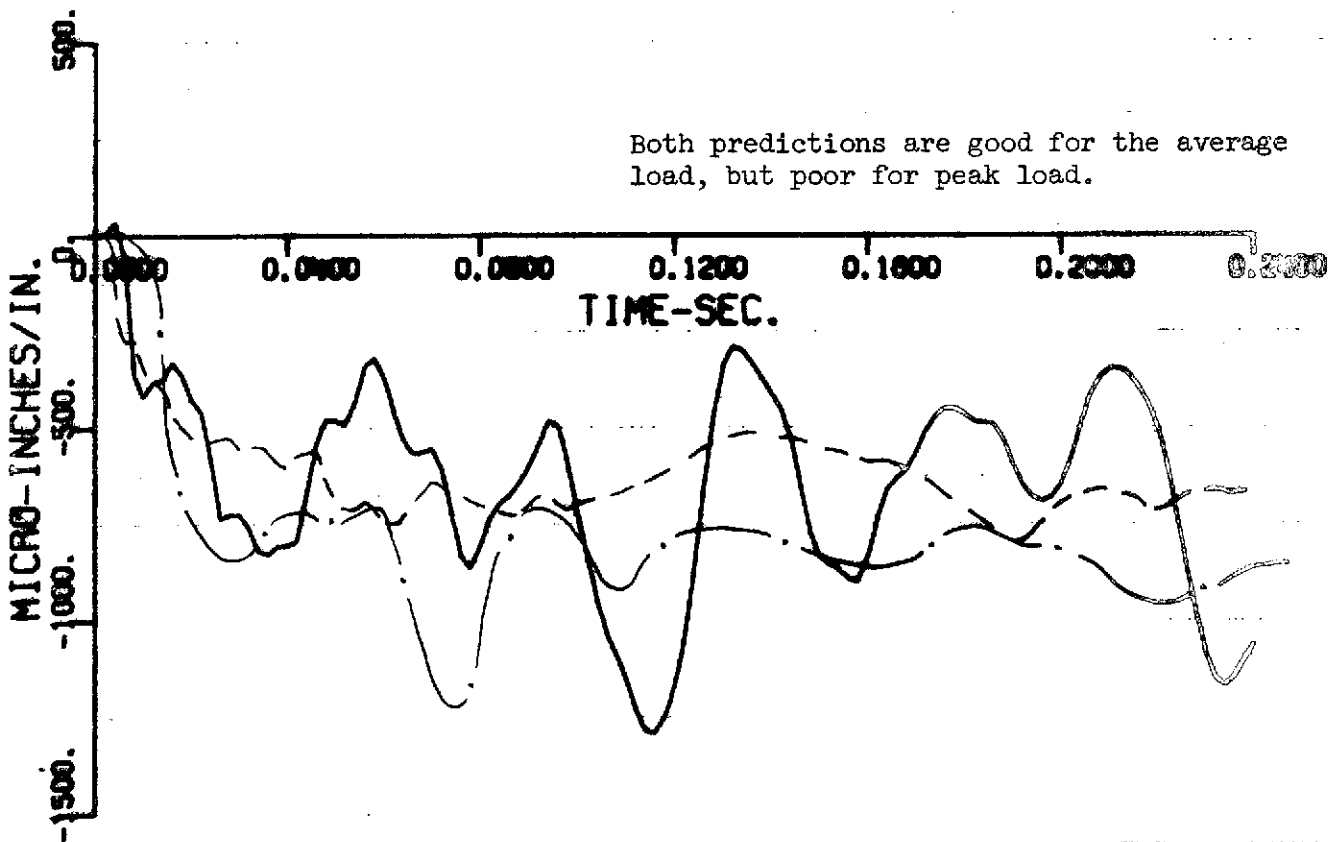
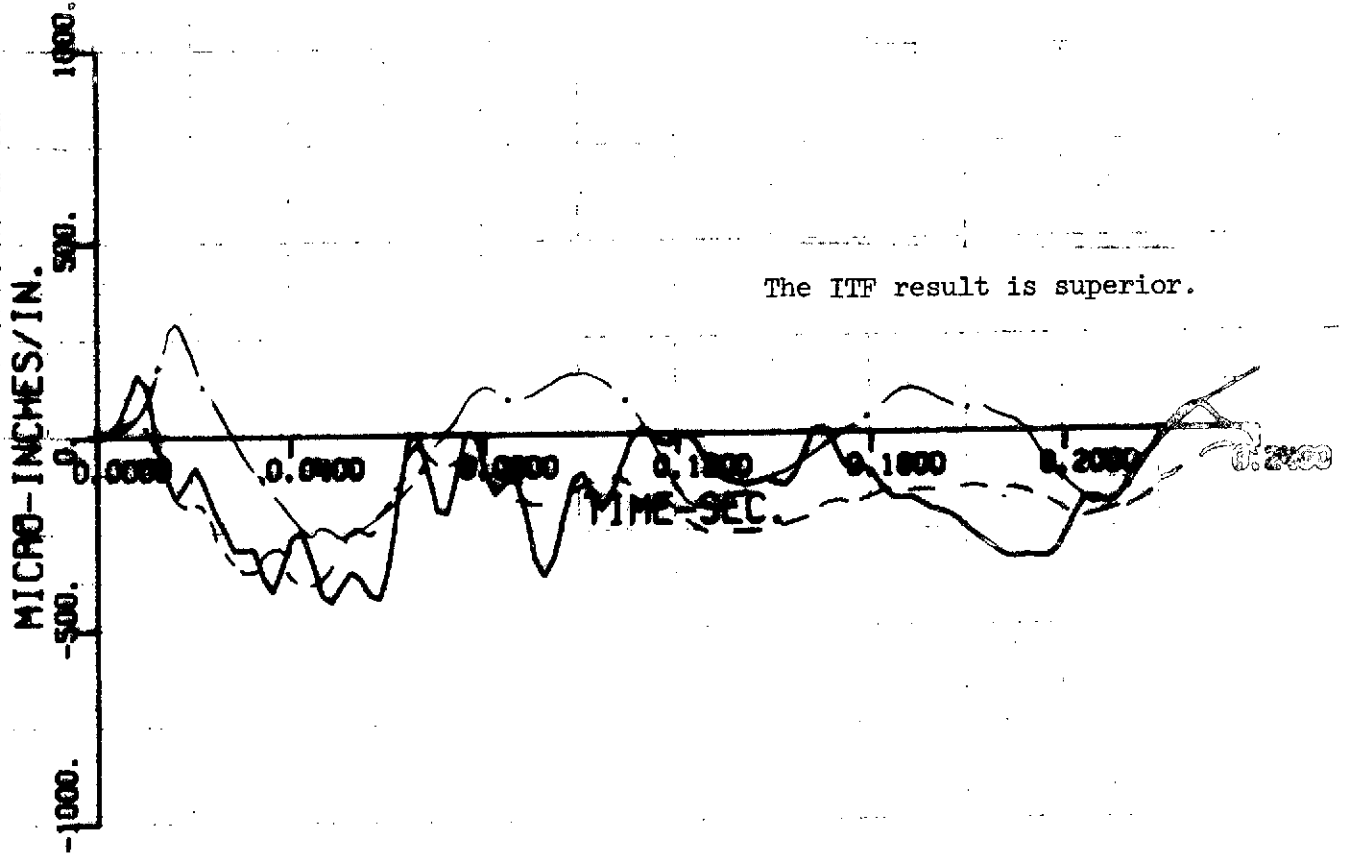


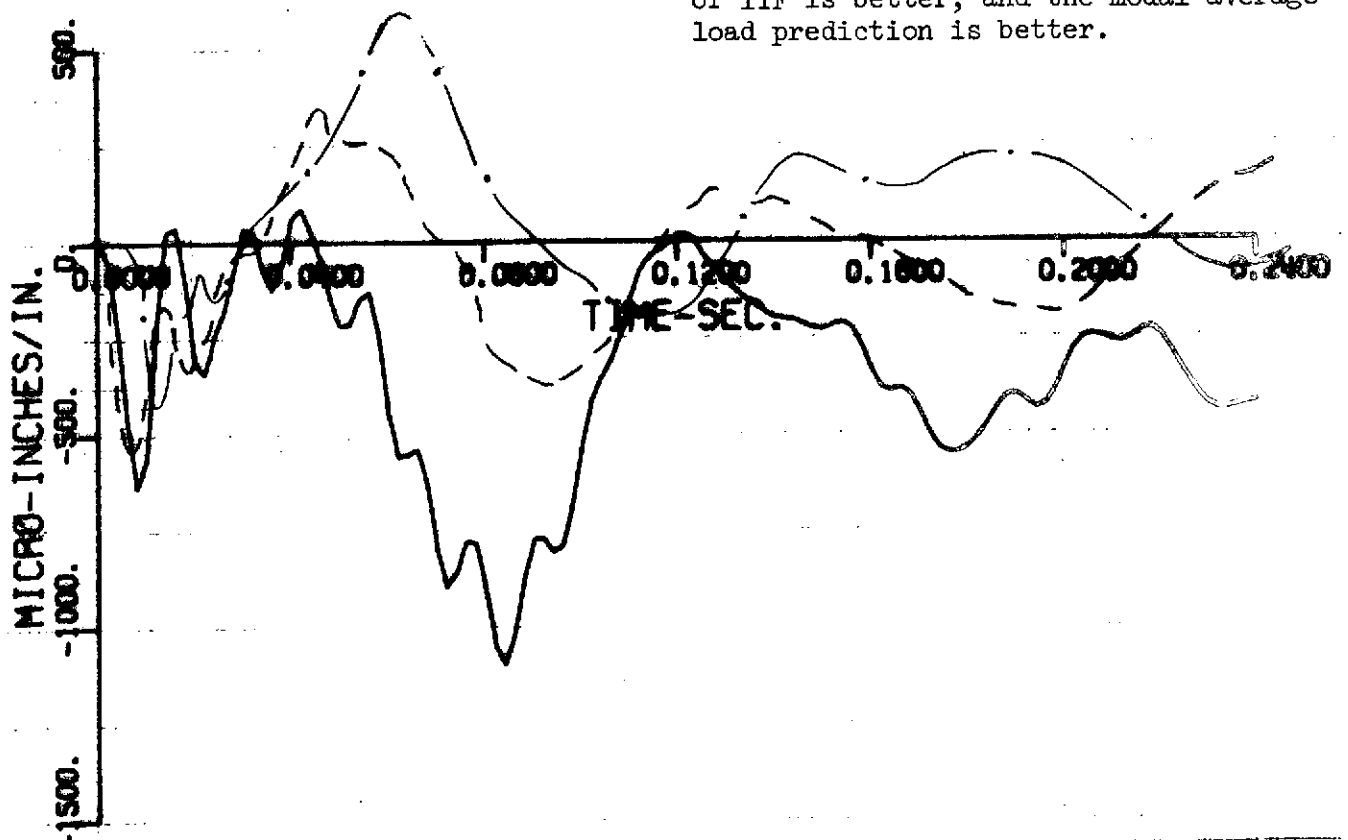
Figure 4b-1 Continued LTA-11 Drop Test Compared With ITF and Modal Analysis Predictions

MEASUREMENT 22 BAR



The ITF result is superior.

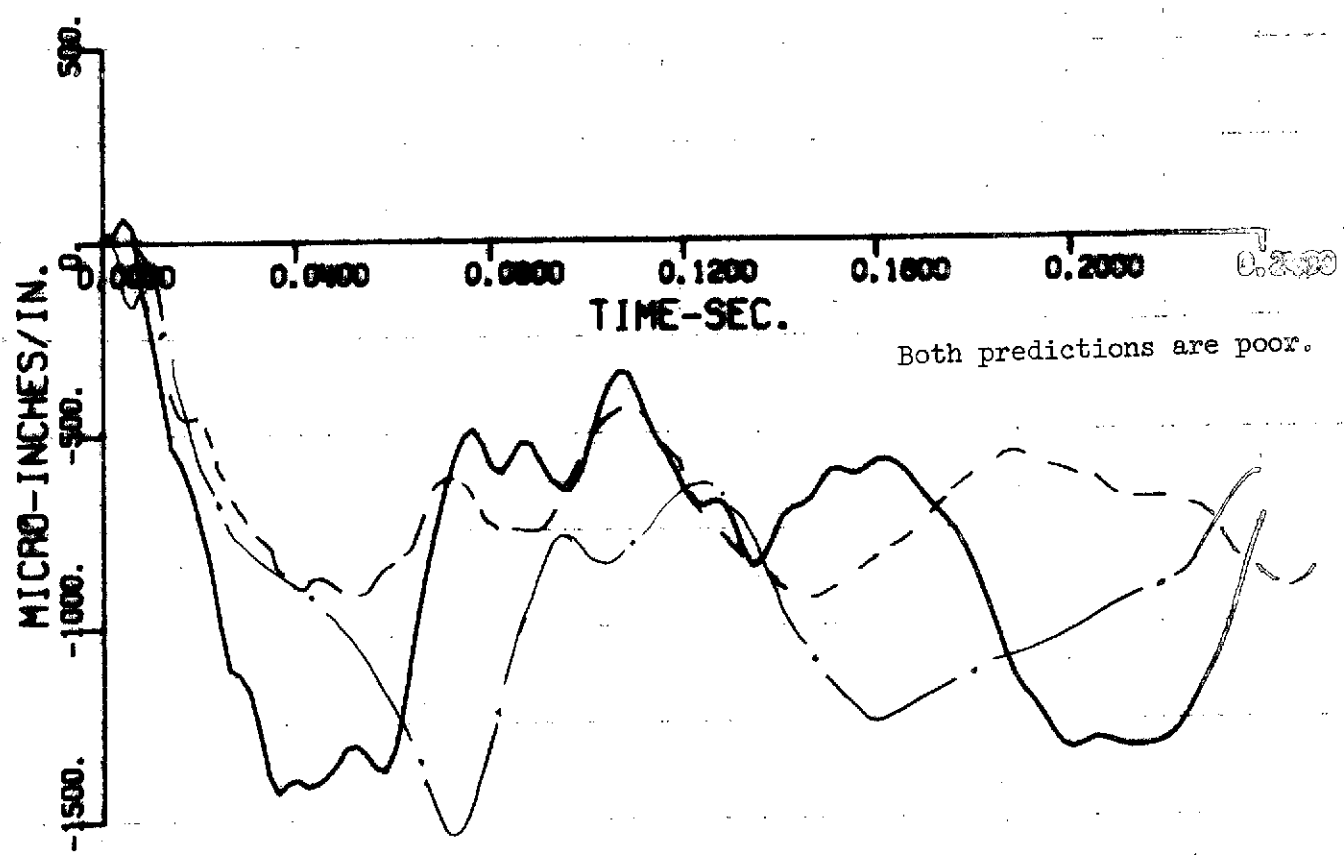
MEASUREMENT 23 BAR



The early high frequency peak prediction of ITF is better, and the modal average load prediction is better.

Figure 4b-1 Continued LTA-11 Drop Test Compared With ITF and Modal Analysis Predictions

MERSUREMENT 24 BAR



MERSUREMENT 25 BAR

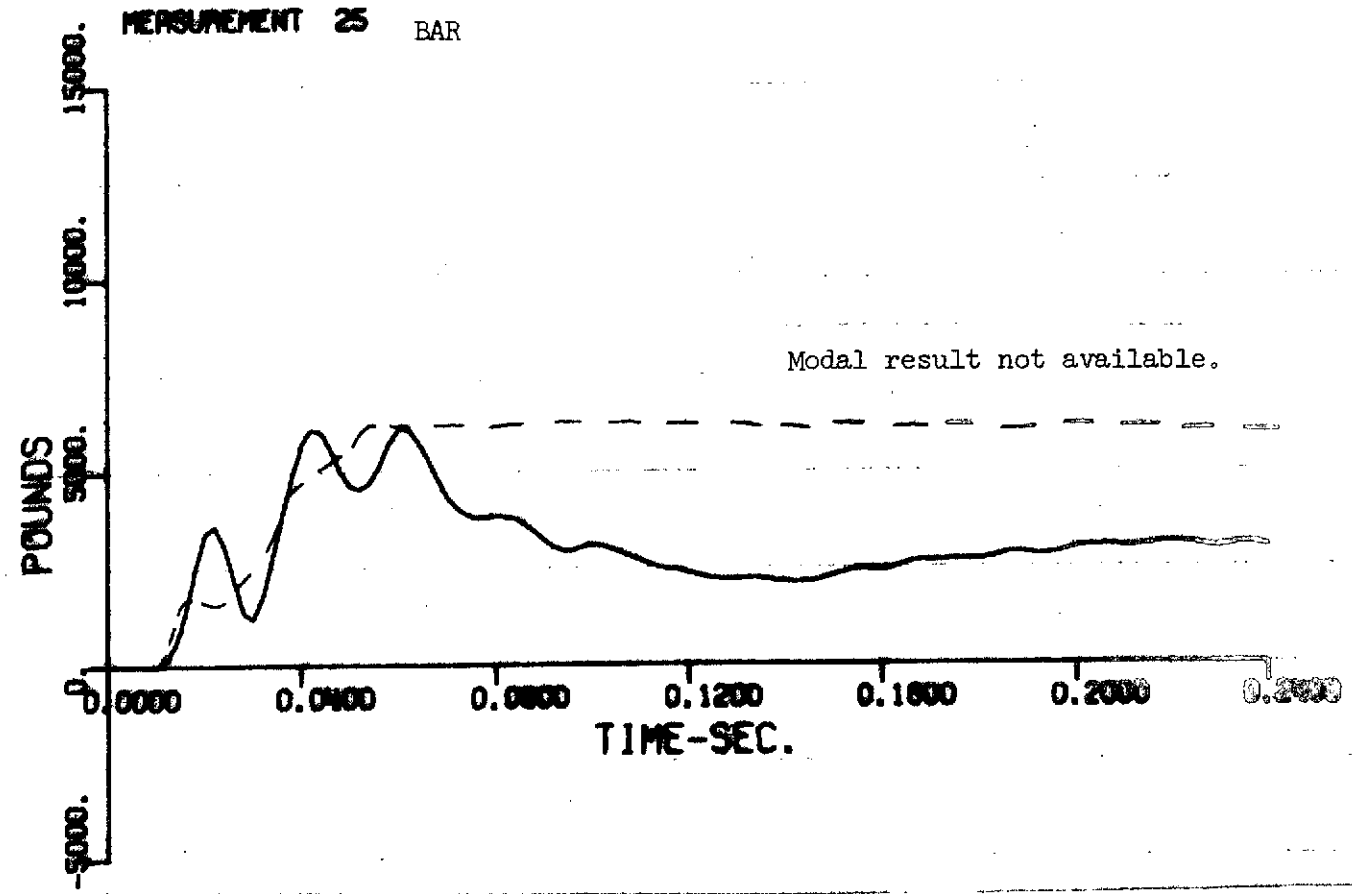


Figure 4b-1 Continued LTA-11 Drop Test Compared With ITF and Modal Analysis Predictions

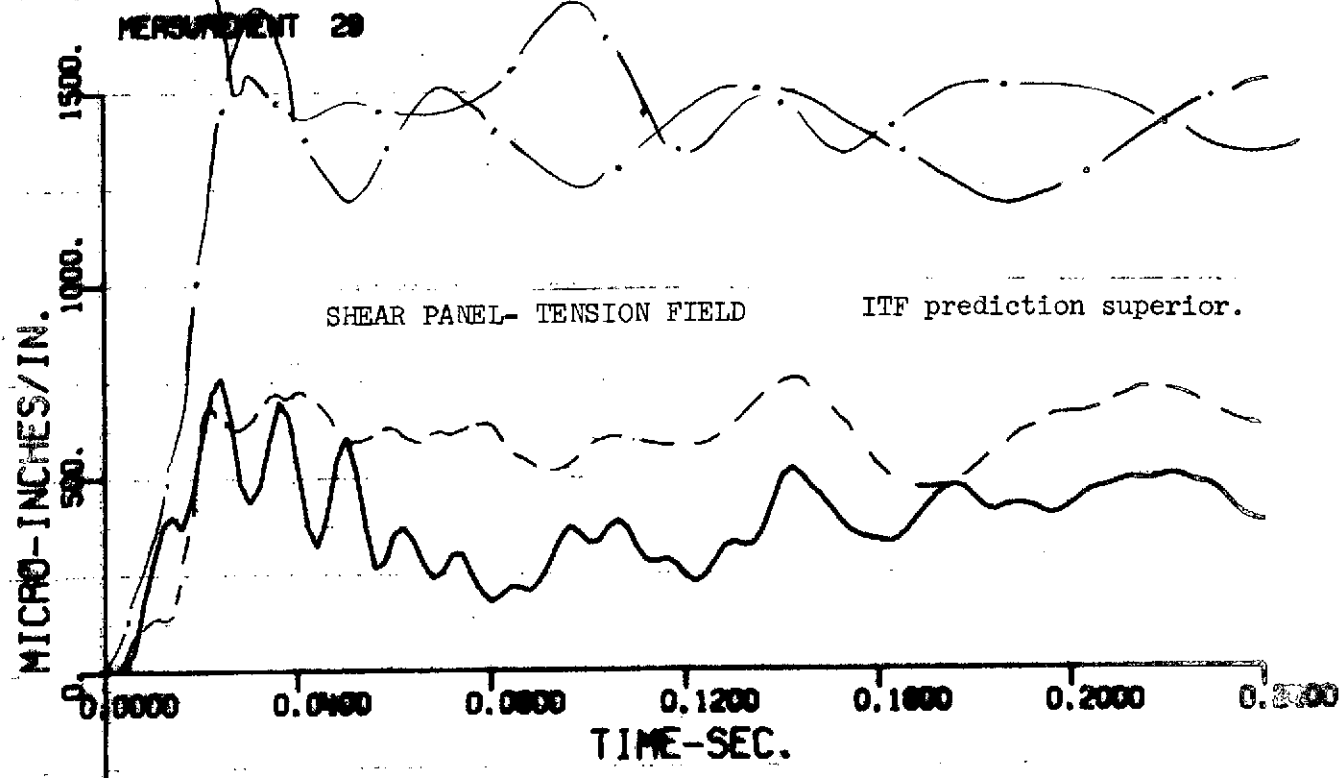
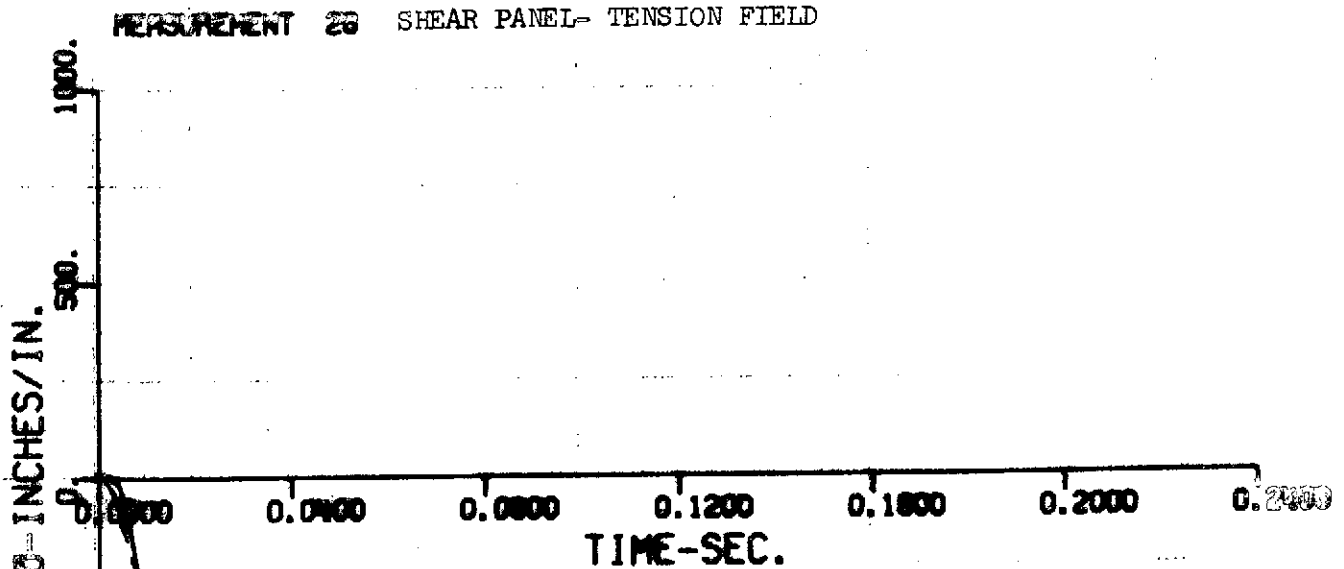


Figure 4b-1 Continued LTA-11 Drop Test Compared With ITF and Modal Analysis Predictions

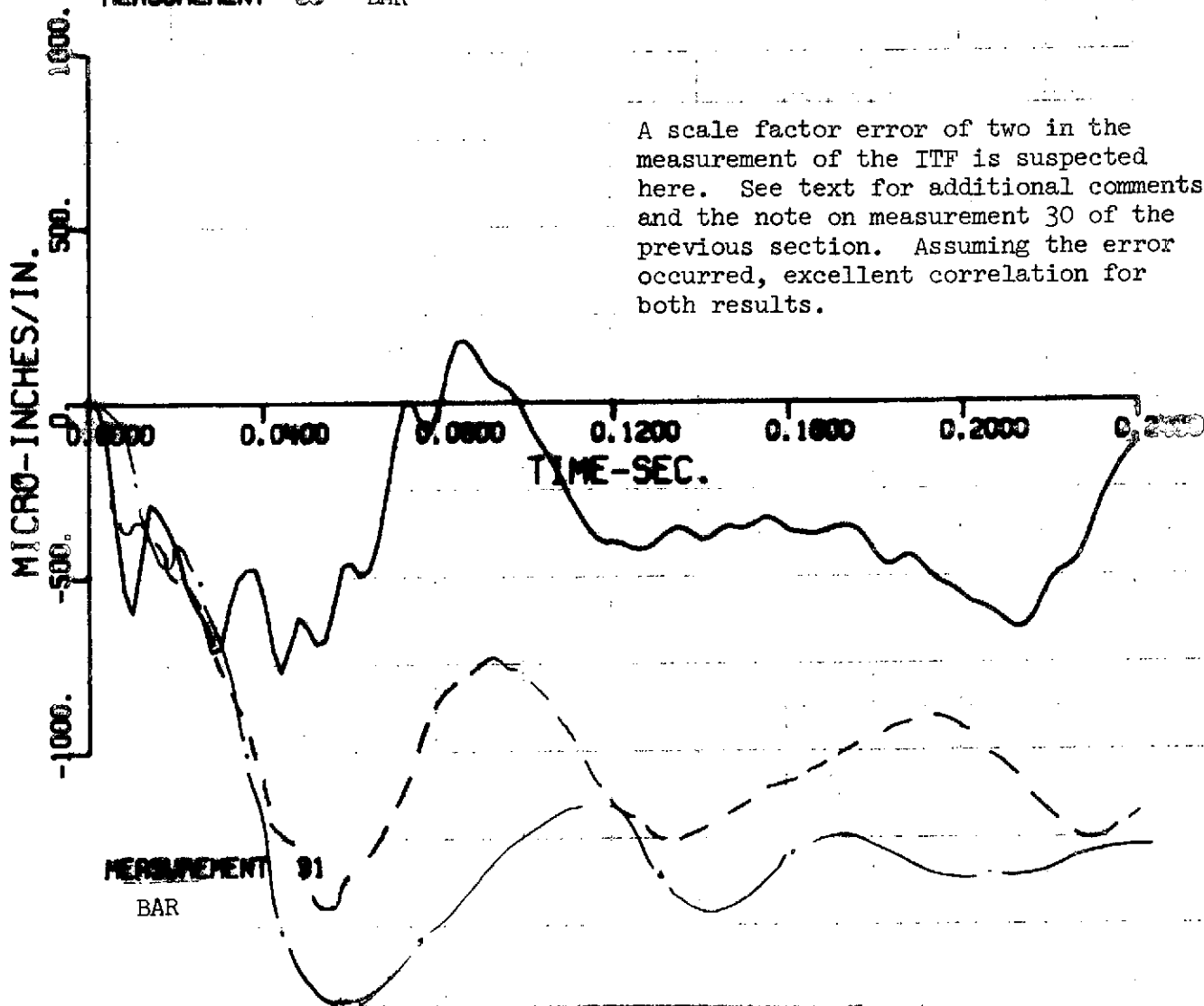
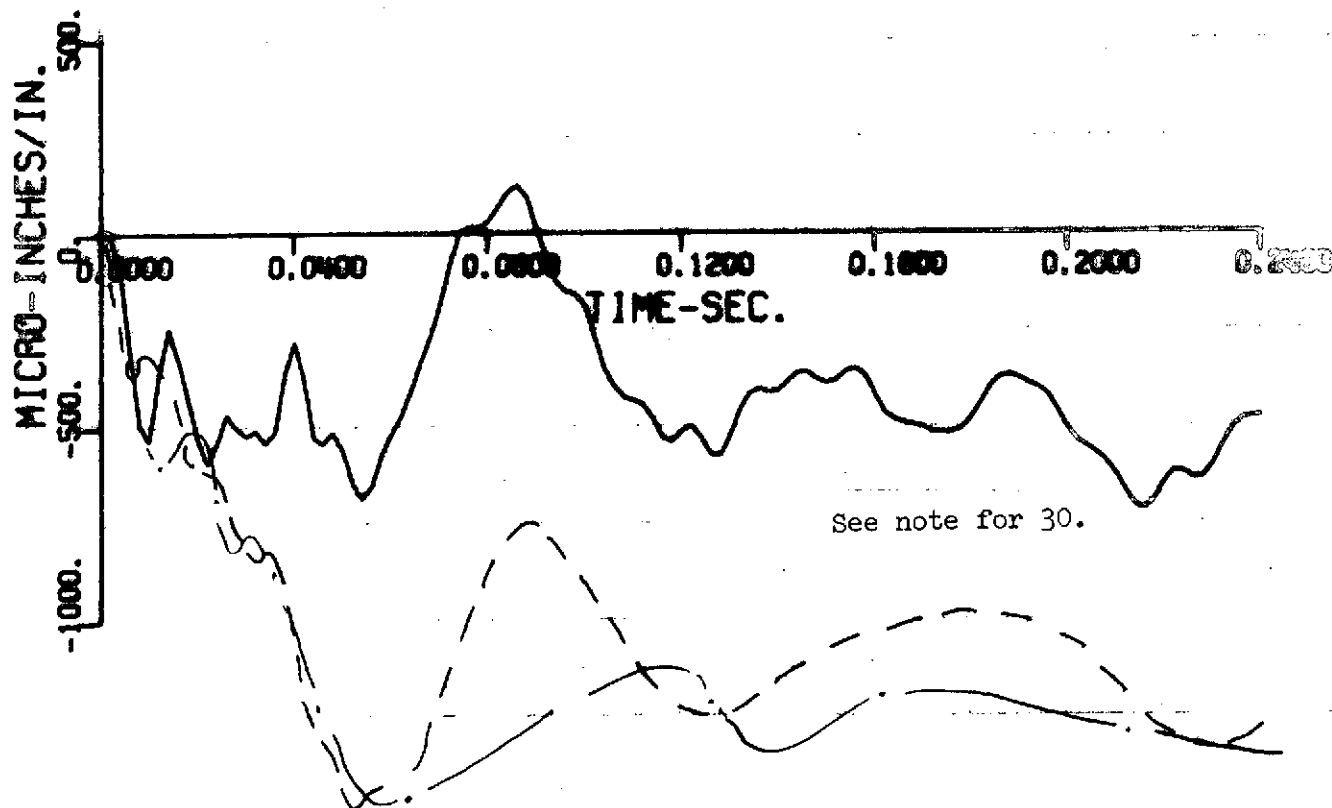


Figure 4b-1 Continued LTA-11 Drop Test Compared With ITF and Modal Analysis Predictions



#### 4c - LM Modal Characteristics From ITF Data

The TRW effort to obtain LM modal characteristics from ITF data is described in detail in References 2 and 3. TRW's procedure determines frequency, damping, modal mass, and mode shape from ITF data. For this computation Grumman supplied 3 seconds of data (3000 points) for accelerometer measurements 42 through 68, and for impulses 4, 13, 17, 18, 19 and 24; data on the measurements and the impulses is given in the Appendices. The frequency determination was reasonably good, and is shown in the accompanying table along with the LM mode survey result for the lowest five modes.

	Frequency, HZ				
TRW	8.4	8.9	11.75	12.3	13.8
LM Mode Survey	7.9	9.3	10.2	12.	13.

Mode shapes, however, were inconsistent and correlated poorly. Mode survey results are given in Appendix F.

Considering the complexity of the LM structure and the fact that this was the first large scale serious attempt at using ITF data for determining modes, this part of the effort may have been too ambitious an undertaking. It is felt that the present analysis would have yielded much better results for simpler, more regular structures such as a wing, fin or stabilizer.

One of the areas in which it is felt a modest amount of development work could improve results considerably is improving the Fourier Transform technique. A key feature of the TRW procedure is to transform the ITF time history to the frequency domain. The transform method used had two significant restrictions. It could handle only a number of data points at an integral power of 2, and the frequency increment is restricted to the reciprocal

of the total time in the time history. These problems are discussed more fully in Reference 2. One restriction was met by using the first 2048( $2^{11}$ ) points of time history; thus the frequency increment in the transform was approximately .5 Hz. Since the modes of interest were closely spaced in the region of 8 to 13 Hz, high order polynomial curve fitting was performed to overcome the coarse frequency increment. Referring to the frequency results above, except for the third mode (10.2 Hz), all the other TRW results correlated consistently within the frequency increment. It is also known that the mode shape prediction degrades much more rapidly than the frequency prediction with reduced time history availability. Considering the cumulative effect of these restrictions it's not surprising that the mode shape predictions were poor.

Grumman has recently developed a transform program which eliminates the first restriction completely, without severely degrading computer time, and is presently working on making the frequency increment restriction less severe.

Another idea which may be useful in improving the accuracy of determining modal information consists of using IITF's from a number of impulses in a way that is analogous to the use of multiple shakers in a vibration test. For example, if an antisymmetric mode were sought in a shake test, shakers would be located and phased so as to excite only this type of mode. It appears that IITF's can be used analogously if responses from a number of impulses are appropriately combined prior to transformation to the frequency domain. Investigation of this approach would require additional development work and revision to existing computer programs.

### 5-CONSIDERATIONS FOR ITF TESTING THE SHUTTLE

Table 5-1 summarizes where it may be possible to utilize ITF testing in determining internal response to transient loading. The first column shows the various loading conditions in the overall Shuttle mission where transient response is of concern. The second column indicates the number of pulses that must be applied to the vehicle in order to define a complete set of applied loads. In the next column the total number of instrumentation channels is estimated. It is interesting to note that the maximum number of ITF time histories that would have to be handled for the estimates shown is 5400 for the landing condition, i.e., 27 applied pulses multiplied by 200 channels. The computer system developed under the present contract can handle this much data if the time interval for storing data were doubled; this would cause no problem for the frequencies of interest on the Shuttle.

The fourth column gives an estimate of the highest statically applied load that would induce internal load approaching limit values. The next column lists an estimate of the highest natural frequency mode that would be excited significantly by the loading condition. One and a half Hz is taken as the lowest natural frequency for all conditions. The data of these two columns is particularly important in estimating the magnitude (area) of the impulse that must be applied for tests of a given condition; subsequent paragraphs will discuss this topic more completely.

In the next to last column the vehicle configuration and the preferred manner of support are given. The suspension system and how it is designed and instrumented is an important consideration that is covered in Appendix A of this report. The last column of the table gives the maximum distance from the point of pulse application to a point where instrumentation may be placed, taking into consideration the load paths that response would travel through component interconnecting structure. Thus, as

is obvious in the table, a distance greater than the overall length of the vehicle is possible. While this column is not of prime importance, it does give an indication as to which conditions will be difficult to excite to measurable response levels.

Examination of the table shows that conditions from main engine startup through orbiter landing have been covered. (Docking is a notable exception. It has not been included in the table because little is known by the authors of the load levels or number of applied pulses necessary to define the applied loads. In any event, the loads associated with docking, and the number of channels and frequencies of interest, should offer no problems more difficult than those posed by conditions listed in the table. Thus, in considering the table as it presently stands, we are probably dealing with the docking problem as well.) Prelaunch conditions, hold-down release and SRB shut-down will be difficult to test because of the size of the configurations and the difficulty of exciting response to an applied pulse of practical size. The SRB shut-down condition where 600,000 lbs is considered limit applied load is the most difficult. Orbiter landing, on the other hand, will most probably be the easiest to cope with. The reasons for this are: the vehicle would be horizontal facilitating application of the impulses; the vehicle is relatively simple; and, the force levels are reasonably low.

A primary question in Shuttle testing is to determine the magnitude and time duration of the impulse necessary to excite measurable response. The following discussion is aimed at providing a method for making the required determination.

Consider a single degree-of-freedom, undamped, mass-spring system subject to an initial velocity and zero initial displacement. The displacement,  $x$ , of the mass is:

$$x = \frac{v_0}{\omega} \sin \omega t \quad (5-1)$$

where  $v_0$  is the initial velocity and  $\omega$  is the natural frequency of the system. For impulse/momentum considerations, and equivalent impulse would be equal to the mass,  $m$ , times  $v_0$ . Substituting  $v_0 = I/m$  into Eq. 5-1 gives:

$$x = \frac{I}{m\omega} \sin \omega t \quad (5-2)$$

Substituting  $m\omega^2 = K$ , the spring stiffness, and rewriting, the spring force can be written as:

$$Kx = I\omega \sin \omega t \quad (5-3)$$

and the maximum spring force can be defined as:

$$(Kx)_{\max} = I\omega \quad (5-4)$$

Now, consider a long-duration force whose maximum value is  $F_0$  (fourth column of Table 5-1). If this force were applied statically to the system, the spring force would be equal to  $F_0$ . We now can form a ratio,  $R$ , which is the maximum dynamic force in the spring to a static value, or:

$$R = \frac{I\omega}{F_0} \quad (5-5)$$

Let us rewrite Eq. 5-5 in terms of frequency,  $f$ , whose units are Hz,

$$\frac{I}{F_0} = \frac{R}{2\pi f} \quad (5-6)$$

Equation 5-6 defines an impulse magnitude necessary to obtain a given portion,  $R$ , of the statically induced spring force for a system with a natural frequency,  $f$ .

Setting aside Eq 5-6 for a moment, let us consider how a single degree-of-freedom system responds to a realistic pulse of finite duration as compared to a theoretical impulse. Reference 5 discusses this matter in some detail for a single degree of freedom system. Figure 5-1, which is taken from this reference, shows the error in peak response as a function of the ratio of pulse duration, ( $\tau$ ), to system natural period,  $T$ . From this figure for a triangular shaped pulse the following data can be found:

<u>% Error (E)</u>	<u><math>\tau/T = \tau f</math></u>
1	.113
2	.157
5	.245
10	.360
15	.443

(A triangular pulse shape has been selected for study since it is representative of the pulse shape obtained in IM testing. Further, little difference exists in the errors associated with a half-sine pulse and a triangular pulse.) Now, the impulse magnitude can be expressed in terms of the peak of the triangular pulse,  $F^*$ , i.e.,

$$I = 1/2 F^* \tau \quad (5-7)$$

Dividing both sides of Eq. 5-7 by  $F_0$  gives

$$\frac{I}{F_0} = \frac{F^*}{F_0} \frac{\tau}{2} \quad (5-8)$$

The error data, and the relationships of Eqs. 5-7 and 5-8 have been plotted in Figure 5-2. The upper right quadrant of the figure shows the relationship given by Eq. 5-8; the upper left quadrant depicts the relationship given by Eq. 5-6; and the lower right quadrant is a graph of the error data for a triangular pulse that is tabulated above.

Figure 5-2 is very useful as an aid in determining impulse requirements for the loading conditions of Table 5-1. For example, consider the main engine start condition. Let us assume that 30,000 lbs is the peak force the impulse generator can supply; thus  $F^*/F_0 = 30,000/115,000 = .26$ , shown as the dashed line in Figure 5-3. Table 5-1 shows that the highest frequency of interest is 15 Hz. If error, E, is limited to 2% the illustrative construction lines of Figure 5-3 can be drawn.

Using 30,000 lbs as the maximum pulse force, the representative data shown in Table 5-2 can be derived. While the data shown in this table is somewhat arbitrary with respect to error, peak impulse force, and induced response, it does give reasonably representative values of the impulse magnitude, peak force level and duration that will be required for the Shuttle. Of course, when firm data on the Shuttle characteristics becomes available, Figure 5-2 can be used to establish final requirements.

Once final impulse requirements are established, impulse generating equipment can be selected. Several considerations will enter into the selection. Among the most important considerations will be the peak force level and the time duration, as well as portability and maneuverability for a particular test condition. At Grumman three devices seem most appropriate for the Shuttle:

- Electrodynamic Shaker
- Hydraulic Shaker
- Stress-wave Riveter

The electrodynamic shaker, programmed to supply an impulse peak force level of about 10,000 lbs and a time duration of 1 millisecond, has been used

in all testing performed to date. This type of shaker can probably be used for output to 30,000 lbs, where the time duration will be limited by the 1/2 inch of stroke available at the shaker head. Thus, data on suspension characteristics and local flexibility will be required before the electrodynamic shaker can be selected for time durations of 10 or more milliseconds.

Electrodynamic shakers of the size used in IM testing have a significant disadvantage with regard to portability. They require a fairly extensive power supply and cooling source, and are difficult to maneuver because of their weight. However, we know they are reliable and have had a significant amount of worthwhile experience in their use.

Hydraulic shakers, to our knowledge, have not been used for impulse generation. However, they appear to have the advantage of long, adjustable stroke and may have an application for use in cases where relatively long time durations are needed.

The Stress-wave riveter is a Grumman developed device for driving rivets with one blow that exhibit improved fatigue life. The device is relatively light (under 100 lbs) and is driven by a modest, portable power supply. Time durations where this device has been used have ranged to 1 millisecond; force levels have been as high as 30,000 lbs.

The procedure we envision for implementing ITF testing for the Shuttle would be along the following lines and in the following rough sequence;

1. Identify dynamic problems where ITF testing can be helpful in the project.
2. Examine existing or scheduled instrumentation and support fixtures in use for ground vibration surveys or other dynamic test and then develop ITF test objectives and schedules.
3. Based on structural data and the data of Table 5-1 and Figure 5-2 establish impulse requirements.
4. Depending on impulse magnitude, initiate a test and analysis program to select impulse generating device. This should be a modest program that could be performed in a few months prior to actual testing.

5. Prepare test plans, design and fabricate any additional fixtures and perform tests.

Another area of possible application of the ITF method is in determining modes from ITF data for special problems. This subject is discussed in some detail in another section of this report.

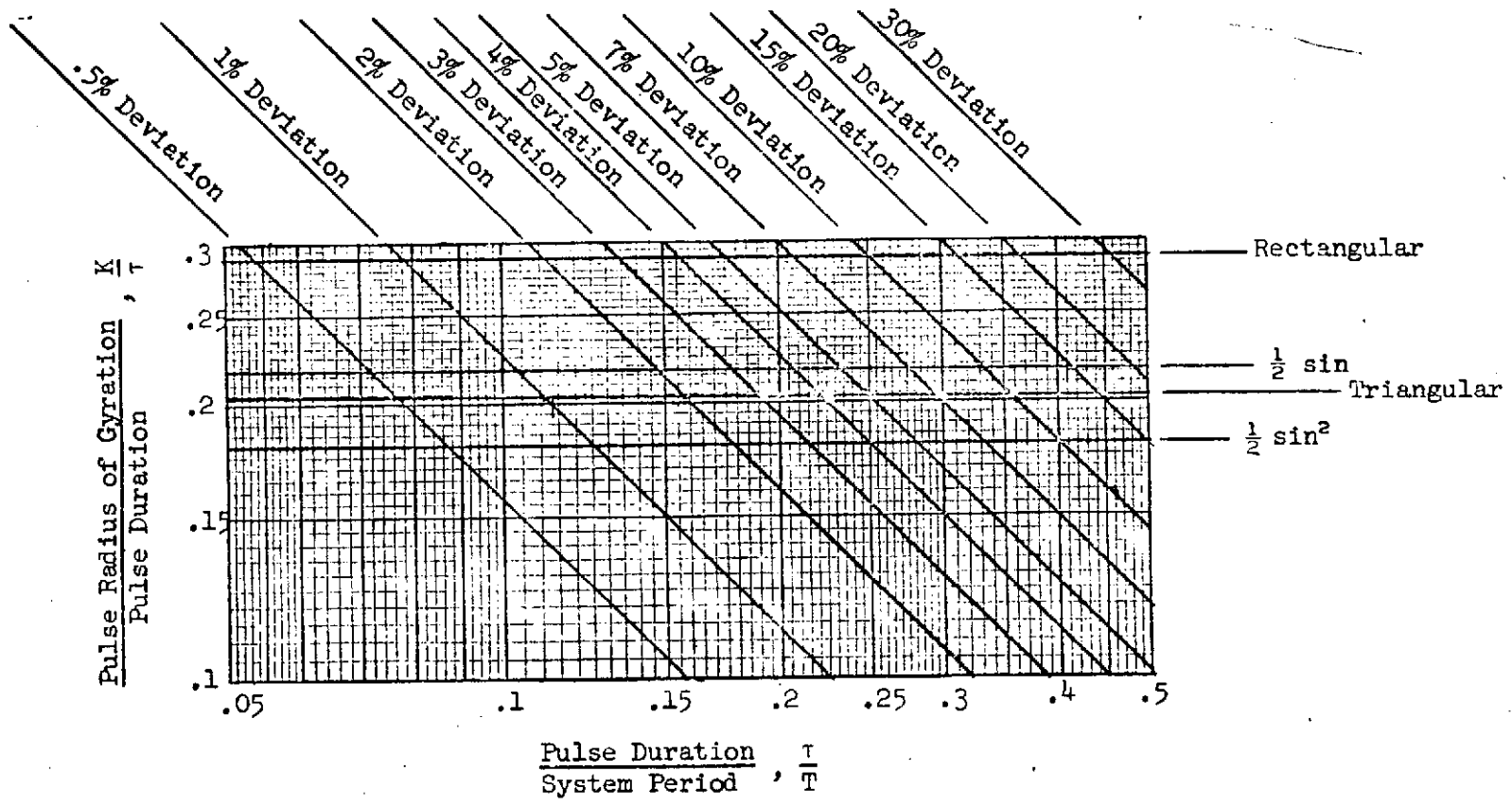
Table 5-1 Possible Application of ITF Method in the Shuttle Program

Loading Condition	No. of Applied Pulses	No. of Responses	Estimated Max Force For Limit Load (Lbs)	Highest Frequency of Interest (Hz)	Vehicle Config. & Support Condition	Max. Distance From Pulse Application Point (In.)
Prelaunch - main engine start & shutdown	9 - (3 ea. at 3 pts.)	~ 400 (~ 200 on orbiter)	115,000	15	Orbiter mounted on booster which is restrained by hold-down mechanism	1500 to Fwd orbiter interstage
Hold-down release	8 - (1 ea. at 8 pts)	~ 400	195,000	15	Launch config.; free-suspension	4000 to orbiter interior; 1600 to ext. tank
SRB Shut down	12 - (1 ea. at hold-down pts. on SRB & 1 at ea. gimbal actuator)	~ 400	600,000 (could use lower value if full decay were not required)	20	Post-launch config.; free suspension	4000 to orbiter interior; 1600 to ext. tank
SRB staging	12 - (6 on SRB & 6 on E.T. at junction pts.)	~ 50 on SRB ~ 100 on E.T. ~ 200 on orbiter	100,000	30	SRB in free suspension, orbiter attached to E.T. in free suspension	2400 to orbiter interior
Orbiter staging	12 - 6 on orbiter & 6 on E.T. at Matching locations	~ 200 on orbiter ~ 100 on E.T.	100,000	30	Orbiter in free suspension, E.T. in free suspension	1300 on orbiter; 1300 on E.T.
Orbiter Engine shut down	9 - (3 ea. on engine thrust structure & 2 on ea. gimbal actuator)	~ 200 on orbiter ~ 100 on E.T.	370,000	35	Orbiter on E.T. in free suspension	1300 on orbiter, 1600 on E.T.
Orbiter Landing	27 - (3 at each tunlion on each gear member)	~ 200 on orbiter	150,000	25	orbiter in free suspension	1300 on orbiter

Table 5-2 Sample Impulse Requirement Data Derived From Table 5-1 and Figure 5-1 and 5-2

See Text For Details

Loading Condition	Highest Frequency of Interest (Hz)	$\left(\frac{F^*}{F_0}\right)$	% Error (E) @ Highest Frequency	Portion of Static Response Induced, R		Pulse Period $\tau$ (Millisec)	Peak Pulse Force $F^*$ (Lbs)
				@ Highest Freq.	@ 1.5 Hz		
Pre launch-main engine start & shut down	15	.26	2	.13	~ .02	10	30,000
Hold-down release	15	.15	5	.12	~ .02	16	30,000
SRB shut down	20	.05	15	.07	~ .01	22	30,000
SRB staging	30	.33	5	.28	.02	8	30,000
Orbiter staging	30	.33	5	.28	.02	8	30,000
Orbiter engine shut down	35	.08	15	.12	~ .01	14	30,000
Orbiter landing	25	.20	10	.25	.02	15	30,000



ITF Accuracy as a Function of  $(\tau/T)$  and  $(K/\tau)$

Figure 5-1

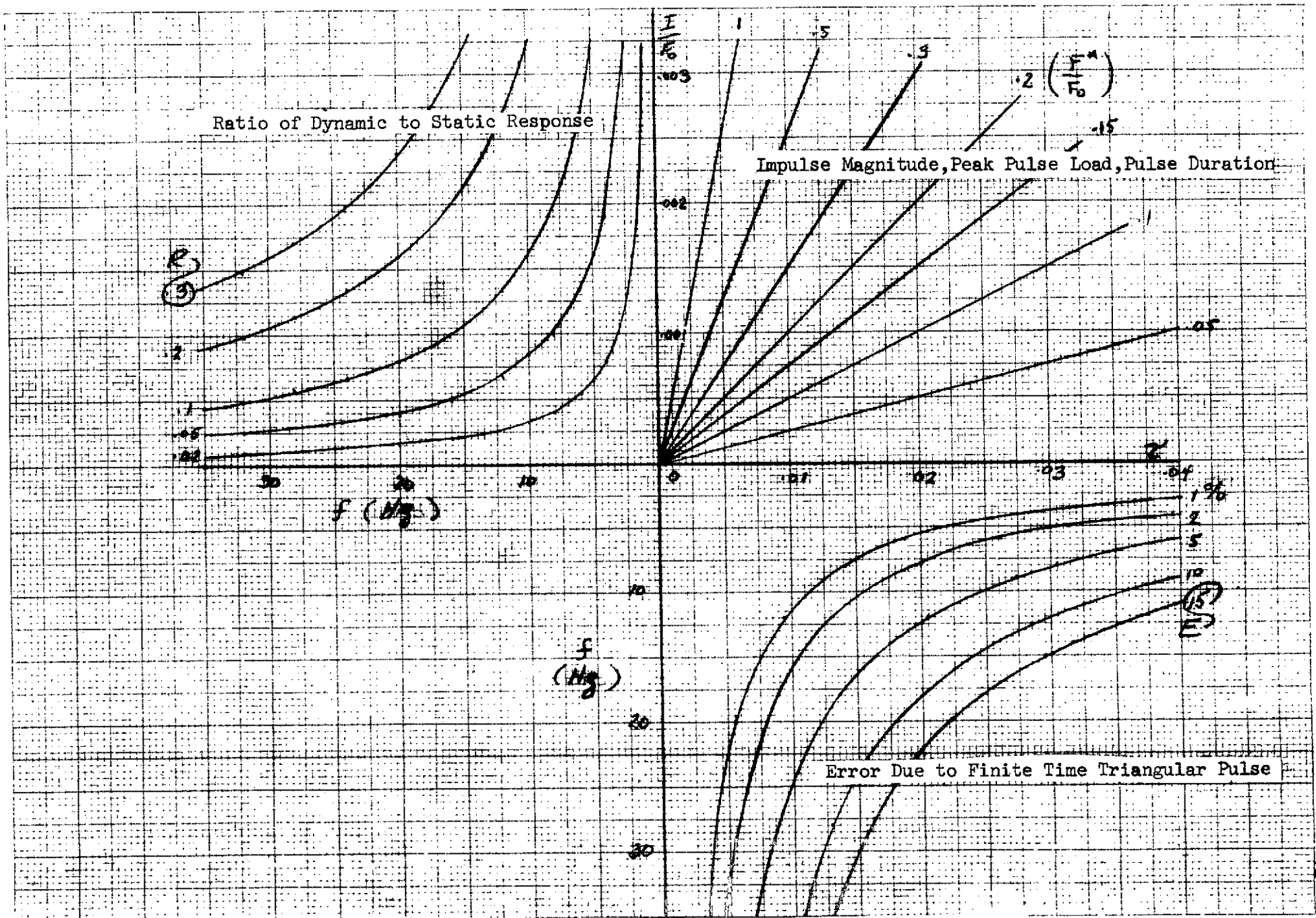


Figure 5-2 Curves For Estimating Impulse Requirements

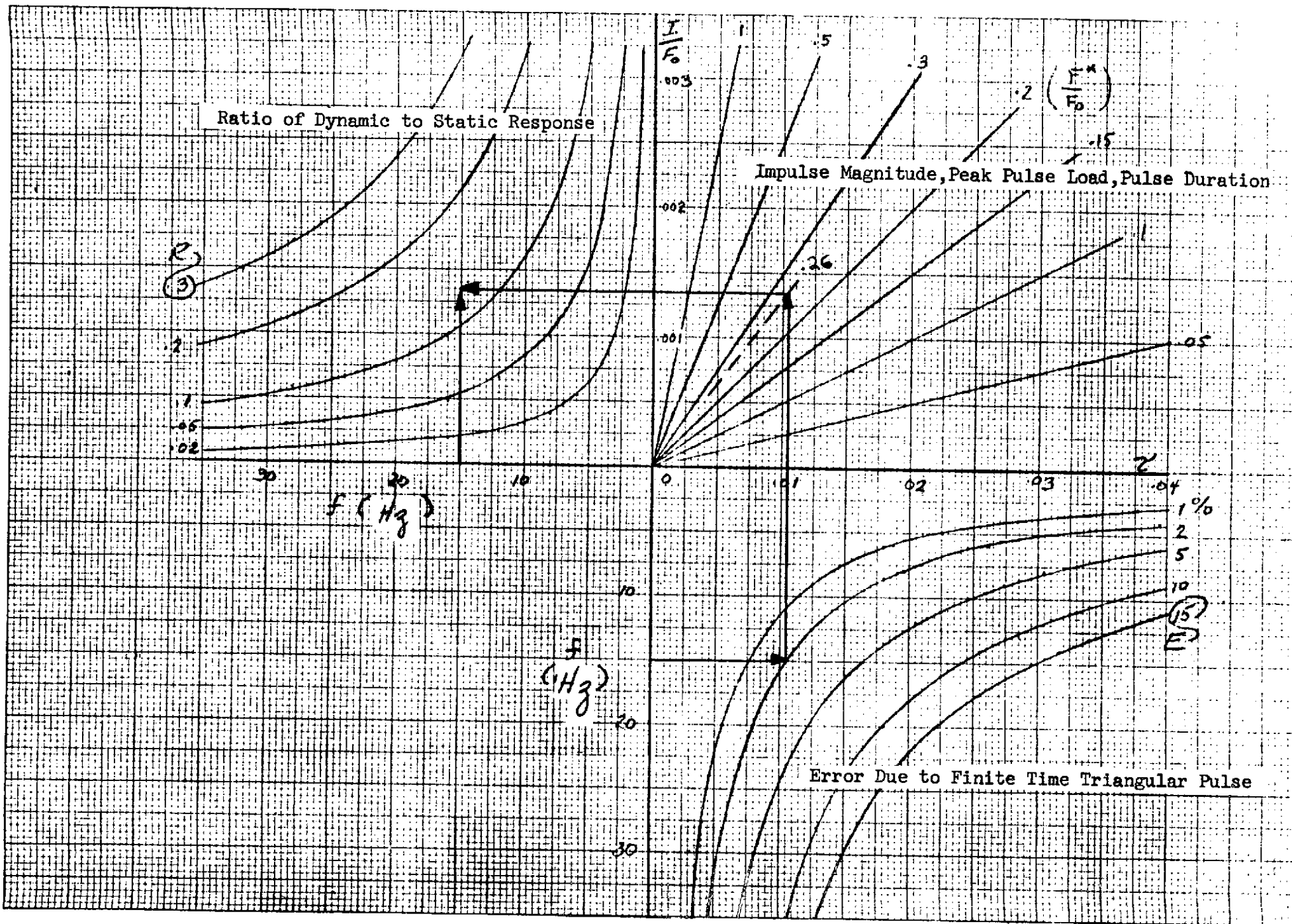


Figure 5-3 An Example Of Estimating Impulse Requirements

## 6-CONCLUSIONS AND RECOMMENDATIONS

Our test work for Langley, Reference 1, demonstrated that an impulse test can be performed on a complicated aerospace structure in a timely fashion. Section 5 of this report outlines test considerations for applying the ITF method to the Shuttle. As discussed, it may be necessary to employ hydraulic shakers as a replacement for the electrodynamic ones used in the LM work in order to deliver the high magnitude impulses necessary to excite the large Shuttle structure. Another impulse generation device that should be considered is the Grumman stress-wave riveter. Prior to any Shuttle application, an exploratory test program will be required in order to insure that candidate test equipment is suitable with regard to impulse magnitude and physical handling characteristics. The data of Section 5 should assist in this work.

Based on the computer program development and the data processing that was accomplished under this contract, it certainly appears practical to handle the large quantity of data that results from an impulse test. Since the data processing package will be available at NASA/MSC and at Grumman, it can be employed immediately as test results become available to insure that the data taken is valid.

Based on the comparison of drop test results and ITF predictions that are presented in Section 4, it appears that the ITF method can often accurately predict both waveform and peak amplitude. In addition, where waveform agreement is lacking, the method is frequently accurate in predicting peak response. The comparison of drop test, ITF predictions, and modal analysis predictions indicates that the ITF approach can be more accurate than a comprehensive modal analysis in computing transient response.

When the test results, the data processing accomplishments, and the correlation studies are considered together, it is our conclusion that the ITF approach can be a valuable supplement to conventional aerospace dynamic testing and analysis practice.

- - - - -

We believe that significant improvements can be made in the accuracy of the ITF method if the lessons of this contract are applied to the testing phase of a new ITF project. Two items are of prime importance. First we strongly urge that data processing be conducted as the test progresses. With the data processing packages now available, it appears possible to complete the processing of an original analog tape a day or two after an impulse is delivered. It would then be possible to conduct various validity checks, i.e., a review for symmetry and obvious data drop-out, so that timely repeat testing can be performed if necessary.

Second, we recommend that considerable attention be given to designing the suspension system so that the rigid body frequencies of the supported vehicle are as far below the structural frequencies as is possible. We believe that the suspension system used in the IM testing was a principal source of inaccuracy in the predicted responses. Since the suspension will never provide a perfectly "free-free" system, methods for eliminating left-over effects should be considered. While the digital filtering methods outlined in Section 4 have been shown to be reasonably effective, it is possible that the spurious effects of the suspension can be more accurately removed by the method outlined in Appendix A. In this method the axial loads in the suspension cables are measured when an impulse is applied. Using the Duhamel integral, the effect of the cable loads are subtracted from the internal response time histories before these responses are considered ITF's. Implementing this approach would require only some minor computer program revisions; no new development work appears to be required. Of course, the

filtering methods that have been included in the computing system are an available back-up and supplement, if needed.

Another area of investigation that was considered under this contract was a study into the feasibility of using ITF data for determining modal information. TRW Systems Group performed this work and reported their results in References 2 and 3. TRW demonstrated that reasonably accurate frequency data could be computed from the ITF's, but mode shape predictions were poor. It is possible that the inaccuracies were due to the highly complicated nature of the LM structure and that further development work is necessary before the method becomes feasible for all applications. We believe, however, that the method should be considered in its present state for special applications on relatively simple structures. Further discussion of this subject may be found in Section 4c.

The impulse testing and correlation studies conducted to date have virtually all been for the LM structure. While this is certainly a realistic and complex space structure, it is not very representative of an aircraft or the Space Shuttle. To gain additional confidence and to uncover any hidden problems in using the method on the Shuttle, we recommend some additional test/analysis work on an aircraft-type structure. Impulse generation, instrumentation requirements, and suspension system design should all be considered. If data is not available upon which to base a correlation study, long duration, transient forcing functions could be applied to the test article. ITF predictions should be made and compared with test results. In addition, it is recommended that a comparison be made with predictions from modal analysis to provide further data on the accuracy of the ITF approach.

A great deal of interest is currently centered on methods of determining total vehicle modes from ground vibration survey data obtained from individual Shuttle component tests. Similar ideas should be entertained for ITF's if the component approach is adopted for the Shuttle. That is, an ITF test could be conducted as part of, or in addition to, a component vibration test program. Impulses would be applied to points where forcing functions exist as well as at the junction points with other components. The data for all the components

would then be combined analytically to obtain ITF's for the total structure. A first phase approach to this problem could be conducted using analysis to simulate test results. Once techniques for accomplishing the coupling were evaluated, they should be employed in a test/analysis project to demonstrate the accuracy of the method.

For both of the test programs described above, a reasonably accurate structural scale model of the Shuttle would be a suitable test article.

In closing, it appears appropriate to list the items that require further resolution prior to applying the ITF method to the Shuttle. These items are:

- Suspension System. A careful design effort is recommended to keep rigid body frequencies well below the lowest elastic frequencies of the test article. In addition to digital filtering, a method for removing remaining suspension system effects should be pursued (Appendix A).
- Impulse Generator. For a given transient response condition, a trade study should be conducted to decide among a hydraulic shaker, an electrodynamic shaker and the Grumman stress-wave riveter, as the impulse delivering device (Section 5).
- Test Procedure. In a new ITF test we strongly recommend that procedures be planned to insure that collected data is reviewed as soon after an impulse is delivered as is possible. We recommend that this analytic effort continue throughout the test period and keep the data validation no more than a few days behind the test program.

7-REFERENCES

1. Mantus, M., "Development and Evaluation of the Impulse Transfer Function Technique," NASA CR-112025, January 1972.
2. Galef, A. E., "Determination of Modal Engineers, Damping, Generalized Mass and Mode Shapes From Impulse Response Measurements, Volume I, Analysis and Results" TRW Systems Group Mechanical Engineering Laboratory Report 72-D-31, November 20, 1972.
3. Wang, T. T., "Determination of Modal Frequencies, Damping, Generalized Mass and Mode Shapes From Impulse Response Measurements, Volume II, Programmers Manual, Users Manual and Program Listing," TRW Systems Group Mechanical Engineering Laboratory Report 72-D-31, November 20, 1972.
4. Goldenberg, S. and Cary, J. W., "An Analytical Method for Predicting the Dynamic Response of a Structure from Experimentally Determined Impulse Transfer Functions," Grumman Report No. 000-SM-010, June 1967.
5. Skipala, R., Birs, C and Schnee, M., "Results of Impulse Testing of LTA-3 Phase 1B," Grumman Report No. LTR-933-100022, 11 December 1969.
6. Baird, E. F., "Transient Loading Considerations for Shuttle Design," presented at the Space Shuttle Symposium, NASA Lewis Research Center, Cleveland, Ohio, July 1970.
7. Goldenberg, S., Kelly, R. F., Catera, J., "User's Manual for Transient Response Computer Program (IDEAS Program V7)", Grumman Report No. 000-SM-019, September 1968.

APPENDICES

### A-Suspension System Considerations

The suspension system used to support a vehicle during ITF testing can be a primary source of inaccuracy in predicted responses. The reason for this lies in the fact that a relatively small error in an ITF can be magnified by the forcing function to a sizeable magnitude. To demonstrate this consider the sketches of Figure A-1. The first grid depicts a measured ITF, in which an error is introduced due to a spurious effect. The remaining two grids show the original ITF dissected into the accurate component plus an error term; the error is represented as a unit step function for simplicity only. Suppose, as is illustrated in Figure A-2, the forcing function is a step at 10,000 lbs. The response due to the error term only, as computed from the Duhamel integral, would be a ramp as shown in the second plot, whose magnitude would be 10,000 lbs after 1 second -- a very sizeable error. This type of effect explains why we addressed a great deal of attention to zero adjust problems and why relatively small errors introduced by a suspension system can be very important to overall results.

We recommend that careful attention be given to designing a suspension system so that rigid body frequencies of the supported vehicle are well below the lowest modal frequencies computed for the elastic "free-free" structure. In a test, we suggest that all rigid body frequencies be measured in all test configurations.

Since any suspension will introduce some restraint, attention should be directed to removing the effect which remains after a concerted design effort. The filtering technique used in this study is one relatively accurate method of eliminating the left-over effect. Another method,

explained below, which involves instrumenting the suspension cables for load, should also be investigated since it may be more accurate in removing suspension effects.

Consider the sketch of Figure A-3. The first sketch depicts an elastic vehicle during an impulse test, where the force induced in the suspension cable is measured along with an ITF time history  $a_1$ . If we could find the response of the system to the cable forces as illustrated in Figure A-3b, then the ITF for the "free-free" system that we seek can be found as

$$h = a_1 - a_2 \quad (\text{A-1})$$

From the original data, we could use a Duhamel integration to predict a response to S:

$$a_3 = \int_0^t S(\tau) a_1 (t-\tau) d\tau \quad (\text{A-2})$$

The question is: How close to  $a_2$  is  $a_3$ , as found from Equation A-2? It would seem that for systems where the low frequency elastic modes are well above frequencies introduced by the suspension system,

$$a_3 \approx a_2 \quad (\text{A-3})$$

and for practical purposes, the "free-free" ITF can be found from

$$h = a_1 - \int_0^t S(\tau) a_1 (t-\tau) d\tau \quad (\text{A-4})$$

While the above discussion does not constitute a proof, it does suggest that this approach is worthy of further investigation as part of a new ITF project. It is interesting to note that the existing computing system would require only minor modification to implement the proposed method. And, of course, since the filtering methods used in the present work are already part of the computer system, they can be used as a back-up or a supplement, as needed.

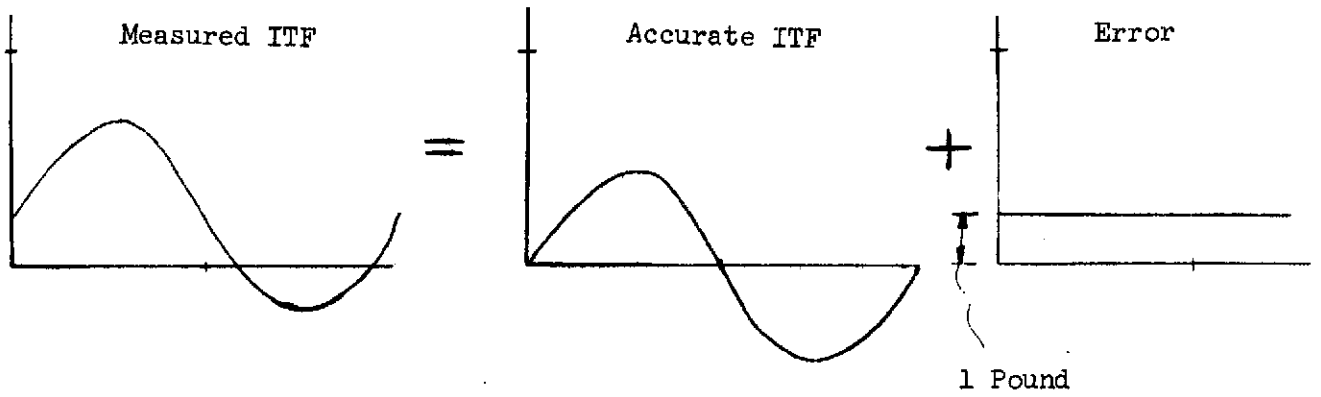


Figure A-1 Error In Measuring An ITF

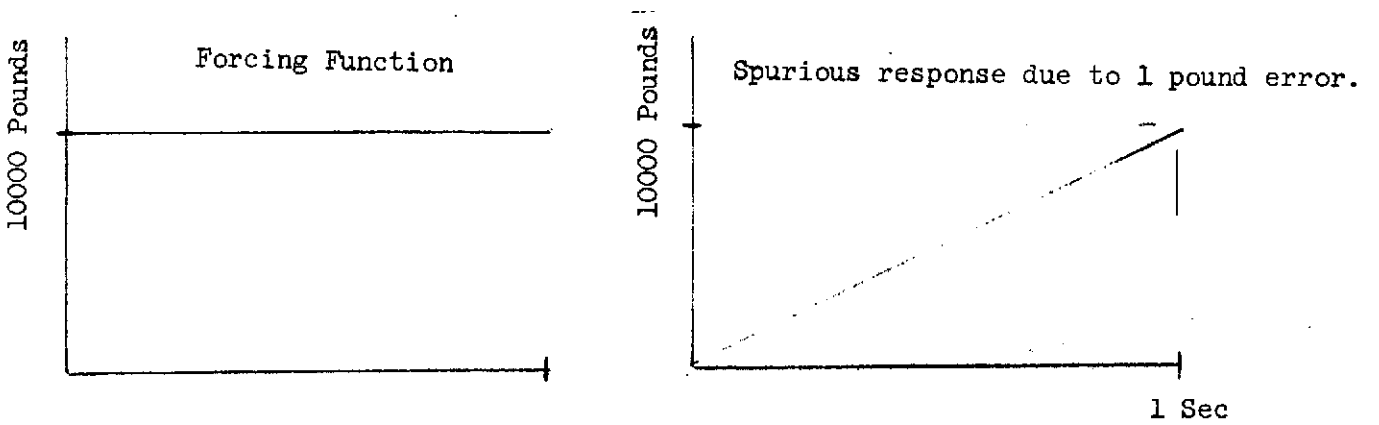


Figure A-2 Result Of Error In An ITF

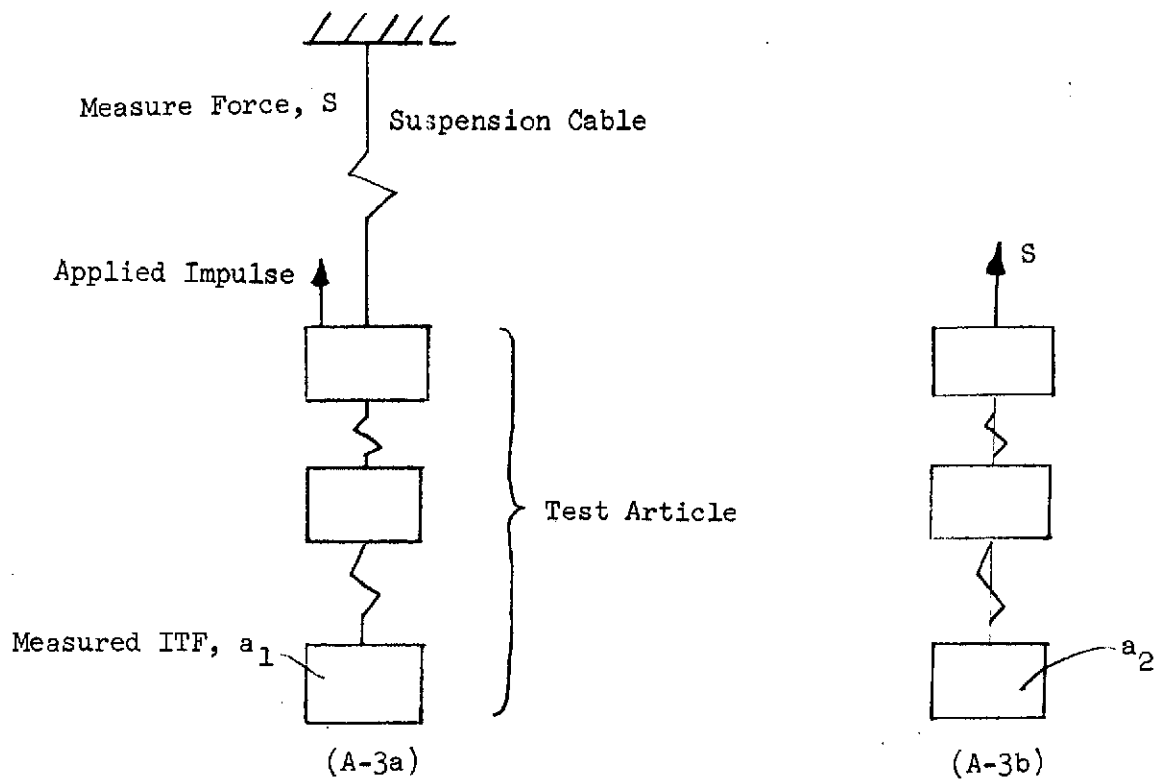


Figure A-3. Suspension System Considerations

B-Instrumentation List

The instrumentation listed in Table B-1 was monitored during LFA-11 impulse testing.

Table B-1 - List of Instrumentation

MEAS. NO.	MEASUREMENT NAME AND LOCATION	TRANSDUCER TYPE & RANGE
1	Input Force	Piezoelectric Impact Force 30,000 lbs
2	Aft Interstage Truss, Outer L.H. GA-12	Axial Strain Gage Ckt 25,000 lbs
3	Aft Interstage Truss, Inner L.H. GA-13	Axial Strain Gage Ckt 10,000 lbs
4	Aft Interstage Truss, Outer R.H. GA-14	Axial Strain Gage Ckt 25,000 lbs
5	Aft Interstage Truss, Inner R.H. GA-15	Axial Strain Gage Ckt 10,000 lbs
6	+Z Outrigger Strut, Upper +Y Side GD-1	Axial Strain Gage Ckt 30,000 lbs
7	+Z Outrigger Strut, Upper -Y Side GD-2	Axial Strain Gage Ckt 30,000 lbs
8	+Z Outrigger Strut, Lower +Y Side GD-3	Axial Strain Gage Ckt 16,000 lbs
9	+Z Outrigger Strut, Lower -Y Side GD-4	Axial Strain Gage Ckt 16,000 lbs
10	Diag. Strap Quad I Upper Center GD-17	Axial Strain 2500 u"/in
11	Diag. Strap Quad I Lower Center GD-18	Axial Strain 2500 u"/in

MEAS. NO.	MEASUREMENT NAME AND LOCATION	TRANSDUCER TYPE & RANGE
12	Diag. Strap Quad II Lower Forward GD-20	Axial Strain 2500 u"/in
13	Diag. Strap Quad III Lower Center GD-23	Axial Strain 2500 u"/in
14	Diag. Strap Quad IV Lower Center GD-25	Axial Strain 2500 u"/in
15	Side Panel Quad II -Z27 Shear GD-28	Shear Strain 2000 u"/in
16	Side Panel Quad II -Y27 Shear GD-29	
17	Side Dec, Quad III -Y27 Shear GD-31	
18	Side Deck Quad IV +Z27 Shear GD-32	
19	Forward Interstage Support R.H. Lateral GD-34	Axial Strain 2500 u"/in
20	Forward Interstage Support, L.H. Diag. "Tee" GD-35	
21	Forward Interstage Support, L.H. Vertical GD-36	
22	Forward Interstage Support, L.H. Lateral GD-37	

MEAS. NO.	MEASUREMENT NAME AND LOCATION	TRANSDUCER TYPE & RANGE
23	Forward Interstage Support, R.H. Diag. "Tee" GD-38	Axial Strain 2500u"/in
24	Forward Interstage Support, R.H. Vertical GD-39	↓
25	Fwd. (+Z) Deployment Int. Cross Member GD-40	Axial Strain 7500 lbs
26	Fwd. (+Z) Deployment -Y Side Member GD-44	Axial Strain 4000 lbs
27	Fwd. (+Z) Deployment -Y Down Lock Member GD-45	Axial Strain 2000 lbs
28	Left (-Y) Upper Deck Fwd. Shear +Z Side GD-65	Shear Strain 4000 u"/in
29	Right (+Y) Upper Deck Fwd. Shear +Z Side GD-68	Shear Strain 1000 u"/in
30	Upper Cap Strip +Y27 Quad IV GD-82	Axial Strain 2000 u"/in
31	Upper Cap Strip -Y27 Quad I GD-83	Axial Strain 2000 u"/in
32	Upper Cap Strip -Z27 Quad III GD-84	Axial Strain 2000 u"/in
33	Upper Cap Strip +Z27 Quad IV GD-85	↓
34	Upper Cap Strip +Y27 Quad III GD-86	↓

MEAS. NO.	MEASUREMENT NAME AND LOCATION	TRANSDUCER TYPE & RANGE
35	Upper Cap Strip -Y27 Quad II GD-87	Axial Strain 2000u"/in
36	Upper Cap Strip -Z27 Quad II GD-88	↓
37	Upper Cap Strip +Z27 Quad I GD-89	Axial Strain 2000 u"/in
38	Mesa End Strut Forward (+Z81) GD-118	Axial Strain 2500 u"/in
39	Mesa End Strut Right Side (+Y81) GD-119	Axial Strain 2500 u"/in
40	Payload Vert. Strut Left Side (-Y) GD-130	Axial Strain 2500 u"/in
41	Payload Vert. Strut Forward (+Z) GD-131	Axial Strain 2500 u"/in
42	Acceleration EA-108 X	Piezoelectric Accelerometer ±1000G
43	Acceleration EA-57 X	
44	Acceleration EA-57 Z	
45	Acceleration EA-58 X	
46	Acceleration EA-58 Y	↓

MEAS. NO.	MEASUREMENT NAME AND LOCATION	TRANSDUCER TYPE & RANGE
47	Acceleration EA-58 Z	Piezoelectric Accelerometer ±1000G
48	Acceleration ED-1 Z	Piezoelectric Accelerometer ±1000G
49	Acceleration ED-2 Z	Piezoelectric Accelerometer ±1000G
50	Acceleration ED-4 Z	
51	Acceleration ED-11 X	
52	Acceleration ED-11 Y	
53	Acceleration ED-12 X	
54	Acceleration ED-12 Z	
55	Acceleration ED-13 X	
56	Acceleration ED-13 Y	
57	Acceleration ED-13 Z	
58	Acceleration ED-14 X	

MEAS. NO.	MEASUREMENT NAME AND LOCATION	TRANSDUCER TYPE & RANGE
59	Acceleration ED-14 Z	Piezoelectric Accelerometer ±1000G
60	Acceleration EA-99 X	Piezoelectric Accelerometer ±1000G
61	Acceleration EA-101 Z	Piezoelectric Accelerometer ±1000 G
62	Acceleration EA-100 X	
63	Acceleration EA-104 Z	
64	Acceleration EA-78 Z	
65	Acceleration EA-95 X	
66	Acceleration EA-95 Y	
67	Acceleration ED-3 X	
68	Acceleration ED-3 Y	
69	Acceleration ED-3 Z	Piezoelectric Accelerometer ±1000G

C-Summary of LTA-11 Impulse Testing

Table C-1 provides a history of impulse testing, including pulse location and direction.

Table C-1 - Summary of LTA-11 Impulse Testing (1971)

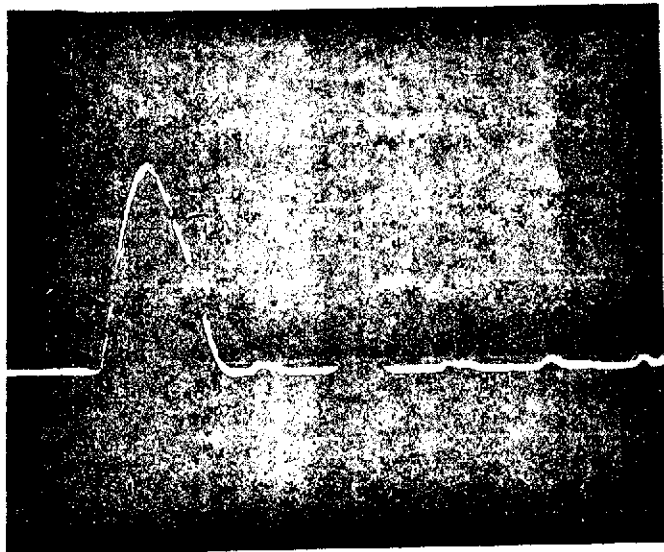
<u>Run No.</u>	<u>Date</u>	<u>Pulse Location</u>	<u>Pulse Direction</u>
1	Aug. 25	+Z Deployment Truss, -Y side	+X
2	Aug. 27	+Z " " , -Y "	-Z
3	Aug. 30	+Z " " , -Y "	+Y
4	Aug. 31	-Y " " , +Z "	-Z
5	Sept. 1	-Y " " , +Z "	+Y
6	Sept. 2	-Y " " , +Z "	+X
7	Sept. 2	-Y " " , -Z "	+X
8	Sept. 3	-Y " " , -Z "	+Y
9	Sept. 3	-Y " " , -Z "	+Z
10	Sept. 7	-Z " " , -Y "	+Y
11	Sept. 9	+Z Apex Fitting	-Z
12	Sept. 10	+Y " "	-Y
13	Sept. 13	-Z " "	+Z
14	Sept. 14	-Y " "	+Y
15	Sept. 15	-Y " "	+Z
16	Sept. 16	+Z " "	+Y
17	Sept. 17	+Y " "	-Z
18	Sept. 17	-Z " "	-Y
19	Sept. 20	-Z " "	+X
20	Sept. 23	+Y " "	+X
21	Sept. 24	+Z " "	+X
22	Sept. 27	-Y " "	+X
23	Sept. 29	-Z Deployment Truss, -Y side	+X
24	Oct. 1	-Z " " , -Y "	+Z
25	Oct. 7	+Z " " , +Y "	-Z
26	Oct. 8	+Z " " , +Y "	-Y
27	Oct. 11	+Z " " , +Y "	+X
28	Oct. 12	+Y " " , +Z "	+X
29	Oct. 12	+Y " " , +Z "	-Z
30	Oct. 13	+Y " " , +Z "	-Y
31	Oct. 15	-Z " " , +Y "	+Z
32	Oct. 15	-Z " " , +Y "	-Y
33	Oct. 18	-Z " " , +Y "	+X
34	Oct. 19	+Y " " , -Z "	+X
35	Oct. 21	+Y " " , -Z "	+Z
36	Oct. 22	+Y " " , -Z "	-Y

NOTE: The pulse direction indicated refers to the ITF testing only. In using the ITF's for the prediction of response, a reversal of sign may be required depending on the direction of a particular forcing function.

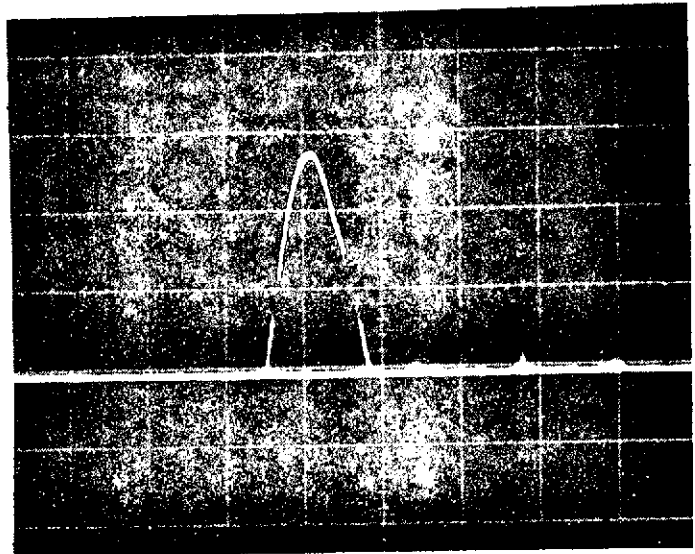
### D-Sample Impulse and Response Time Histories

Figure D-1 shows time histories of the impulses delivered to the outrigger truss apex fittings. These pulses closely resemble half sine waves for about .5 milliseconds and are typical of the 36 applied to the test article.

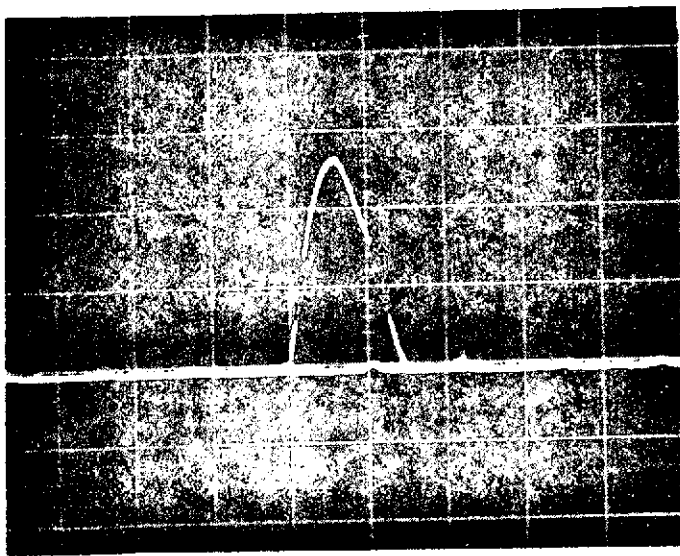
Two response time histories, typical of the response throughout the vehicle, are shown in Figure D-2. One strain gage and one accelerometer response, played back from the original analog tape, are given. The only filter in the system was a 1000 Hz filter used in the data acquisition system.



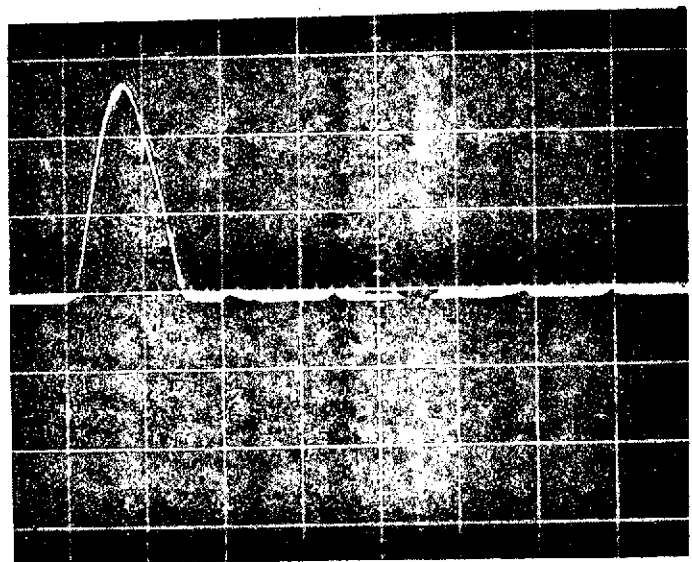
+Z APEX



-Z APEX



+Y APEX



-Y APEX

Vertical Scale = 5000lb./division  
Horizontal Scale = .5 millisecond/division

Figure D-1 - Pulses Applied to Outrigger Truss Apex Fittings in the X Direction

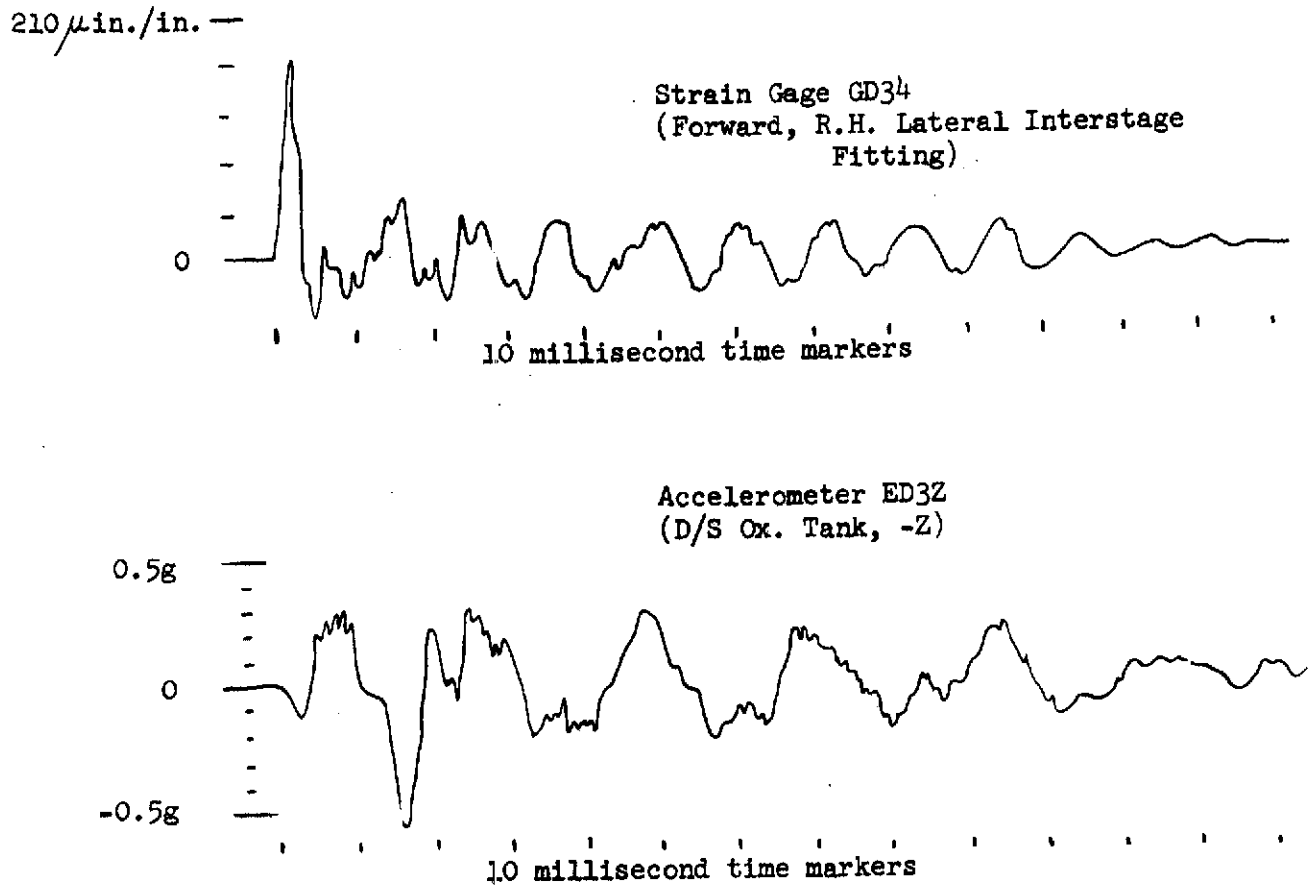


Figure D-2 - Typical Impulse Response Time Histories

C2

E-LTA-11 Finite Element Idealization

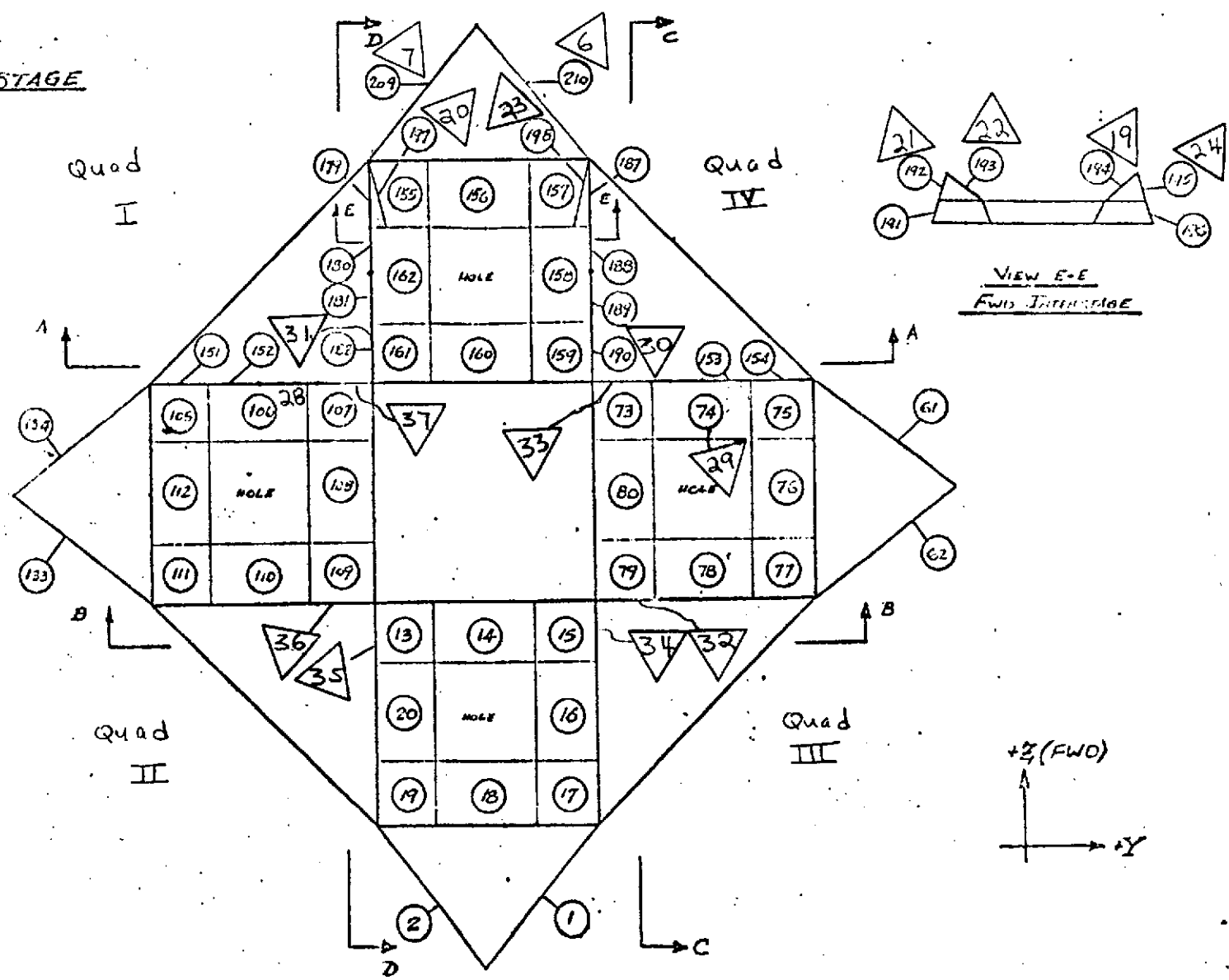
Table E-1 shows the correspondence of ITF measurement number with the finite element number shown in the sketches of Figure E-1. In these sketches the finite element number is shown circled while the corresponding measurement number is shown within a triangle.

Table E-1 Impulse Test Measurement Number - Finite Element Number

Measurement Number	Finite Element Number	Measurement Number	Finite Element Number
6	210	18	148
7	209	19	194
8	212	20	197
9	211	21	192
11	200	22	193
12	34	23	198
13	33	24	195
14	199	28	106
15	45	29	74
16	40	30	190
17	36	31	182

LMMP DESCENT STAGE

UPPER DECK

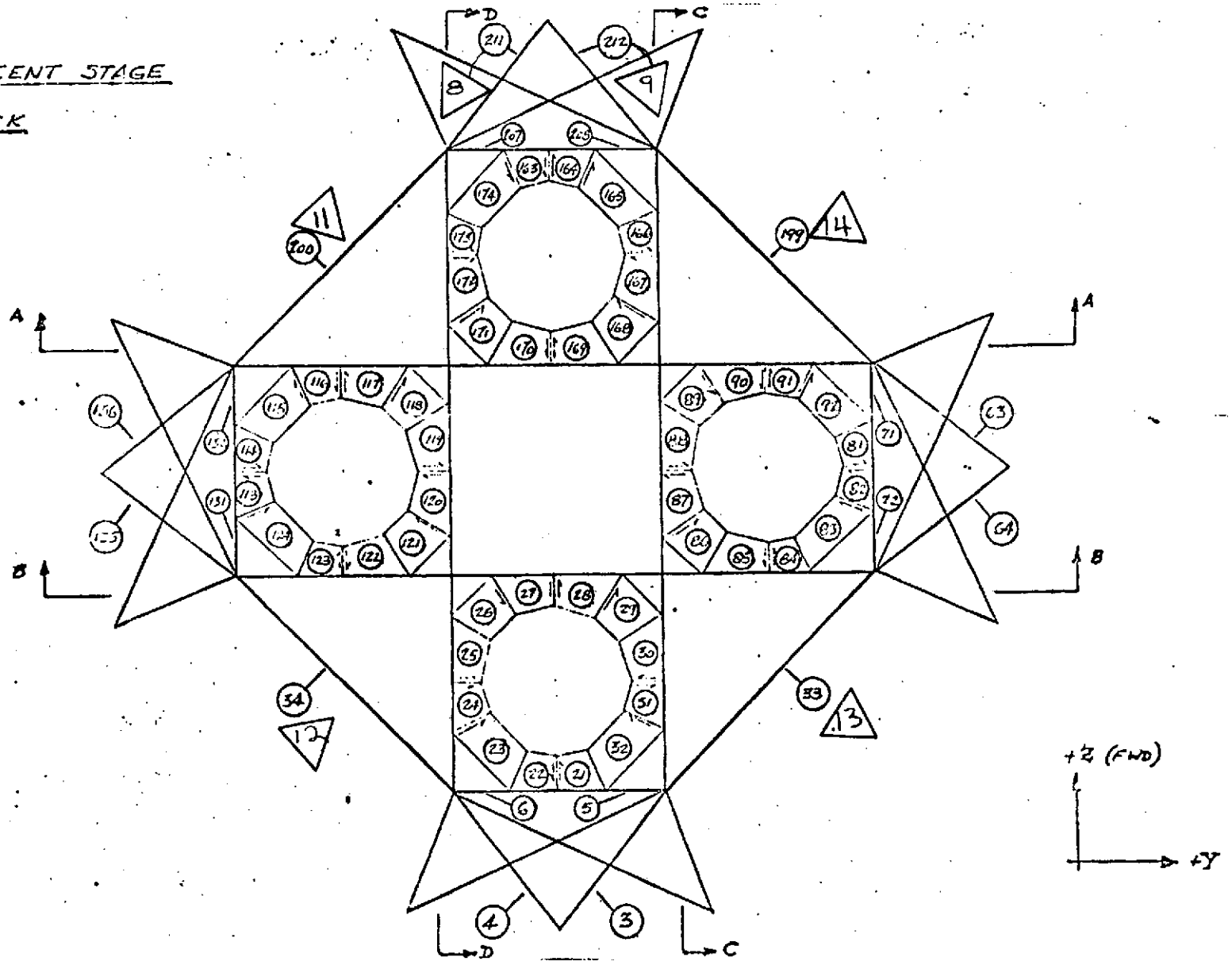


NOTE: The numbers in the triangles indicate the impulse test measurement number.

Figure E-1a LTA-11 Finite Element Idealization

LINAP DESCENT STAGE

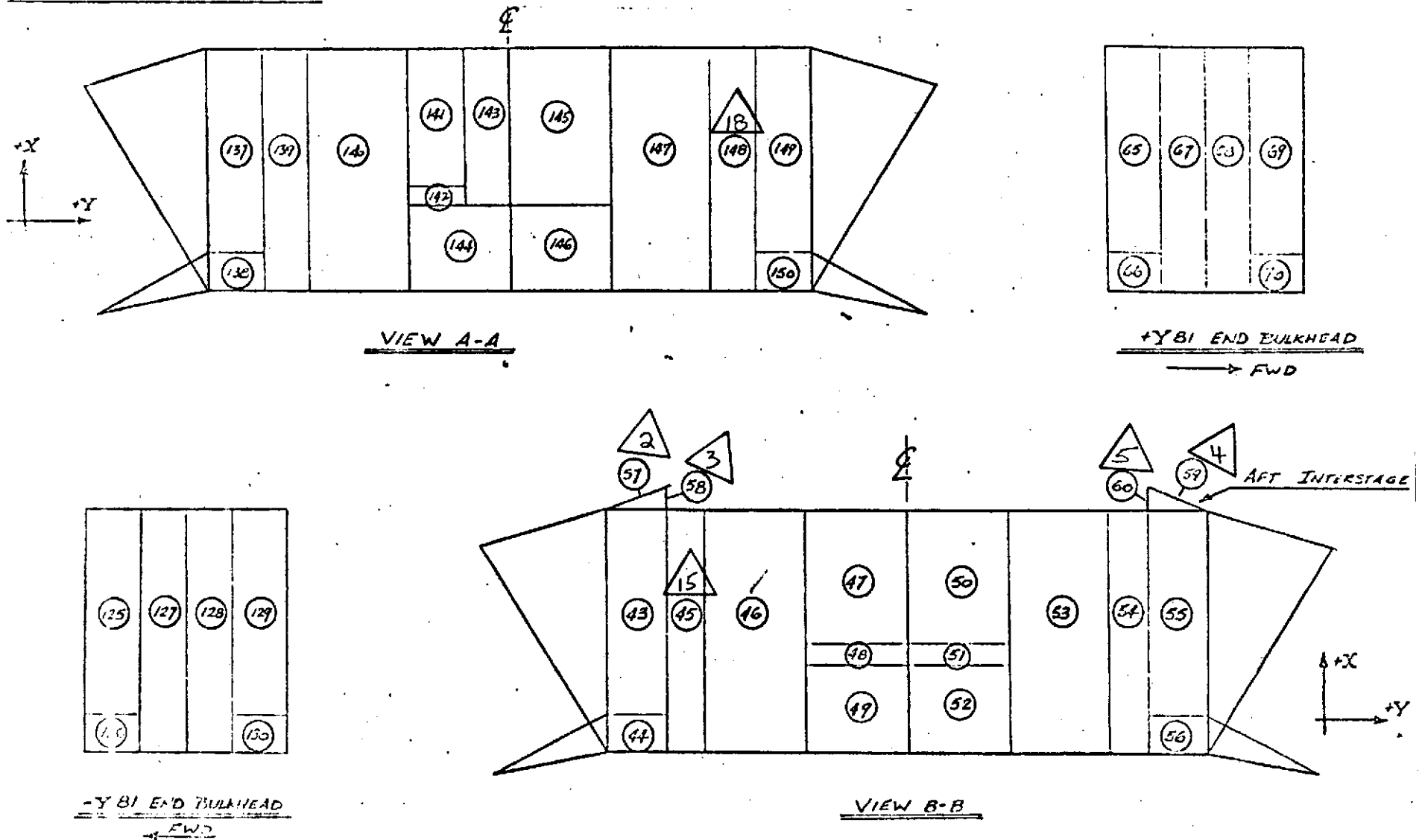
LOWER DECK



NOTE: The numbers in the triangles indicate the impulse test measurement number.

Figure E-1b LTA-11 Finite Element Idealization

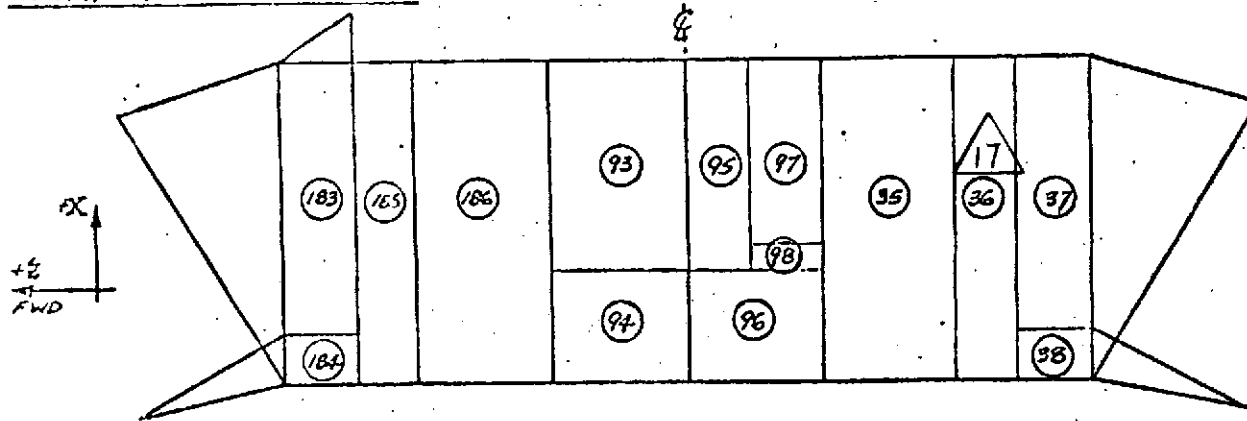
LMMP DESCENT STAGE



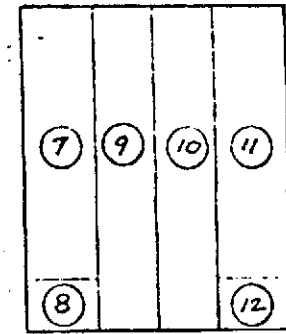
NOTE: The numbers in the triangles indicate the impulse test measurement number.

Figure E-1c LMA-11 Finite Element Idealization

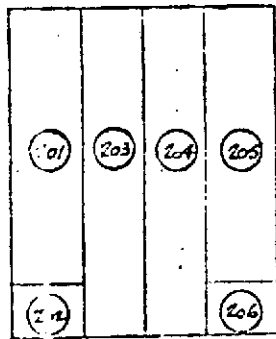
LMMP DESCENT STAGE



VIEW C-C

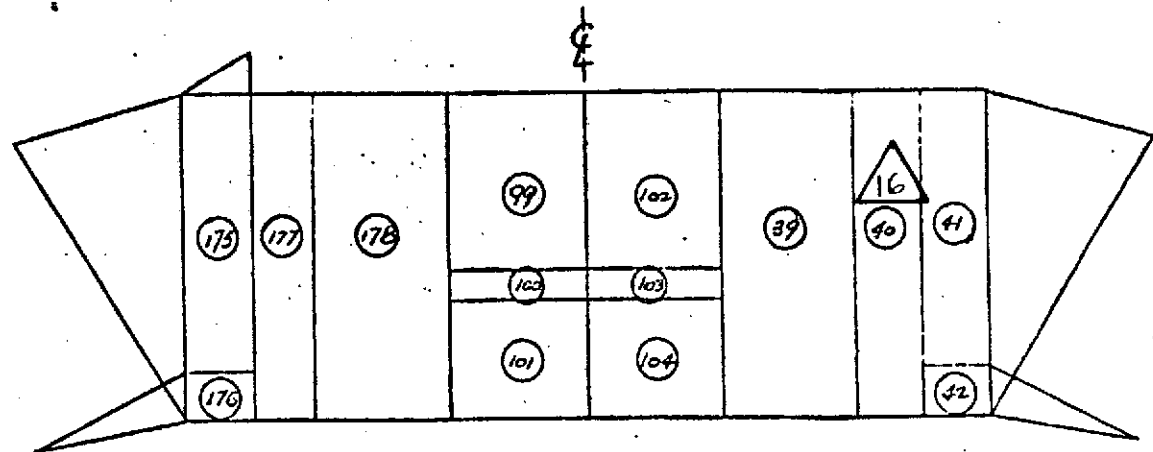


-2.81 (AFT) END BULKHEAD



2.81 (FWD) END BULKHEAD

+Y



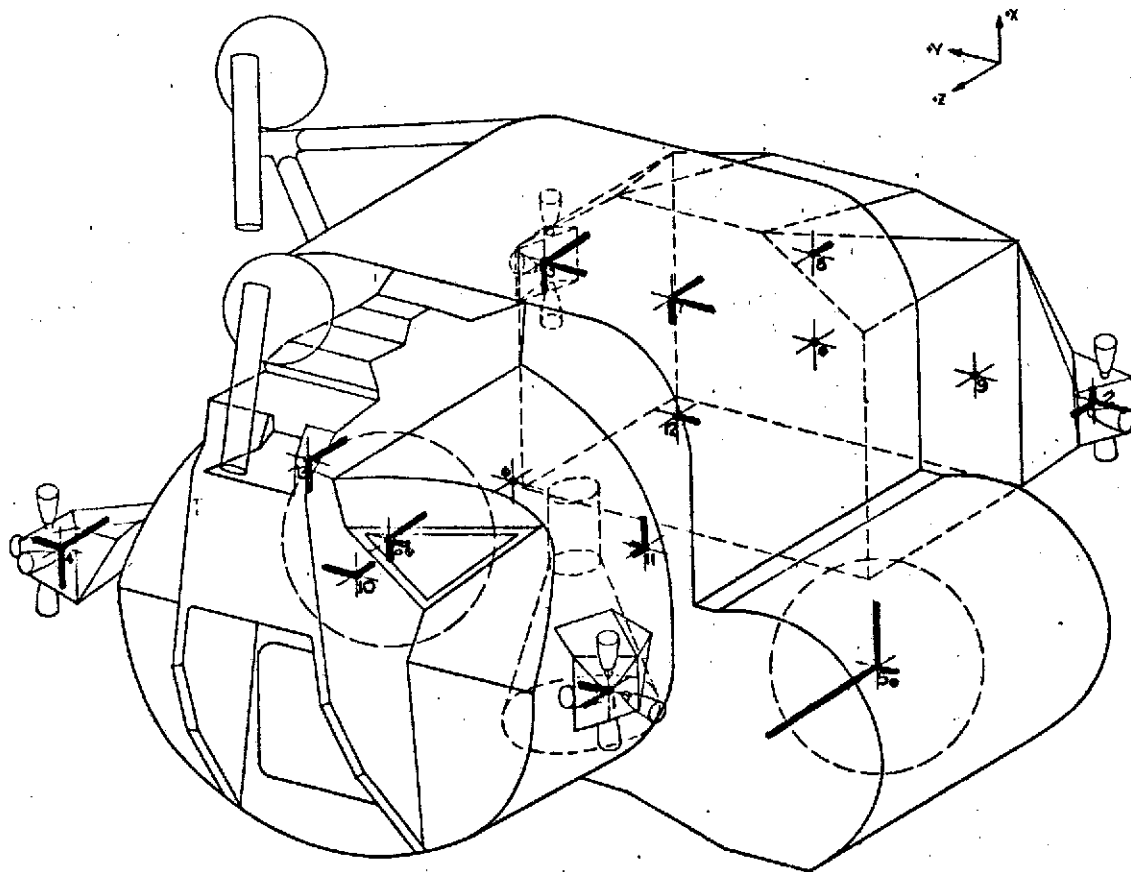
VIEW D-D

NOTE: The numbers in the triangles indicate the impulse test measurement number.

Figure E-1d LTA-11 Finite Element Idealization

### F-LTA-11 Mode Survey Results

Figures F-1 through F-5 present the mode shapes and frequencies measured in the LTA-11 ground vibration survey. Figure F-6 is a sketch showing accelerometer location and measurement direction for the ITF program. These figures may be useful in interpreting the results of Reference 2.



◆ C.G. OF UNIT

LTA-11  
ASCENT STAGE

CONFIGURATION — LUNAR LANDING  
 FREQUENCY — CPS — 7.91 Hz  
 RUN #10

Figure F-1a LTA-11 Mode Survey Result - Ascent Stage First Mode

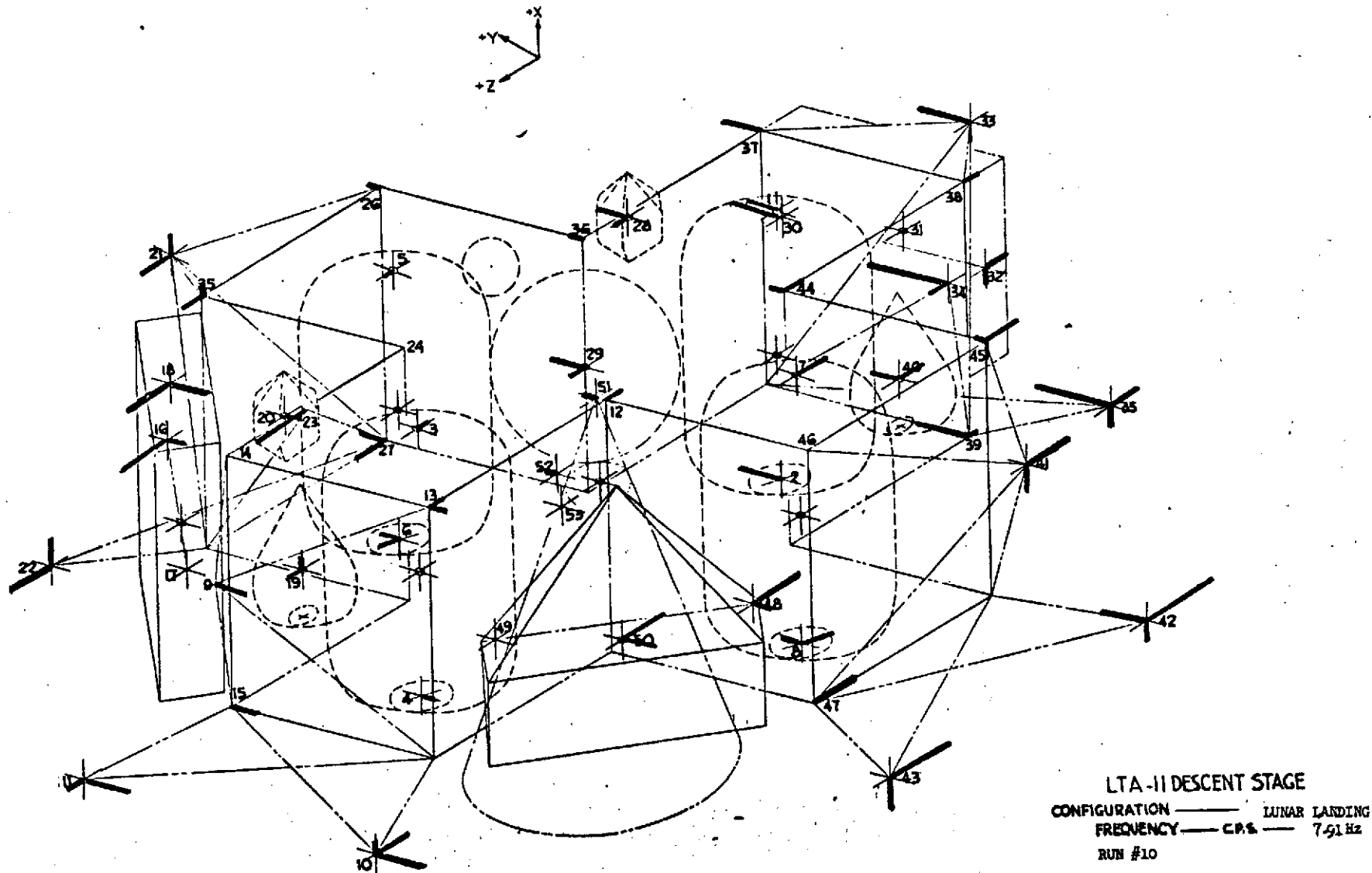
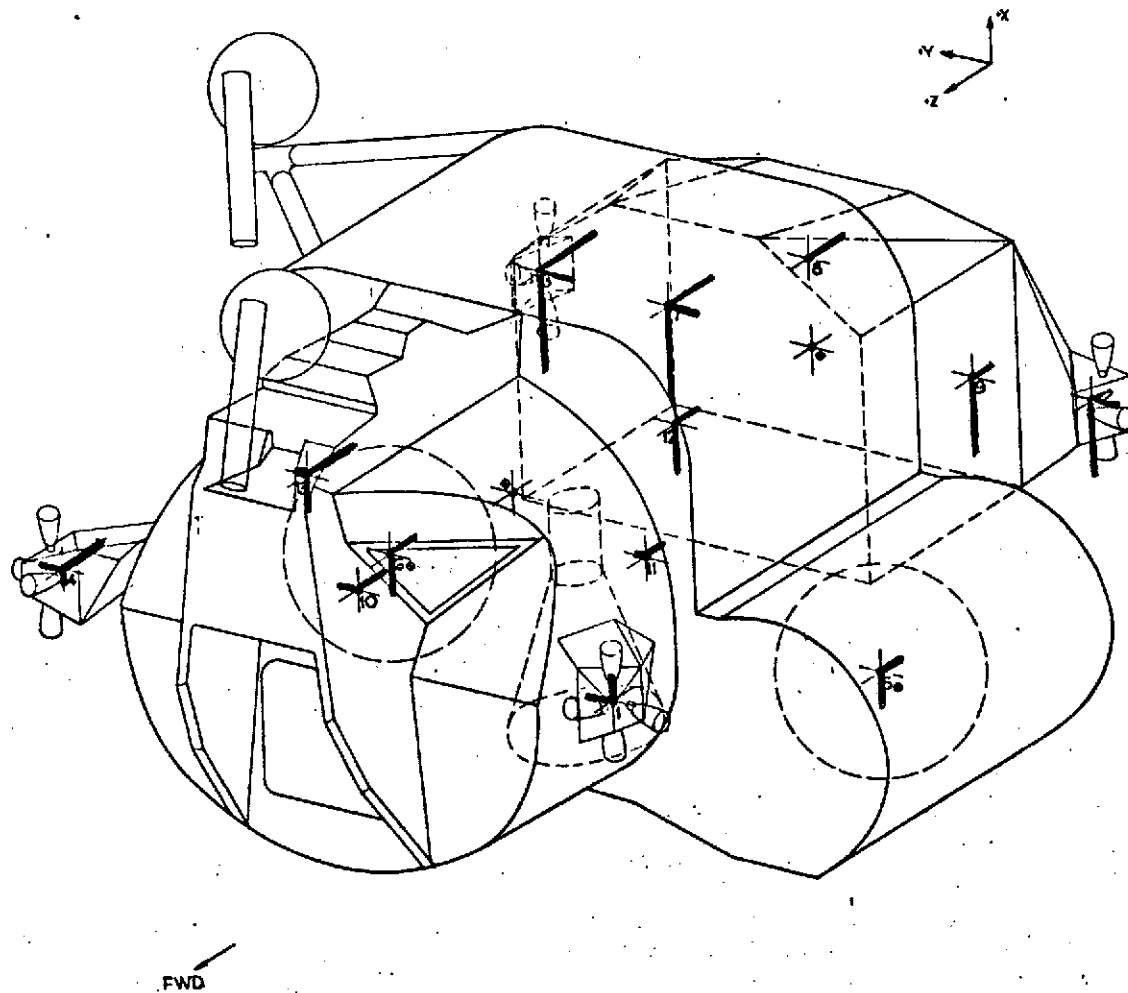


Figure F-1b IFA-11 Mode Survey Result - Descent Stage First Mode



◆ C.G. OF UNIT

LTA-11  
ASCENT STAGE

CONFIGURATION ——— LUNAR LANDING  
 FREQUENCY — CPS — 9.30 Hz  
 RUN #110

Figure F-2a LTA-11 Mode Survey Result - Ascent Stage Second Mode

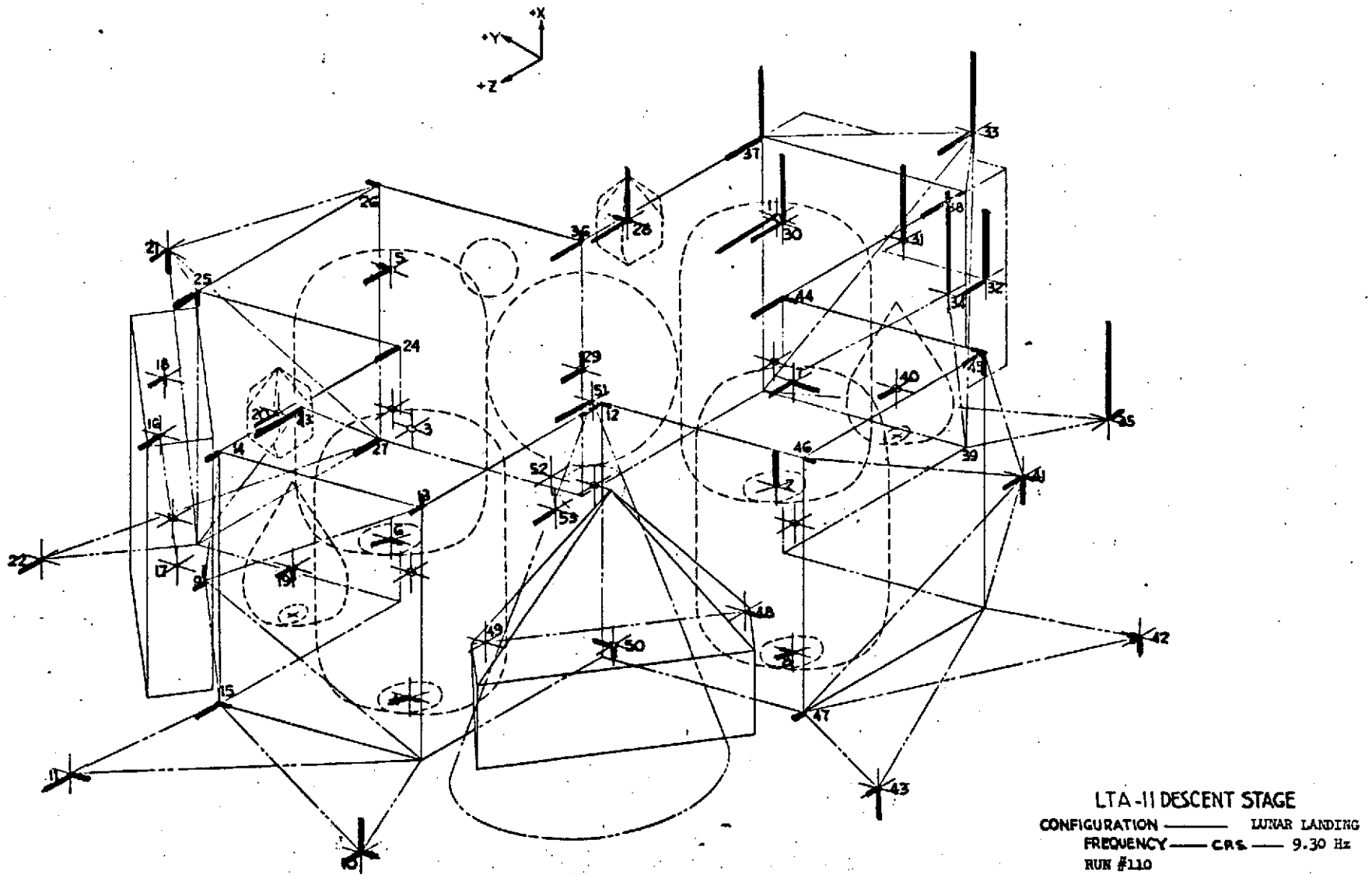
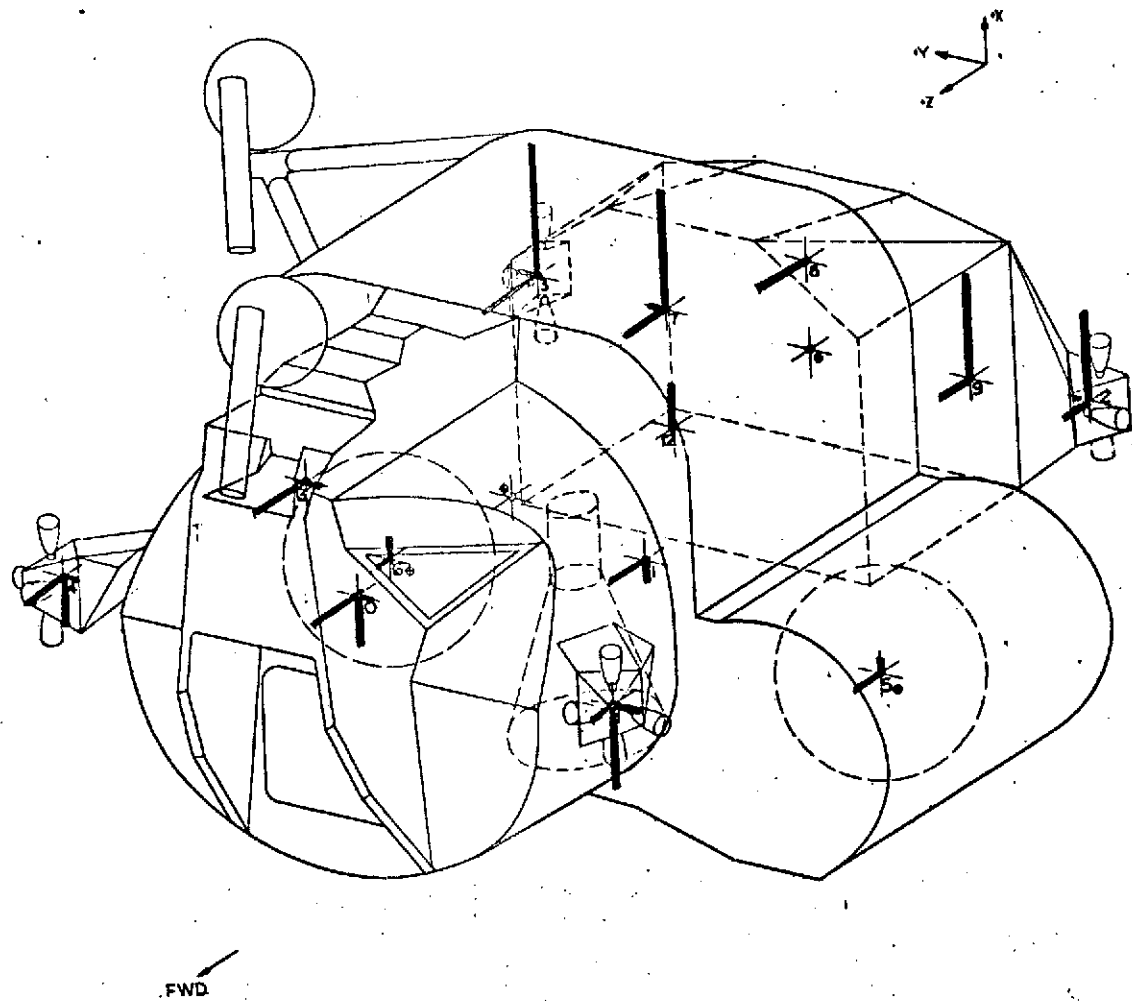


Figure F-2b LTA-11 Mode Survey Result - Descent Stage Second Mode



◆ C.G. OF UNIT

LTA-11  
ASCENT STAGE

CONFIGURATION ——— LUNAR LANDING  
 FREQUENCY — CPS — 10.19 Hz  
 RUN #96

Figure F-3a LTA-11 Mode Survey Result - Ascent Stage Third Mode

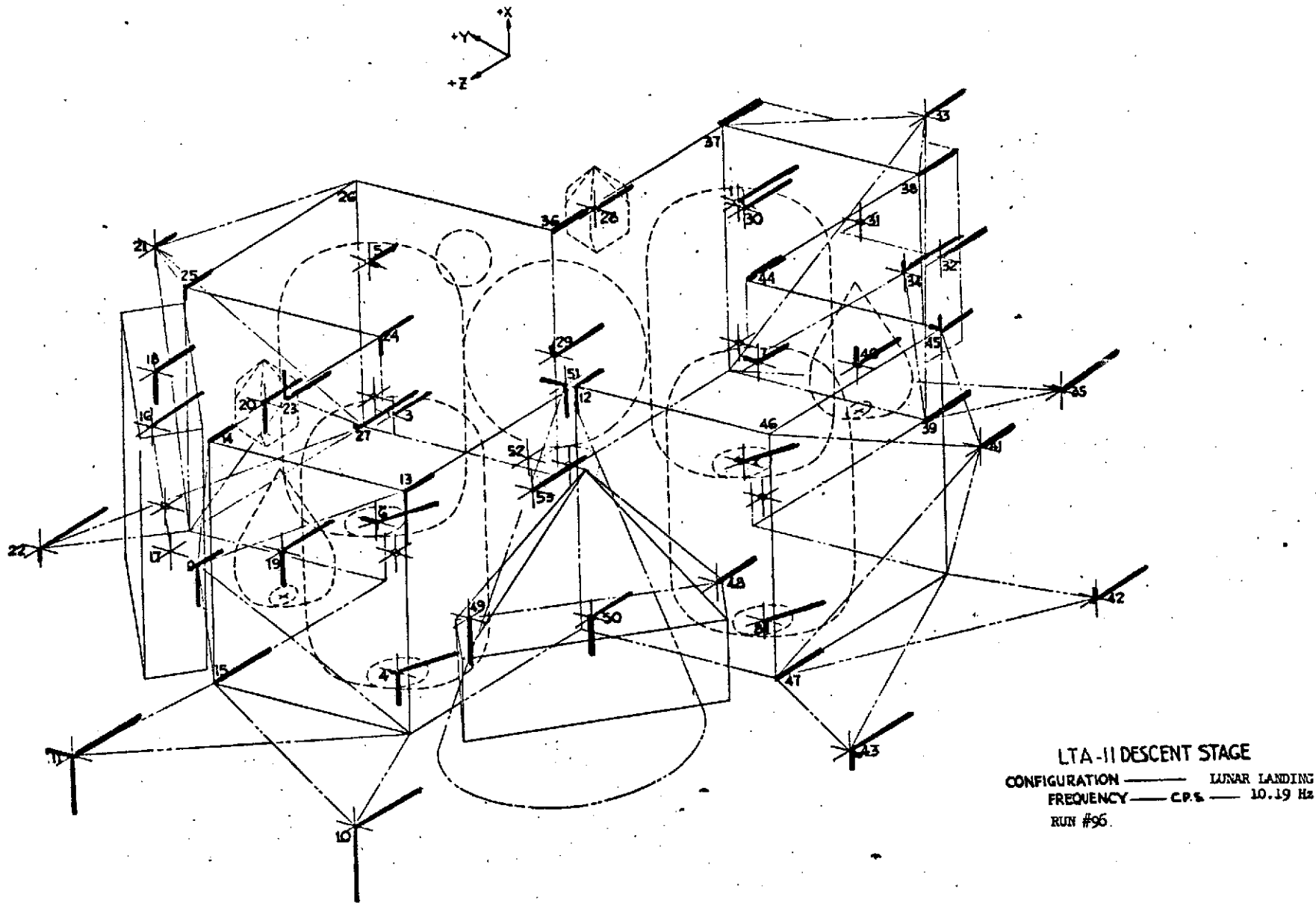
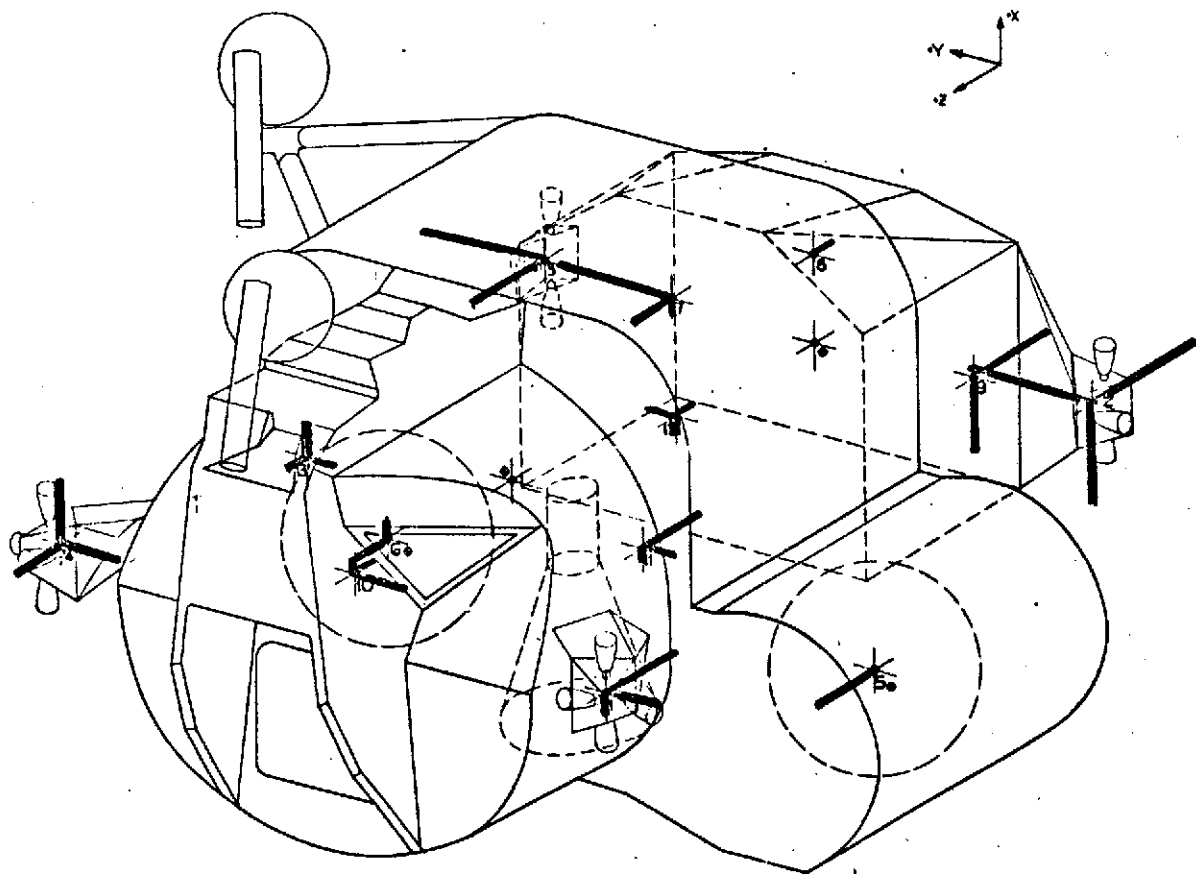


Figure F-3b LTA-11 Mode Survey Result - Descent Stage Third Mode



◆ C.G. OF UNIT

LTA-11  
ASCENT STAGE

CONFIGURATION          LUNAR LANDING  
 FREQUENCY          CPS          12.00 Hz  
 RUN #111

Figure F-4a LTA-11 Mode Survey Result - Ascent Stage Fourth Mode

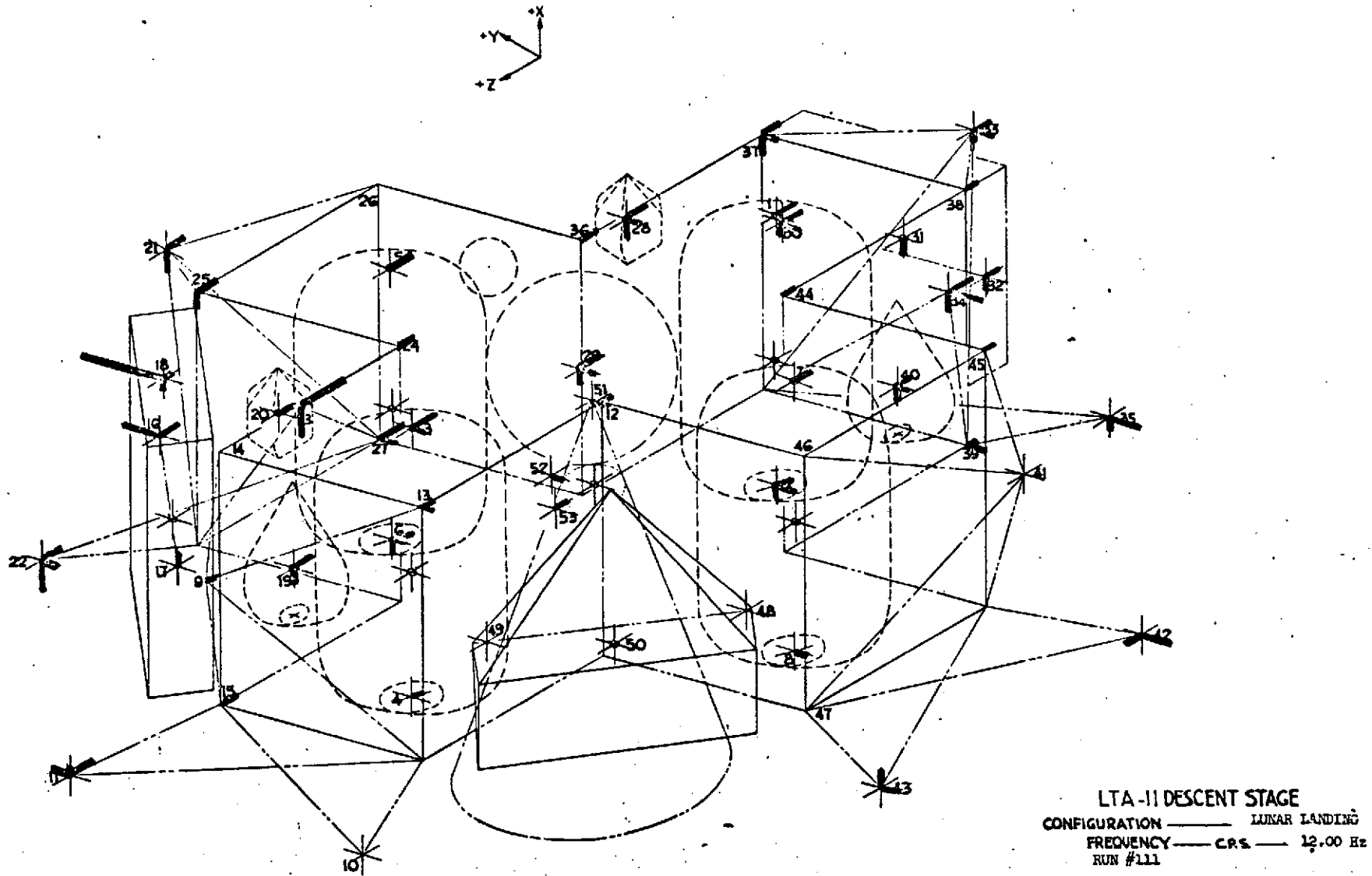
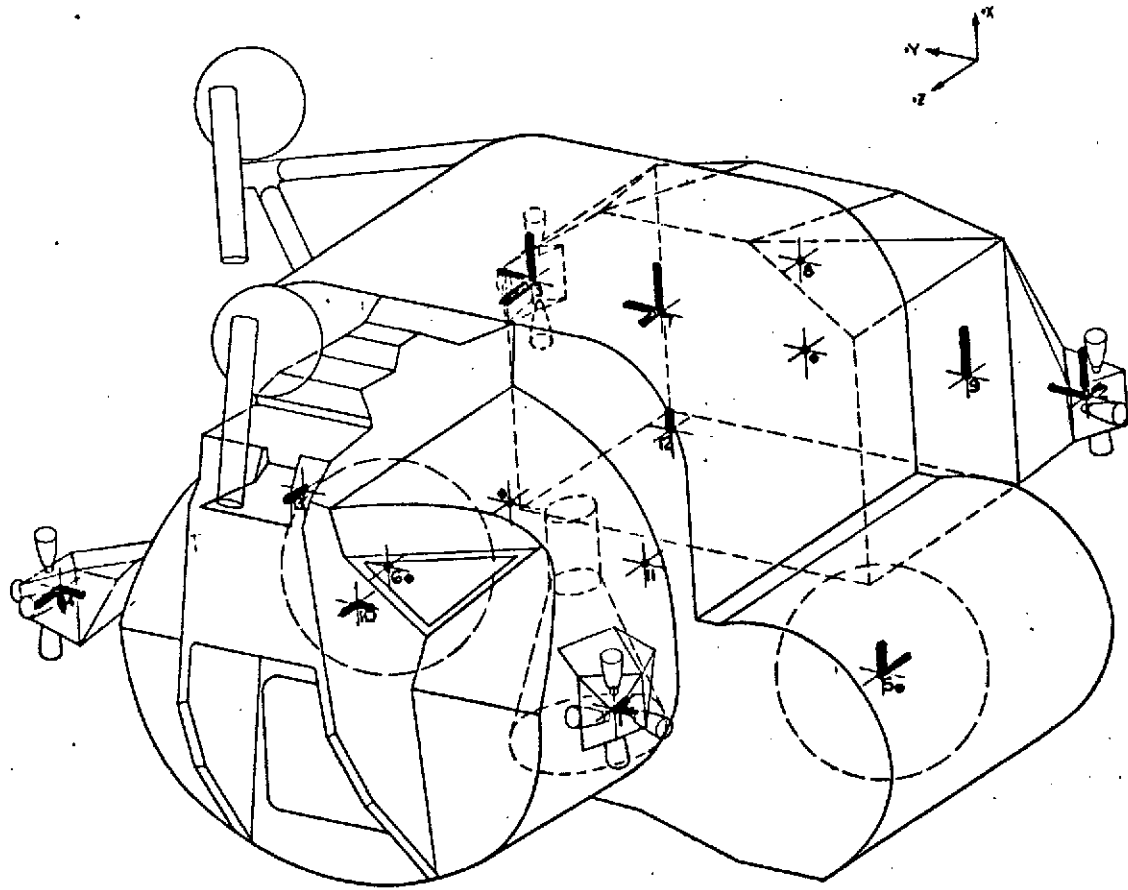


Figure F-4b LTA-11 Mode Survey Result - Descent Stage Fourth Mode



◆ CG OF UNIT

LTA-11  
ASCENT STAGE

CONFIGURATION — LUNAR LANDING  
 FREQUENCY — CPS — 13.02 Hz  
 RUN #115

Figure F-5a LTA-11 Mode Survey Result - Ascent Stage Fifth Mode

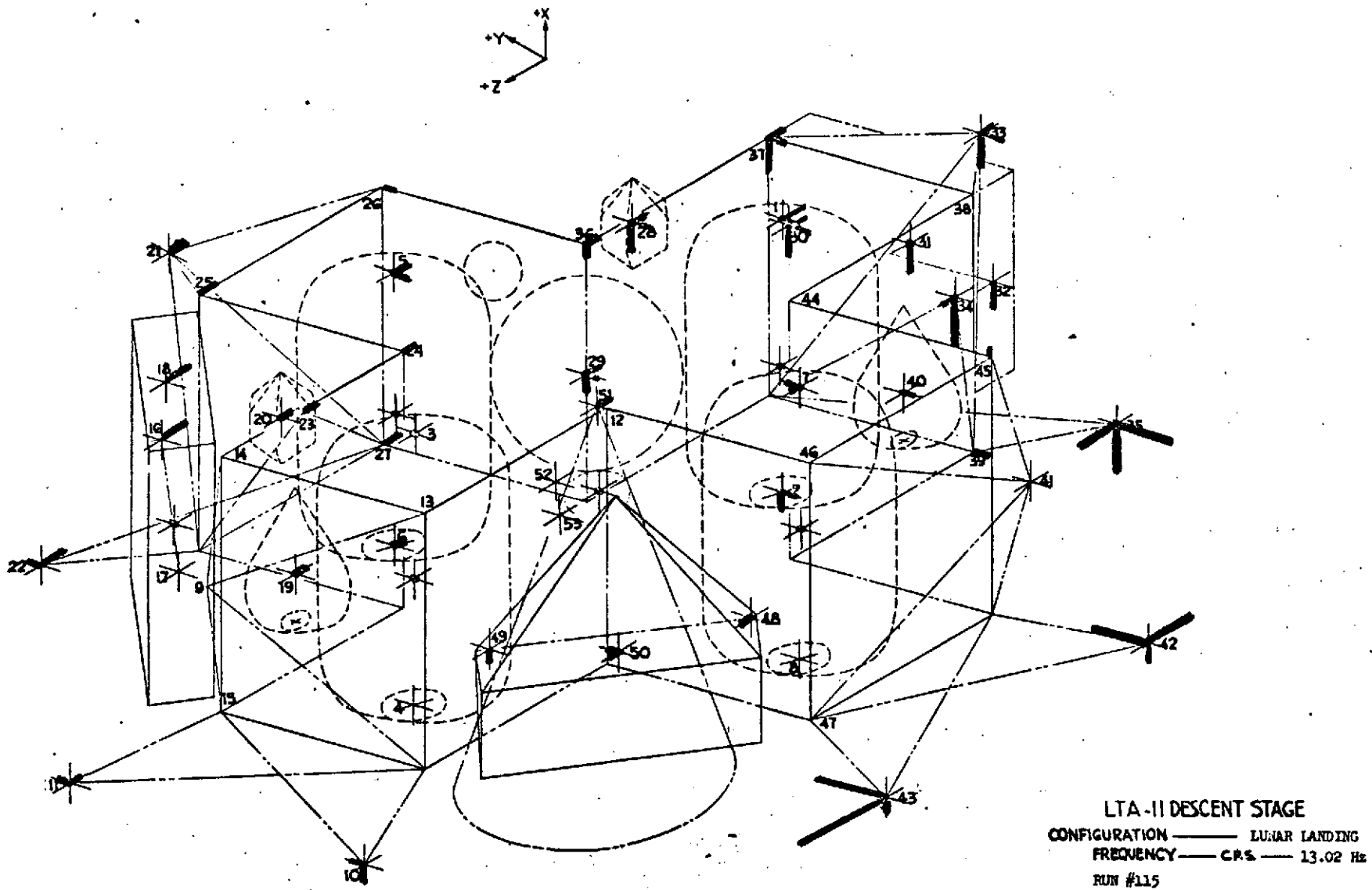
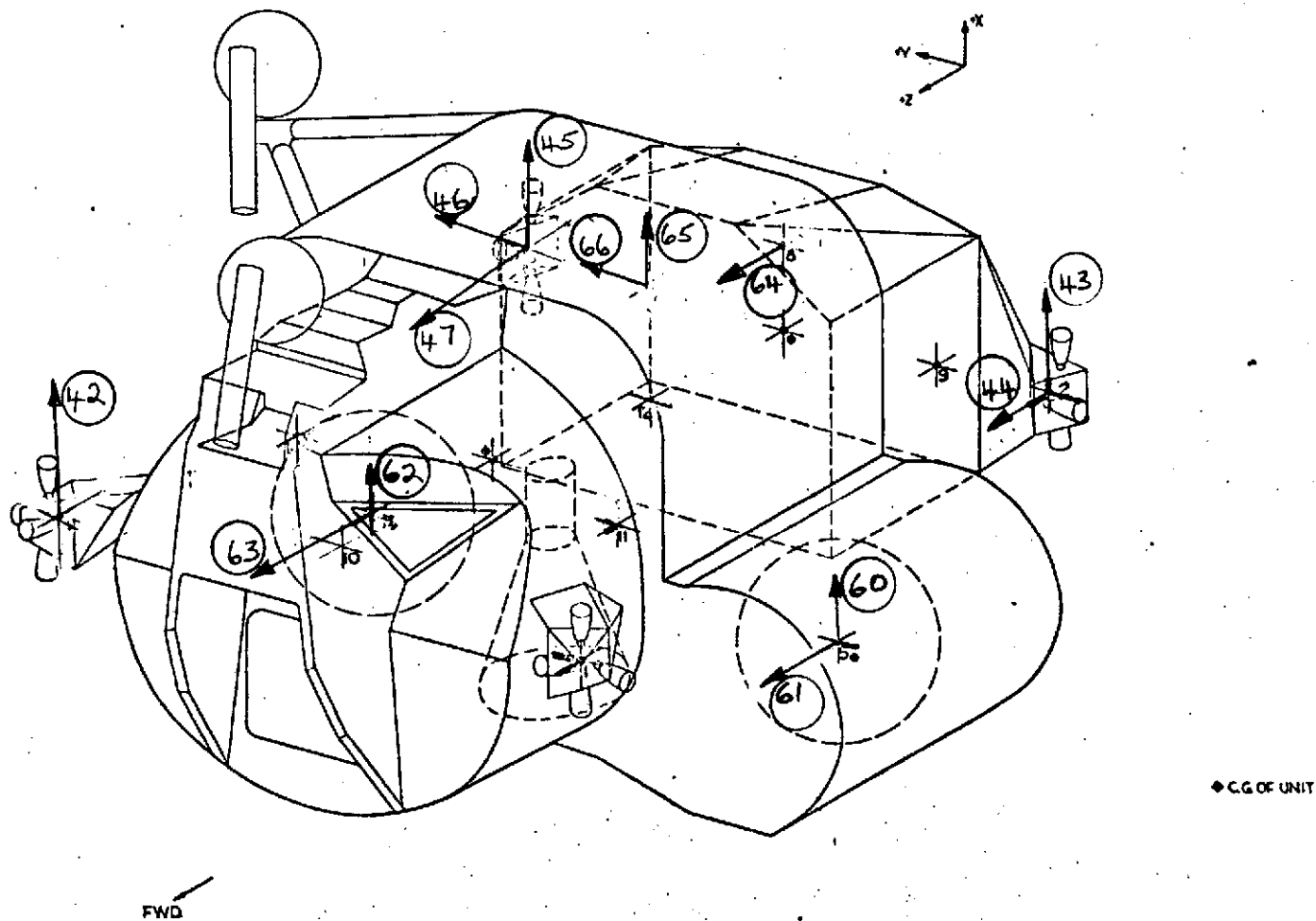
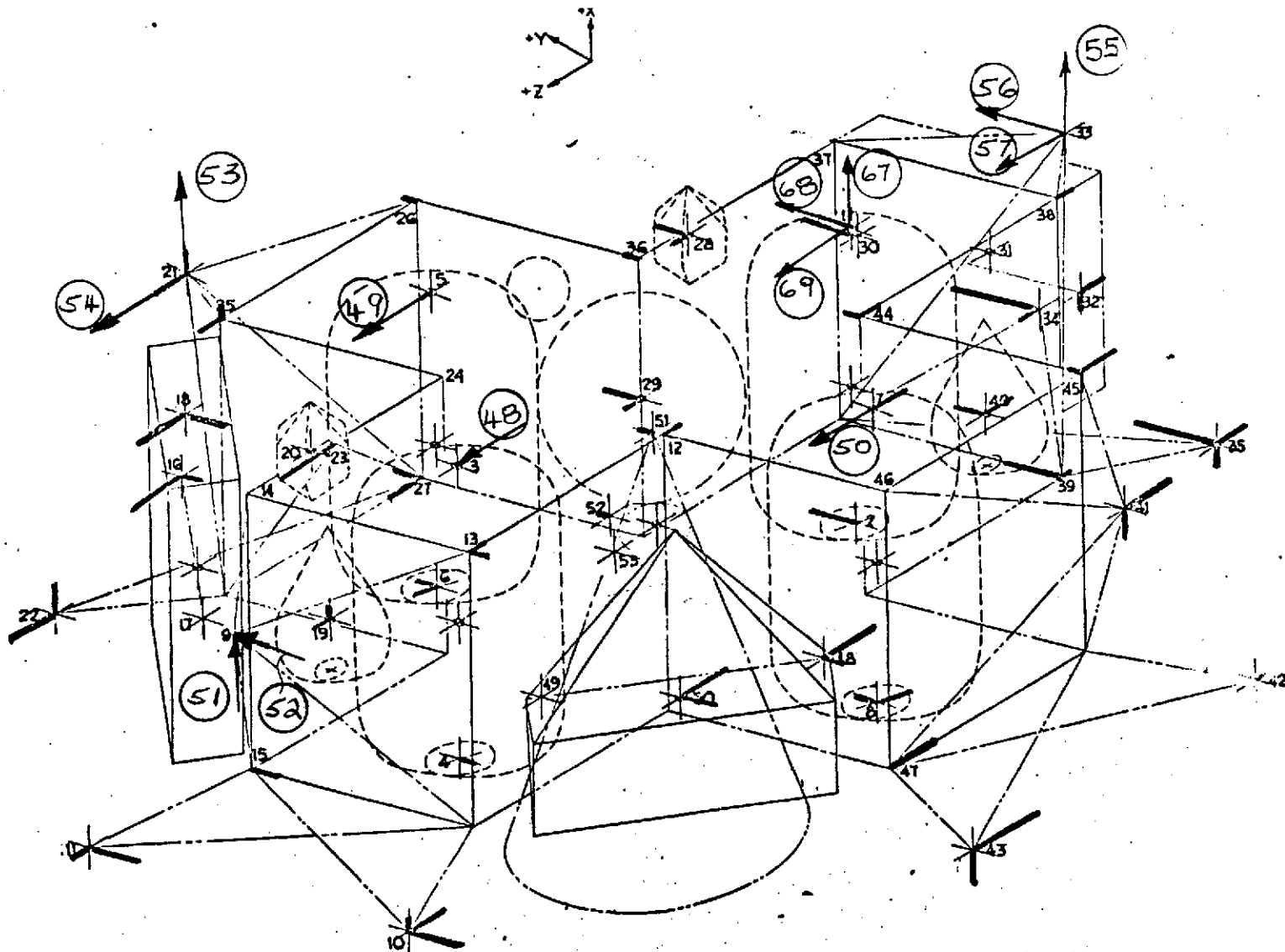


Figure F-5b LTA-11 Mode Survey Result - Descent Stage Fifth Mode



NOTE: Accelerometer locations and measurement direction used in the impulse tests are shown by the circled numbers.

Figure F-6a Accelerometer Locations For Impulse Test - Descent Stage



NOTE: Accelerometer locations and measurement direction used in the impulse tests are shown by the circled numbers.

Figure F-6b Accelerometer Locations For Impulse Test - Ascent Stage